THESIS REPORT

Ph.D.

Control of Bifurcations and Routes to Chaos in Dynamical Systems

by H. Wang
Advisor: E.H. Abed

Ph.D. 93-10

The Institute for Systems Research is supported by the National Science Foundation Engineering Research Center Program (NSFD CD 8803012), the University of Maryland, Harvard University, and Industry

Abstract

Title of Dissertation: Control of Bifurcations and Routes to Chaos in Dynamical Systems

Hua Wang, Doctor of Philosophy, 1993

Dissertation directed by: Professor Eyad H. Abed
Department of Electrical Engineering

This dissertation addresses issues in the control of nonlinear instabilities in high performance engineering systems. Specifically, we consider nonlinear control systems near the limits of their operating envelope. These are highly nonlinear situations occuring in the high-performance operation of a wide variety of systems. Such systems tend to exhibit nonlinear stabilities in terms of a jump to a new low-performance operating point, oscillatory behavior, chaotic behavior or system collapse in the absence of appropriate control action. Such situations necessitate the study of controlling nonlinear phenomena such as bifurcations and chaos.

A new approach to the control of chaotic dynamical systems is introduced, namely control of routes to chaos. The theme is to design feedback control laws which ensure a sufficient degree of stability for a primary bifurcation in the routes to chaos. A thermal convection loop is used as a vehicle to illustrate the idea. Moreover, as the period doubling cascade is one of the most famous routes to chaos, the stabilization of period doubling bifurcations for general n-dimensional discrete-time nonlinear systems is investigated. The technique presented here

affords considerable flexibility in terms of achievable behavior of the nonlinear system over a range of parameter values.

One contribution is the modeling, analysis and control of voltage collapse in electric power systems. A new mechanism of voltage collapse is suggested based on the framework of catastrophic bifurcations. Bifurcation control laws are designed to control these nonlinear phenomena at the inception of voltage collapse. The control laws are shown to result in improved performance of the system for a greater range of parameter values.

Another important application considered is the stall phenomenon in axial flow compressors. A combination of bifurcation analysis and nonlinear control is used to study the dynamics and active control of rotating stall in an axial flow compressor model. Both smooth and nonsmooth feedbacks are considered. Successful experimental verifications have been reported on these results.

Control of Bifurcations and Routes to Chaos in Dynamical Systems

by

Hua Wang

Dissertation submitted to the Faculty of the Graduate School
of The University of Maryland in partial fulfillment
of the requirements for the degree of
Doctor of Philosophy
1993

Advisory Committee:

Professor Eyad H. Abed, Chairman/Advisor
Professor P. S. Krishnaprasad
Associate Professor Mark A. Shayman
Asst. Research Scientist Raymond A. Adomaitis
Professor Celso Grebogi

Dedication

To my parents, sisters

and my wife

Acknowledgements

I would like to express my gratitude in the strongest possible terms to my advisor Dr. Eyad H. Abed, who is not only a superb advisor but also a thoughtful, sensitive and generous friend, for his support, encouragement and guidance. It is he who taught me that good research and decency can go hand-in-hand. It is he who taught me the art of scientific writing. His poetic research and writing style will hold influence throughout my research career.

Acknowledgements are also due to my advisory committee: Drs. Raymond A. Adomaitis, Celso Grebogi, P.S. Krishnaprasad and Mark A. Shayman for their reading of this dissertation and for providing fruitful comments.

I wish to thank Dr. Raymond A. Adomaitis for numerous technical discussions, helpful suggestions and casual chats. It has been important to me that the door to Ray's office was always open. Thanks are also due to Drs. Anan M.A. Hamdan, James C. Alexander, Hsien-Chiarn Lee, Alberto Tesi and Roberto Genesio for helpful suggestions. I thank Drs. Jyun-Horng Fu, Der-Cherng Liaw and Lahcen Saydy for their encouragement and support. I am also grateful to Dr. David L. Elliott for many enlightening conversations and helpful suggestions.

I wish to express my sincere thanks to Dr. Petar V. Kokotovic for featuring our work on controlling chaos in his Bode Prize Lecture at the 1991 IEEE Conference on Decision and Control, for his encouragement in a time when control is facing 'hardship.' I am also grateful to Drs. James A. Yorke, Celso Grebogi and Edward Ott for inviting me to communicate our work at their pizza lunch seminars, and for their invitation to work at the headquarters of chaos research.

To my family, especially my parents, I express my deepest thanks for their

unending love, encouragement and support. To my wife, Wai Chin, it is a dream comes true that we hold together in 'chaos' and 'turbulence.' I thank her for her love, understanding, patience and encouragement over the years.

I would like to extend my thanks to the faculty, staff and fellow students at the Institute for Systems Research for providing an excellent and stimulating environment for study and research.

This research has been supported in part by the National Science Foundation's Engineering Research Centers Program: NSFD CDR-88-03012, by the NSF under Grant ECS-86-57561, by the Air Force Office of Scientific Research under URI Grant AFOSR-87-0073 and Grant AFOSR and by the TRW Foundation.

TABLE OF CONTENTS

List of Tables

List of Figures

Chapter 1

Introduction

Every engineering system has limits on its operating envelope, past which it will no longer function in a useful manner. In response to today's ever-increasing demands on the performance of many engineering systems, there is considerable interest in operating systems near the edge of these limits. These are highly nonlinear situations occurring in the high-performance operation of a wide variety of systems. This dissertation focuses on the control of nonlinear instabilities in high performance engineering systems. These belong to the type of problems that cannot be adequately addressed without recourse to results from nonlinear dynamics. For instance, one needs to study control of nonlinear phenomena such as bifurcations and chaos. Theoretical problems as well as applications in search of theory are considered. Applications are drawn from thermal convection, electric power systems and jet engine dynamics.

1.1 Motivation

The angles of the boundary of stability
are always directed outside,
driving a wedge into the domain of instability.
This is apparently the consequence of a very general principle,
according to which everything good is fragile.

– Vladimir Arnold [17]

The important role played by concepts from bifurcation theory in the sciences, engineering and the social sciences is well-established. Nonlinear phenomena such as the appearance of limit cycles, divergence to new steady states, and transition to chaotic behavior have been observed and studied for a great variety of systems. Only recently have issues of the control of such nonlinear phenomena been given serious consideration (e.g., [2], [3], [58], [60], [77], [21], [101], [9], [62], [103], [104]). Interest in these control problems is partially due to the increased performance that is potentially achievable in modern engineering systems when operating near their stability limits. Systems which function at or near the limits of their operating envelopes tend to experience bifurcations under moderate disturbances. These bifurcations can results in:

- A jump to a new low-performance operating point
- Oscillatory behavior
- Chaotic behavior
- System collapse

Examples of the consequences of operating a system close to its inherent limits include:

- Aircraft stall in supermaneuvers;
- Blackout of a heavily loaded electric power system; and
- Aircraft engine stall.

Although a system is operated within physical limits, it may still undergo such catastrophic events if operated too close to these limits. In such an operating mode, the system is highly vulnerable to even small or moderate external disturbances. Very often, one finds that in this type of operating mode, mathematical models which are relevant must be nonlinear. That is, linearized models cannot be used to predict the system's response subsequent to a destabilizing disturbance.

Despite the foregoing observations, interest exists in a variety of application areas in operating a system very near the limits of its envelope. This is in response to today's ever-increasing demands on the performance of many engineering systems. Achieving increases in performance while maintaining an acceptable safety margin presents an important current engineering challenge. An essential aspect of this challenge is the design of control systems for these *stressed nonlinear systems.* This is the type of control problem considered in this dissertation.

To understand any of the complex behaviors which may characterize the instability of a stressed nonlinear system, one resorts to mathematical modeling. Since transients dominate these phenomena, useful mathematical models fall in the broad class of dynamic models. That is, one deals with systems of evolution equations in an independent time parameter. These may include differential or difference equations of various types. Of course, the evolution equations may be subject to algebraic constraints, boundary conditions, etc.

Qualitative changes in the behavior of nonlinear systems subjected to disturbances is an issue closely linked to concepts of bifurcation theory. This theory has become an indispensable tool in the analysis of many problems of modern applied mathematics. Bifurcation theory, whose history is so closely linked with applications, has been applied successfully in diverse problems of science and technology.

One purpose of this dissertation is to study various bifurcation phenomena in some real world systems. In doing so the objective is to determine the mechanism of certain catastrophic events, such as voltage collapse in power systems. The analysis involves study of local and global bifurcations, including those involving chaotic motions.

In the control of stressed nonlinear systems, interest exists in the implications of bifurcation theory for the control of nonlinear systems with a small margin of stability. A heavily load electric power systems is an example of a highly stressed nonlinear system with a small margin of stability. A variety of bifurcations, static and dynamic, local and global, occur in power system models exhibiting voltage collapse, In order to control voltage collapse in these power system models, one has to design control laws to deal with these various nonlinear phenomena, namely, bifurcations, chaos and crises.

Similar concepts can be applied to the control of axial flow compressor jet engines. Compressor stall is a kind of bifurcation phenomenon of jet engines [4] characterized by large drops in mass flow (in average) which lead the engine to run at a very inefficient operating condition. In particular, the rotating stall type of stall is very difficult to recover from, usually requiring a complete shutdown and subsequent re-start [44]. Since the most efficient operating condition is at

the point where the compressor is about to stall, the normal operating condition will be very close to the stall point. Therefore, the engine has a nonnegligible possibility to run into stall following a large disturbance or during a transition period. Design active control to improve the operability in the vicinity of stall point and to recover the engine to go back to the normal operating conditions in the face of disturbance will be very useful.

Investigations have also been carried out regarding control of chaotic systems, i.e., deterministic systems which can display seemingly random behavior. Since period doubling route to chaos is one of the most important routes to chaos, stabilization of period doubling bifurcations and the implication for control of chaos are explored.

1.2 Linear Control, Nonlinear Control and Bifurcation Control

Traditionally, approximate linearization and linear control design have been the main methodology for the development of control theory and applications. The control laws are mostly designed with reference to a fixed operating condition, such as a fixed equilibrium point. Later, gain scheduling control design is employed to adjust to different (changing) operating conditions.

From the beginning, control engineering is concerned with performance of nonlinear control systems. Questions often asked are: is linearization a reasonable step? Are the results adequate? In the process of evaluating the performance of nonlinear control systems, people start being interested in the nonlinear dynamics of control systems. Most existing results linking nonlinear dynamics

to control are of this type [19] [45] [40] [23] [67] [25].

Chang and his co-workers have done systematic work on the dynamics of control systems [23], [67], [25]. It is well known that the stability criteria established in linear control theory are valid only in the local neighborhood of a set point for a nonlinear system. Away from this immediate neighborhood, other attracting equilibrium states, which cannot be studied with the localized linear model, can destroy the global stability of the locally stabilized set point and, with it, much of the power of the linear theories. In [23] [67] [25] a bifurcation approach is proposed to study the bifurcation characteristics and global dynamics of controlled nonlinear systems. The main idea is to treat the controller gain as a bifurcation parameter and study the qualitative change of the system behavior as the controller gain varies. In particular, [23] studies the bifurcation characteristics of nonlinear systems under conventional PID control. A substrate inhibition model of bioreactors is used to illustrate the richness of dynamic behaviors that can be instigated by a simple controller. These dynamic behaviors in the closed-loop system includes multiple equilibrium points, limit-cycles, tori and strange attractors. In another work [67] the global dynamics of an autothermal reactor under linear feedback control is also studied. It is found that the global stability of the set point is destroyed as the control gain crosses beyond the marginal value, and that further variation of the control gain results in loss of stability at a Hopf bifurcation point. In the case of a subcritical Hopf bifurcation, a locally stable set point can coexist with a large amplitude, stable limit-cycle. This is an example of a so-called "dangerous" stability boundary [92]. Continuing the work of [23], [67], the global effects of controller *saturation* on closed-loop dynamics are investigated in [25].

In this dissertation, we are mainly interested in the control of nonlinear dynamics. The main framework is *bifurcation control.* The type of work of Chang and his co-workers is closely related to bifurcation control but there are major differences. In the study of nonlinear dynamics of control systems, the bifurcation characteristics and dynamics of controlled systems are analyzed passively. Whereas bifurcation control involves design of feedback controls to actively modify the stability and amplitude of bifurcated solutions in general nonlinear control systems.

There has been increased interest in the implications of bifurcation theory for the control of nonlinear systems with a small margin of stability [2], [3], [58], [60], [101], [9], [62], [103], [104]. In [2], the local stabilization control for systems displaying Hopf bifurcation is considered. In [3], local feedback stabilization and bifurcation control are studied for systems displaying stationary bifurcation. In [58], [59], the results of [2] are extended by employing washout filter-aided dynamic feedbacks. The main advantage of using washout filters in the feedback loop is the preservation of all system equilibria even under uncertainty. Also considered in [59] are washout filter-aided control laws for systems possessing a stationary pitchfork bifurcation, and systems possessing double pairs of pure imaginary eigenvalues. Concepts from bifurcation theory have been successfully applied to control problems in high angle of attack flight [58, 59], stall of jet engines [62], [103], [14], oscillatory behavior of tethered satellites [60], electric power system voltage collapse [104] as well as chaotic dynamical systems [101] [9]. For a review of control of chaotic systems see [88].

Mehar [70] and Mehra, Kessel, Carroll [71] have studied global removal of bifurcations by state feedback. Their control result applies only to stationary

bifurcations, since it is obtained bby appealing to a global implicit function theorem. This differs markedly from the local bifurcation control problems considered here, in which one seeks only to modify the stability properties of the bifurcated solutions.

Optimal control and optimization of bifurcating systems have been considered by several authors. Theoretical work on this topic has been reported by Qin [82] and Russell [86]. Doedel, Keller and Kernévez have considered the global numerical optimization of bifurcation problems.

A related subject is the so-called structural or branching control of nonlinear systems [90], [89], [91]. In this approach, the branching ("bifurcation") phenomena for degenerate systems are realized by synthesis problems for attractors having a prescribed nature in a neighborhood of a fixed point. Specifically, the problem considered is how to synthesize a feedback for a completely controllable nonlinear dynamic system to ensure that the dynamics of the closed-loop system is qualitatively equivalent to the dynamics of the original system. The results are applied to synthesize stable periodic trajectories in a given neighborhood of equilibrium. There the idea is to augment the system with a parameter dynamics and then apply the Hopf Bifurcation Theorem to the supercritical case.

1.3 Outline

The development of this dissertation is as follows. In Chapter 2, some basic concepts related to bifurcation along with notation and terminology are reviewed. Basic results related to local and global bifurcations are collected. Complex nonlinear phenomena such as chaos and crises are discussed. Finally, washout

filters and some of their basic properties are introduced.

In Chapter 3, a new approach to the control of chaotic dynamical systems is presented. The idea is illustrated in the context of a thermal convection loop model. A washout filter-aided feedback control stabilizes a primary bifurcation in a sequence of bifurcations leading to chaos. For the example considered, the primary bifurcation is a Hopf bifurcation. A feedback control achieving a sufficient degree of stability for this bifurcation also extinguishes chaos. The technique results in equilibrium preservation even in the face of model uncertainty.

In Chapter 4, continuing the work of controlling bifurcations and chaos, the stabilization of period doubling bifurcations for discrete-time nonlinear systems is investigated. Both static and dynamic feedback controllers have been studied. It is shown that generically such bifurcations can be stabilized using smooth feedback, even if the linearized system is uncontrollable at criticality. In the course of the analysis, expressions are derived for bifurcation stability coefficients of general n-dimensional systems undergoing period doubling bifurcation. A connection is determined between control of the amplitude of a period doubled orbit and the elimination of a period doubling cascade to chaos. For illustration, the results are applied to the Hénon system.

In Chapter 5, modeling, analysis and control of voltage collapse in a model electric power system are considered. We challenge the existing theory of linking voltage collapse exclusively to a saddle node bifurcation by showing a variety of nonlinear phenomena existing in power system models exhibiting voltage collapse. These nonlinear phenomena include local and global bifurcations, chaos and crises. A new view of voltage collapse is suggested based on the framework of catastrophic bifurcations. Bifurcation control laws are designed to control the

nonlinear phenomena at the inception of voltage collapse. The control laws are shown to result in improved performance of the system for a greater range of parameter values.

In Chapter 6, another example of an engineering system near the limits of its operating envelope is considered, namely, stall phenomena in axial flow compressors. A combination of theoretical and computational nonlinear analysis techniques is used to study the scenario of bifurcations at the inception of rotating stall in an axial flow compressor model. Using the throttle opening as a control, it is found that the bifurcations to stall are not linearly stabilizable. Nonlinear stabilization techniques are necessary. Both smooth and nonsmooth feedback of the first mode amplitude are considered. The operability and nonlinear stability of the compression system near the stall point are improved.

Conclusions and suggestions for further research are collected in Chapter 7.

Chapter 2

Nonlinear Phenomena: Preliminaries

In this chapter, we review some basic results relating to bifurcation theory, chaos and crises. Some mathematical tools such as multilinear functions are also discussed. The summary follows [7] and [97]. Since washout filters are employed in the design of control laws in later chapters, basic results on washout filters are recalled as well.

2.1 Local bifurcations

There are many types of bifurcations. Of particular interest in many practical engineering systems are the local bifurcations, i.e., those which result from loss of stability of an equilibrium. Global bifurcations are those which take place over some domain in state space.

2.1.1 Low-Dimensional Examples

The term *bifurcation* refers to qualitative changes in the phase portraits of dynamical systems occurring with slight variation in system parameters. A pa-

rameter value at which such a change occurs is called a critical parameter value. Originally, Poincaré [81] used the term "bifurcation" to describe the splitting of equilibrium solutions for a family of differential equations. Bifurcations involving only equilibrium points are known as stationary or static bifurcations. There are also bifurcations, such as the Hopf bifurcation, which involve both equilibria and periodic solutions. Consider a system

$$\dot{x} = f(x, \mu) \tag{2.1}$$

where $x \in \mathbb{R}^n$ is the system state and $\mu \in \mathbb{R}^k$ denotes a k-dimensional parameter; k can be any positive integer. In this work, we restrict k to be 1 so that μ is a scaler. The equilibrium solutions are given by the solutions of the equation $f_\mu(x) = 0$. By the implicit function theorem, as μ varies, these equilibria are smooth functions of μ as long as $D_x f_\mu$, the Frechet derivative of $f_\mu(x)$ with respect to x, does not have zero eigenvalue. The graph of each of these functions of equilibria in (x, μ) space is a *branch* of an equilibrium of the system. An equilibrium point for a given parameter value is called a "stationary bifurcation point" if several equilibria join at that point. A necessary condition for an equilibrium (x^0, μ_0) to be a (stationary) bifurcation point is that the Jacobian $D_x f_\mu$ has a zero eigenvalues.

Bifurcations are often classified according to the codimension of $D_x f$. Using a linear coordinate transformation, $D_x f$ can be represented in block-diagonal form

$$D_x f := \begin{pmatrix} A_c & 0 \\ 0 & A_s \end{pmatrix} \tag{2.2}$$

where A_c is the Jordan block corresponding to the critical modes and A_s involves the remaining stable modes. Bifurcations from an equilibrium of codi-

mension 1 and 2 fall into one of the following situations:

Codimension 1 bifurcations:

1. $A_c = 0$, a scalar. (This is associated with stationary bifurcation.)

2. A_c is 2×2 and has a pair of pure imaginary eigenvalues. (This is associated with Hopf bifurcation.)

Codimension 2 bifurcations:

1. A_c is 2×2 and is nondiagonalizable with a double zero eigenvalue, that is

$$A_c = \begin{pmatrix} 0 & 1 \\ 0 & 0 \end{pmatrix}. \tag{2.3}$$

2. A_c is 2×2 and is diagonalizable with a double zero eigenvalue, that is

$$A_c = \begin{pmatrix} 0 & 0 \\ 0 & 0 \end{pmatrix}. \tag{2.4}$$

3. A_c is 3×3 and has one zero and one pair of pure imaginary eigenvalues, that is

$$A_c = \begin{pmatrix} 0 & -\omega_c & 0 \\ \omega_c & 0 & 0 \\ 0 & 0 & 0 \end{pmatrix} \tag{2.5}$$

4. A_c is 4×4 and has two pairs of pure imaginary eigenvalues, that is

$$A_c = \begin{pmatrix} 0 & -\omega_1 & 0 & 0 \\ \omega_1 & 0 & 0 & 0 \\ 0 & 0 & 0 & -\omega_2 \\ 0 & 0 & \omega_2 & 0 \end{pmatrix}. \tag{2.6}$$

By using the center manifold reduction technique and normal form transformations, we can reduce system (2.1) to a lower order simplified system called a *normal form.* Normal forms preserve the qualitative properties of the solutions near the bifurcation. Analyzing the dynamics of normal forms yields a qualitative picture of the solutions for each type of bifurcation. The normal forms of codimension one bifurcations are summarized as follows:

i) **Saddle-node bifurcation:** The normal form is given by

$$\dot{x} = \mu - x^2. \tag{2.7}$$

The bifurcated equilibrium solutions exist for $\mu > 0$ and are given by $x = \pm\sqrt{\mu}$. The branch $x = \sqrt{\mu}$, is stable while the other branch, $x = -\sqrt{\mu}$, is unstable.

ii) **Transcritical bifurcation:** The normal form is given by

$$\dot{x} = \mu x - x^2. \tag{2.8}$$

The bifurcated equilibrium, $x = \mu$, exists for both $\mu > 0$ and $\mu < 0$. For $\mu > 0$ (resp. $\mu < 0$), the bifurcated branch is stable (resp. unstable).

iii) **Pitchfork bifurcation:** The normal form (for the *supercritical* case) is given by

$$\dot{x} = \mu x - x^3. \tag{2.9}$$

There are two bifurcated equilibrium branches, $x = \pm\sqrt{\mu}$, for $\mu > 0$, and they are both stable.

iv) **Hopf bifurcation:** The normal form is given by

$$\dot{x} = -y + x(\mu - (x^2 + y^2)); \tag{2.10}$$

$$\dot{y} = x + y(\mu - (x^2 + y^2)). \tag{2.11}$$

The associated bifurcated solutions are nonconstant periodic trajectories.

2.1.2 Bifurcation Theorems

Bifurcations, especially catastrophic bifurcations, play a decisive role in certain catastrophic events to be studied in this thesis. Chaos is also very closely related to bifurcations. Therefore, it is felt that a more detailed discussions of some bifurcations which arise is in order. Generally, we are interested in nonlinear autonomous systems (2.1).

Suppose that (2.1) possesses an equilibrium point $x_0(\mu)$ for a range of values of the parameter μ of interest. We assume that this is an asymptotically stable equilibrium for a large portion of this range. Thus, the equilibrium can qualify as a possible operating condition for the physical system modeled by (2.1). When the system operates in a highly stressed condition, it is possible for the equilibrium $x_0(\mu)$ to lose stability for some parameter value μ_c. At such a loss of stability, the nonlinear system (2.1) typically undergoes a local bifurcation. Such a bifurcation can give rise to new equilibria or periodic orbits of (2.1).

In applications, it may happen that an asymptotically stable equilibrium loses stability through a stationary bifurcation, but the equilibrium solution itself survives. In such a case, either a transcritical bifurcation or a pitchfork bifurcation occurs. This is treated in the following theorem.

Theorem 2.1 (A Stationary Bifurcation Theorem) [51] *Suppose f of system (2.1) is sufficiently smooth with respect to both x and μ, $f(0,\mu) = 0$ for μ near the critical value $\mu_c = 0$, and the Jacobian of f, $A(\mu) := D_x f(0,\mu)$, possesses a simple eigenvalue $\lambda(\mu)$ such that at the critical parameter value $\mu_c = 0$,* $\lambda(0) = 0$,

$$\lambda'(0) := \frac{d\lambda}{d\mu}\Big|_{\mu=0} \neq 0, \tag{2.12}$$

and all the remaining eigenvalues of A_0 have strictly negative real part. Then:

i) There is an $\epsilon_0 > 0$ and a function

$$\mu(\epsilon) = \mu_1\epsilon + \mu_2\epsilon^2 + O(\epsilon^3) \tag{2.13}$$

such that if $\mu_1 \neq 0$, there is a nontrivial equilibrium $x(\mu)$ near $x = 0$ for each $\epsilon \in \{[-\epsilon_0, 0) \cup (0, \epsilon_0]\}$; if $\mu_1 = 0$ and $\mu_2 > 0$ (resp. < 0), there are two equilibrium points $x_\pm(\mu)$ near $x = 0$ for each $\mu \in (0, \epsilon_0]$ (resp. $\mu \in [-\epsilon_0, 0)$).

ii) Exactly one eigenvalue $\beta(\epsilon)$ of the Jacobian evaluated with respect to each of the nontrivial equilibrium points in (i) approaches 0 as $\epsilon \to 0$ and it is given by a real function

$$\beta(\epsilon) = \beta_1\epsilon + \beta_2\epsilon^2 + O(\epsilon^3). \tag{2.14}$$

The coefficient β_1 of this function satisfies $\beta_1 = -\lambda'(0)\mu_1$. The nontrivial equilibrium x_- (resp. x_+) is stable (resp. unstable) if $\beta_1\epsilon < 0$ and is unstable (resp. stable) if $\beta_1\epsilon > 0$. The nominal equilibrium point is unstable at bifurcation. If $\beta_1 = 0$, then $\beta_2 = -2\lambda'(0)\mu_2$, and the nontrivial equilibria are asymptotically stable if $\beta_2 < 0$ and are unstable if $\beta_2 > 0$.

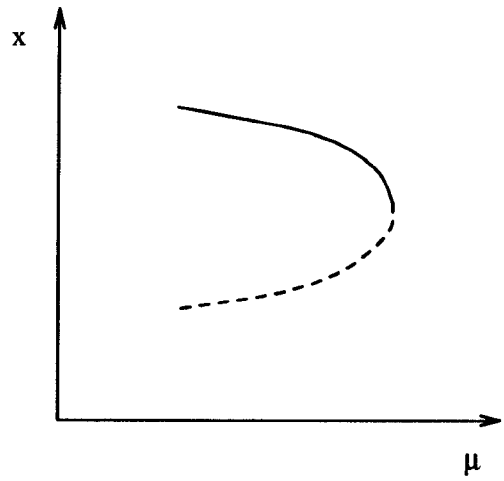

Figure 2.1: Saddle node bifurcation

The assumptions of the theorem above are not generic for the case of a single parameter μ. A result that is generic is one which gives conditions for a saddle node bifurcation. In this case the bifurcation of $x_0(\mu)$ is the merging of this nominal, stable equilibrium with another, unstable equilibrium. Figure 2.1 depicts a saddle node bifurcation for the case of a scalar state vector. Of course, the terminology saddle node bifurcation is inspired by the generalization to systems of dimension two or higher, but the figure addresses the scalar case for simplicity.

To state a theorem on saddle node bifurcation, we consider system (2.1) where f is sufficiently smooth and $f(0,0) = 0$. Express the expansion of $f(x,\mu)$ in a Taylor series about $x = 0, \mu = 0$ in the form

$$f(x,\mu) = Ax + b\mu + Q(x,x) + \cdots \tag{2.15}$$

Note that $A = D_x f(0,0)$ is simply the Jacobian matrix of f at the origin for $\mu = 0$. The next hypothesis is basic to the saddle node bifurcation, as well as other stationary bifurcations of equilibria.

(SN1) The Jacobian A possesses a simple zero eigenvalue.

Let (SN1) hold, and denote by r (resp. l) the right column (resp. left row) eigenvector of the critical Jacobian A corresponding to the zero eigenvalue. Normalize r and l by setting the first component of r to 1 and then chosing l so that $lr = 1$. (This may require one to interchange the position of the first state variable with that of another state variable.) The next hypothesis, along with (SN1), ensures that Eq. (2.1) undergoes a saddle node bifurcation from the origin at $\mu = 0$.

(SN2) $lb \neq 0$ and $lQ(r,r) \neq 0$.

The precise statement is given in the following theorem. Note that usually this result is stated for a one-dimensional reduced system model, whereas we give a statement which applies directly to a general n-dimensional system [7].

Theorem 2.2 (Saddle Node Bifurcation Theorem) *With the notation and assumptions above, if (SN1) and (SN2) hold, then there is an $\epsilon_0 > 0$ and a function*

$$\mu(\epsilon) = \mu_2\epsilon^2 + O(\epsilon^3) \tag{2.16}$$

such that $\mu_2 \neq 0$ and for each $\epsilon \in (0, \epsilon_0]$, Eq. (2.1) has a nontrivial equilibrium $x(\epsilon)$ near 0 for $\mu = \mu(\epsilon)$. The equilibrium point $x = 0$ is unstable at bifurcation, i.e., for $\mu = 0$.

This is the type of bifurcation which has been linked to voltage collapse in [34], [15]. From the point of view of this work, the most important feature of the saddle node bifurcation is the *disappearance, locally, of any stable bounded solution of the system* (2.1). In the following subsections, we give other, more complicated (nonlocal) examples of bifurcations displaying this same feature.

Suppose that the instability of the nominal equilibrium $x_0(\mu)$ is the result of a pair of eigenvalues of the system linearization crossing the imaginary axis in the complex plane. Then, as is well known [47], [65], generically it will be the case that a small amplitude periodic orbit of (2.1) emerges from the equilibrium $x_0(\mu)$. The following hypotheses are invoked in the theorem statement below.

(H1) The Jacobian $D_x f(0,\mu)$ possesses a pair of complex-conjugate simple eigenvalues $\lambda(\mu) = \alpha(\mu) + i\omega(\mu)$, $\overline{\lambda(\mu)}$, such that $\alpha(0) = 0$, $\alpha'(0) \neq 0$ and $\omega_c := \omega(0) > 0$.

(H2) $\pm i\omega_c$ are the only pure imaginary eigenvalues of the critical Jacobian $D_x f(0,0)$.

Theorem 2.3 (Hopf Bifurcation Theorem) *Suppose the vector field f of system (2.1) is sufficiently smooth and $f(0,\mu) \equiv 0$. Given (H1) and (H2) above, then the following hold:*

(a) *(Existence) There is a $\epsilon_0 > 0$ and a smooth function $\mu(\epsilon) = \mu_2\epsilon^2 + O(\epsilon^3)$, such that for each $\epsilon \in (0, \epsilon_0]$ there is a nonconstant periodic solution $p_\epsilon(t)$ of system (2.1) near $x_0(\mu)$ for $\mu = \mu(\epsilon)$. The period of $p_\epsilon(t)$ is a smooth function $T(\epsilon) = 2\pi\omega_c^{-1}[1 + T_2\epsilon^2] + O(\epsilon^3)$, and its amplitude grows as $O(\epsilon)$.*

(b) *(Uniqueness) If $\mu_2 \neq 0$, there is a $\epsilon_1 \in (0, \epsilon_0]$ such that for each $\epsilon \in (0, \epsilon_1]$, the periodic orbit p_ϵ is the only periodic solution of system (2.1) for $\mu = \mu(\epsilon)$ lying in a neighborhood of $x_0(\mu(\epsilon))$.*

(c) *(Stability) Exactly one of the characteristic exponents of $p_\epsilon(t)$ approaches 0 as $\epsilon \downarrow 0$, and it is given by a real smooth function $\beta(\epsilon) = \beta_2\epsilon^2 + O(\epsilon^3)$. The relationship*

$$\beta_2 = -2\alpha'(0)\mu_2 \tag{2.17}$$

holds. Moreover, if all eigenvalues of $D_x f(0,0)$ *besides* $\pm i\omega_c$ *have negative real parts, then* $p_\epsilon(t)$ *is orbitally asymptotically stable with asymptotic phase if* $\beta(\epsilon) < 0$ *but is unstable if* $\beta(\epsilon) > 0$.

The theorems above are of course not sufficient to address all types of catastrophic or jump phenomena in nonlinear systems. Besides these local bifurcations, other bifurcations involving considerations which are not localized in state space near an equilibrium point, can and do arise. However, since an engineering system normally functions at a stable operating *point*, it is the equilibrium condition which must yield, after one or several bifurcations, the decisive bifurcation after which collapse ensues. In the next section we discuss mechanisms of global bifurcation, namely blue sky bifurcations, by which a limit cycle or a strange attractor may disappear through interaction with other invariant sets. First, however, some common mathematical tools largely used in bifurcation analysis are collected.

2.1.3 Multilinear Functions

Multivariate Taylor series expansions are used extensively in our derivation of local stability conditions for bifurcating systems and critical systems. It is very convenient in dealing with these expansions to employ the notation of multilinear functions. The following are some basic definitions and properties of these functions.

Definition 2.1 *Let* V_1, V_2,...,V_k *and* W *be vector spaces over the same field. A map* $\psi : V_1 \times V_2 \times \ldots \times V_k \mapsto W$ *is said to be multilinear (or k-linear) if it is linear in each of its variables. That is ([20], p. 76), for arbitrary* $v^i, \tilde{v}^i \in V_i$,

$i = 1, \ldots, k$, *and for arbitrary scalars* $a, \tilde{a}$, *we have*

$$\begin{aligned} &\psi(v^1, \ldots, av^i + \tilde{a}\tilde{v}^i, \ldots, v^k) \\ &\quad = a\psi(v^1, \ldots, v^i, \ldots, v^k) + \tilde{a}\psi(v^1, \ldots, \tilde{v}^i, \ldots, v^k). \end{aligned} \tag{2.18}$$

We refer to k as the *degree* of the multilinear function ψ. In particular, multilinear functions of degree two, three and four are referred to as *bilinear*, *trilinear* and *tetralinear functions*, respectively.

We shall in the sequel deal exclusively with multilinear functions ψ whose domain is the product space of k *identical* vector spaces $V_1 = V_2 = \ldots = V_k = V$. For such multilinear functions, we have the following notion of symmetry.

Definition 2.2 *A* k*-linear function* $\psi : V \times V \times \ldots \times V \mapsto W$ *is symmetric if, for any* $v^i \in V$, $i = 1, \ldots, k$, *the vector*

$$\psi(v^1, v^2, \ldots, v^k) \tag{2.19}$$

is invariant under arbitrary permutations of the argument vectors v^i.

With an arbitrary multilinear function ψ, we associate a symmetric multilinear function ψ_s by the *symmetrization operation* ([20], pp. 88-89). Given a multilinear function $\psi(x^1, x^2, \ldots, x^k)$, define a new (symmetric) multilinear function Sym ψ as follows:

$$\text{Sym } \psi(x^1, x^2, \ldots, x^k) := \frac{1}{k!} \sum_{(i_1, i_2, \ldots, i_k)} \psi(x^{i_1}, x^{i_2}, \ldots, x^{i_k}), \tag{2.20}$$

where the sum is taken over the $k!$ permutations of the integers $1, 2, ..., k$.

An important property of homogeneous functions represented in terms of multilinear functions is given next.

Proposition 2.4 *[39] Let $\psi : (\mathbb{R}^n)^k \to \mathbb{R}^m$ be a symmetric k-linear function. For any vector $v \in \Re^n$,*

$$D\psi(\eta, \eta, \ldots, \eta) \cdot v = k\psi(\eta, \eta, \ldots, \eta, v). \tag{2.21}$$

2.1.4 The Fredholm Alternative

Consider the system of linear equations

$$Ax = b \tag{2.22}$$

where A is a real $n \times n$ matrix and $b \in \mathbb{R}^n$. It is natural to seek necessary and sufficient conditions for (2.22) to possess solutions $x \in \mathbb{R}^n$. If the coefficient matrix A is nonsingular, then (2.22) has a unique solution, given by $A^{-1}b$. Existence of solutions for cases in which A is singular is the subject of the Fredholm Alternative. Below, we first present this result for the general case of a singular coefficient matrix A, and then employ it for the particular case in which A has a simple zero eigenvalue.

Theorem 2.5 (The Fredholm Alternative) [96] *Let $\mathcal{N}(A)$ be k-dimensional, with basis $r^1, \ldots, r^k$, and dual basis $l^1, \ldots, l^k$. Then (2.22) has at least one solution in $\mathbb{R}^n$ if and only if $l^i b = 0$ for $i = 1, \ldots, k$. Moreover, in such a case, the general solution of (2.22) has the representation*

$$x = x^0 + \sum_{i=1}^{k} \alpha_i r^i \tag{2.23}$$

where x^0 is any particular solution of (2.22) and the α_i are arbitrary real scalars.

Suppose now that A has a simple zero eigenvalue. Let r and l denote right (column) and left (row) eigenvectors of A, respectively, corresponding to the

zero eigenvalue, and require that these be chosen to satisfy $lr = 1$. Under these conditions, the Fredholm Alternative asserts that (2.22) has a solution if and only if $lb = 0$. Moreover, the Fredholm Alternative also implies that, if (2.22) has a solution x^0, then the totality of solutions is given by the one-parameter family $x = x^0 + \alpha r$ where $\alpha \in \mathbb{R}$ is arbitrary. The solution is rendered unique upon imposing a normalization condition which specifies the value of lx.

Introduce subspaces $E^c, E^s \subset \mathbb{R}^n$ as follows: E^c is the one-dimensional subspace

$$E^c := \text{span}\{r\}, \tag{2.24}$$

and E^s is the $(n-1)$-dimensional subspace

$$E^s := \{x \in \mathbb{R}^n | \ lx = 0\}. \tag{2.25}$$

From the foregoing, we have in particular that if $lb = 0$ then the system $Ax = b$, $lx = 0$ has a unique solution. *Equivalently,* (2.22) *has a unique solution in* E^s *for any vector* $b \in E^s$. This proves that the *restriction* ([48], p. 199) $A|_{E^s}$ of the linear map A to E^s defines an invertible (one-to-one and onto) map. In the next result, we exhibit the unique solution which lies in $E^s$of the system $Ax = b$, $lx = 0$. The proof is elementary [3].

Proposition 2.6 *Suppose* A *has a simple zero eigenvalue. Then the unique solution of* $Ax = b$, $lx = 0$ *given that* $lb = 0$ *is*

$$x = (A^T A + l^T l)^{-1} A^T b. \tag{2.26}$$

This result motivates the following introduction of notation:

$$A^- := (A^T A + l^T l)^{-1} A^T. \tag{2.27}$$

Thus, the inverse of the restricted map $A|_{E^s}$ exists and is given by

$$(A|_{E^s})^{-1} = A^{-}. \tag{2.28}$$

2.2 Global Bifurcations, Chaos and Crises

Thompson and Stewart [97] (p.268) refer to a type of global bifurcation in state space involving the discontinuous disappearance of a limit cycle through collision with an equilibrium point as a *blue sky catastrophe.* This is not a local bifurcation. However it does possess the feature noted above for the saddle node bifurcation, namely the disappearance of the attractor by collision with a saddle, in this case a saddle equilibrium point. Here, we find it useful to refer to this and other bifurcations also as blue sky bifurcations since they possess the same feature, namely the disappearance of a (stable) solution of the system (2.1) by a collision with a saddle invariant motion. Thus in this sense saddle node bifurcation may be viewed as a blue sky bifurcation of a stable equilibrium.

The blue sky bifurcation for a periodic orbit is the sudden disappearance of a limit cycle trough collision with a saddle equilibrium point. Prior to the critical parameter value μ_c at which the collision occurs, a saddle equilibrium coexists with the limit cycle. At μ_c the limit cycle and a branch of both the stable and unstable manifolds of the saddle point coincide, forming a *homoclinic connection.* Past μ_c the limit cycle no longer exists. Collision with a saddle fixed point is a typical mechanism by which a limit cycle can abruptly vanish from state space. This blue sky bifurcation can take two forms: the disappearance of a stable limit cycle and the disappearance of an unstable limit cycle. Moreover, it is a global, discontinuous or catastrophic bifurcation. It also serves as a prototype of a blue

sky bifurcation for a strange attractor (an attractor exhibiting chaotic behavior).

Chaos is an irregular, seemingly random dynamic behavior displaying extreme sensitivity to initial conditions [78, 97]. Nearby initial conditions result, at least initially, in trajectories that diverge exponentially fast.

One type of global bifurcation involving a strange attractor is the sudden death of the attractor. Such a blue sky bifurcation occurs commonly for strange attractors of differential equations. Like the blue sky bifurcation for a limit cycle, a chaotic blue sky bifurcation involves a collision with an object of saddle type and is analogous to the blue sky disappearance of a limit cycle discussed above. The chaotic blue sky bifurcation is also known by another term, namely the *boundary crisis of a strange attractor.*

The term *crisis* was introduced in [42], [43], and applies to sudden qualitative changes in strange attractors with quasistatic changes in parameters. A crisis involving the sudden destruction of a strange attractor through collision with a saddle point, an unstable periodic orbit, or the stable manifold of such, is known as a *boundary crisis.* In a boundary crisis, a strange attractor exists for parameter values up to the critical value, at which the collision takes place. Subsequent to this value, the strange attractor no longer exists, but it leaves a signature, namely a transient chaotic motion. The transient chaotic motion appears chaotic for a relatively long time (depending on the initial condition), and then suddenly experiences a sharp excursion either to another, probably distant attractor, or to infinity. This excursion occurs through a "tunnel" in state space which necessarily follows the unstable manifold of the saddle point or orbit with which the collision takes place. The result is a discontinuous, catastrophic disappearance of the strange attractor. Such a bifurcation is always a global

bifurcation involving a homoclinic or heteroclinic event. In this thesis, we shall use the terms chaotic blue sky bifurcation and boundary crisis of a strange attractor synonymously, although boundary crisis was originally introduced for one-dimensional maps.

2.3 Catastrophic Bifurcations

In the classification of bifurcations, it is very useful to distinguish between continuous and discontinuous (or catastrophic) bifurcations. In the case of discontinuous bifurcations, the system exhibits a jump from the nominal to another attractor, possibly infinity. While in the case of continuous bifurcations, the system evolves continuously onto another attractor. The saddle node bifurcation, in which a pair of equilibria (a saddle and a node) disappear simultaneously as a parameter passes a critical value, is a fundamental bifurcation in nonlinear dynamics. It is also the simplest example of a discontinuous or catastrophic bifurcation. Other examples of catastrophic bifurcations are all the bifurcations appearing in subcritical form, e.g., subcritical Hopf bifurcation and subcritical pitchfork bifurcation.

In the case of saddle node bifurcation, the interrupted path of the attractor (stable equilibrium) indicates a discontinuous bifurcation. A contrasting case is the stable (supercritical) pitchfork bifurcation which is a *continuous bifurcation.*

One way to define a discontinuous or continuous bifurcation is to use the so-called parameter-phase function, which maps each parameter value μ to the corresponding attractor-basin portrait [97]. Using this notion, a *discontinuous bifurcation* occurs at a parameter value μ where the parameter-phase function is

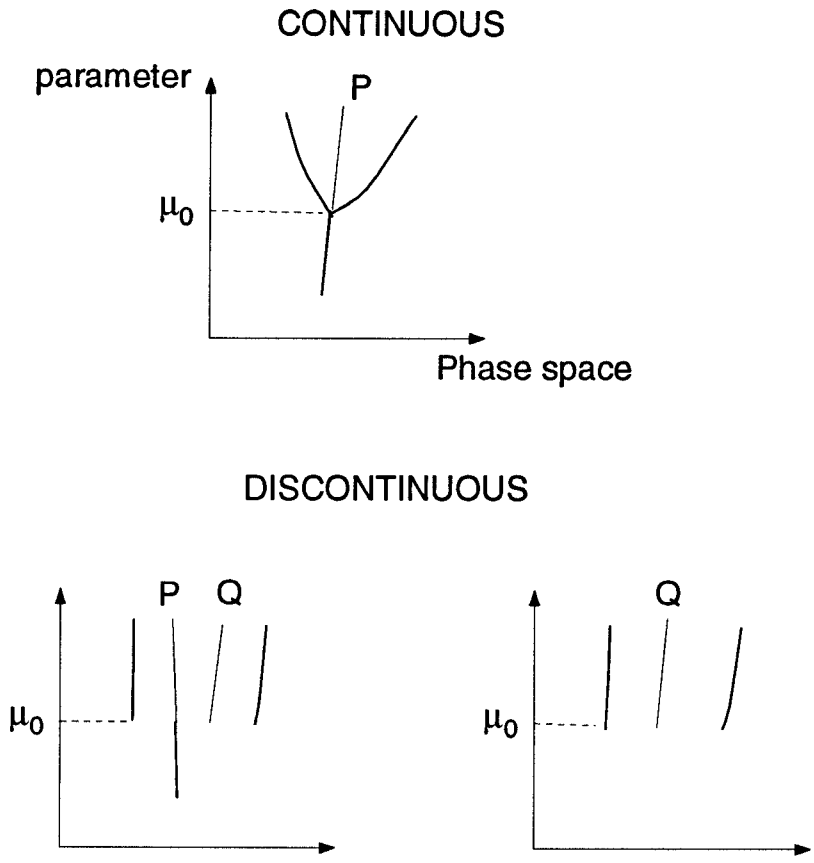

Figure 2.2: Schematic parameter-phase space diagrams of continuous and discontinuous bifurcations at $\mu = \mu_0$; attractrix paths P continue across the bifurcation point, while paths Q are interrupted

discontinuous.

Schematic diagrams of continuous and discontinuous bifurcation $\mu = \mu_0$ are shown in Fig. 2.2 [97]. We shall use the terms discontinuous bifurcation and catastrophic bifurcation synonymously for any bifurcation in which some attracting set paths are interrupted. A theoretical framework for these ideas can be found in [11].

Based on the observation of catastrophic and continuous bifurcations, the supercritical bifurcations result in a more desirable system response than the

subcritical bifurcations, locally near $\mu = \mu_c$. This constitutes our main philosophy in the local stabilization of bifurcations from equilibria of system (2.1). The control strategy is to design a feedback to transform a subcritical bifurcation into a supercritical one or to enhance the stability of a supercritical bifurcation.

2.4 Washout Filters

Washout filters are used commonly in control systems for power systems [16] and aircraft [68]. The main advantage of using these filters is the resulting robustness of the system operating point to model uncertainty and to other control actions which may be used. In this section, we give a brief discussion of these filters, their use in control of parametrized systems and especially bifurcation problems.

A *washout filter* (or washout circuit) is a stable high pass filter with transfer function [38, p. 477]

$$\begin{aligned} G(s) &= \frac{y(s)}{x(s)} = \frac{s}{(s+a)} \\ &= 1 - \frac{a}{(s+a)}. \end{aligned} \tag{2.29}$$

Here, $a > 0$ is the inverse of the filter time constant. Letting

$$z(s) := \frac{1}{(s+a)} x(s), \tag{2.30}$$

the dynamics of the filter can be written as

$$\dot{z} = x - az, \tag{2.31}$$

and

$$y = x - az. \tag{2.32}$$

Feedback through washout filters results in *equilibrium preservation* in the presence of system uncertainties and other control mechanisms that they inherently offer. Indeed, the most striking property of a system controlled through a washout filter is that all the original equilibria are preserved. Thus, one can concentrate on the design of controllers emphasizing the increase in performance achieved for a particular equilibrium, without the risk of affecting the location of other equilibria. As has been observed in [6], even with careful curve-fitting, it is possible that extraneous equilibria will be brought very close to the nominal equilibrium, significantly increasing the stability vulnerability of that equilibrium. Here, vulnerability occurs because the domain of attraction for the nominal equilibrium will be compromised in the direction of a nearby extraneous equilibrium.

Equilibrium points represent, in some sense, a system's capability to perform in a certain manner at steady state. There are cases in which such a capability should not be altered by the introduced control strategy. For instance, in the problem of lateral control design for an aircraft, the yaw rate signal is fed back to the rudder to increase the Dutch roll damping factor. The control is usually designed assuming a level flight condition. That is, one works with a linearized model obtained relative to a level flight condition. Unfortunately, this type of feedback tends to oppose the aircraft's tendency to turn. To remedy this situation, a washout filter is included in the feedback loop. This filter, which rejects steady-state input signals, has the effect of "washing out" the yaw rate signal at steady-state and thus minimizes the tendency opposing a steady turn. In other words, the lateral control designed for level flight does not impact the open-loop equilibrium for turning flight. Moreover, if the controller is purely

nonlinear, the linear stability of each equilibrium point will also be preserved.

Washout filters reject steady-state inputs, while passing transient inputs. At steady-state,

$$z = \frac{x}{a}, \tag{2.33}$$

the output $y = 0$, and the steady-state input signal has been washed out.

Consider a system

$$\dot{x} = f(x, u) \tag{2.34}$$

with

$$f(x_e, 0) = 0, \tag{2.35}$$

where u is the control input and x_e is an equilibrium point for the system with zero input. Let the control input u be a function of y, defined in Eq. (1.3b): u = h(y), and let h satisfy

$$h(0) = 0. \tag{2.36}$$

From Eq. (2.31)-(2.32), it is clear that y vanishes at steady-state. Hence

$$f(x_e, h(y_e)) = f(x_e, 0) = 0, \tag{2.37}$$

and x_e remains an equilibrium point of the closed-loop system. This shows that by incorporating a washout filter in the feedback, the equilibrium points of the original system are preserved.

Chapter 3

Bifurcation Control of Chaotic Dynamical Systems

In this chapter nonlinear system which exhibits bifurcations, transient chaos, and fully developed chaos is considered. This is to illustrate the role of two ideas in the control of chaotic dynamical systems. The first of these ideas is the need for *robust control*, in the sense that, even with an uncertain dynamic model of the system, the design ensures stabilization without at the same time changing the underlying equilibrium structure of the system. The second idea is that focusing on the control of primary bifurcations in the routes to chaos can result in the taming of chaos. The latter is an example of the 'bifurcation control' approach. When employed along with a dynamic feedback approach to equilibrium structure preservation, this results in a family of robust feedback controllers by which one can achieve various types of 'stability' for the system.

3.1 Introduction

Recently, significant attention has been focused on developing techniques for the control of chaotic dynamical systems [93, 77, 85, 37, 99, 52, 88]. Of course, at the outset, one must realize that there is no obvious way to define the 'control of chaos' problem. This is in direct contrast to more traditional dynamical system control problems, such as the textbook problem of stabilization of an equilibrium position of a nonlinear system. Although even this textbook problem allows for various interpretations for the achieved margin of stability, decay rate, etc., these can all be viewed within the same basic framework. Chaos, on the other hand, is a rich, global dynamic behavior, and its 'stabilization' can have vastly differing interpretations. For example, references [77, 85] employ a small amplitude control law in a restricted region of the state space, thereby stabilizing a pre-existing equilibrium or periodic orbit. Since the control vanishes in most of the state space, closed-loop system trajectories follow erratic paths for some time, until they enter part of the neighborhood in which the control is effective, after which they are attracted to the equilibrium or periodic orbit of interest. Other authors apply nonlocal linear or nonlinear feedback to stabilize nominal equilibrium points [93, 99]. Also, some authors are taking a control systems approach to the analysis of chaos, which may prove useful in control design (see [69, 19, 41]). This summary of previous work on control of chaos is of necessity very brief, and the reader is referred to the original papers for details.

In general, the techniques for feedback control of chaos presented thus far in the literature have some common features, which we feel are important to briefly summarize. The control is usually designed for parameter values where the system is known to exhibit chaotic motion, and is typically of the form $u = u(x - x_0)$

where x is the system state vector, and x_0 is an unstable equilibrium of interest, which lies on a chaotic attractor. The control function u is not necessarily smooth. Thus, the control consists of direct state (or output) feedback around x_0, a specific equilibrium of interest. Note that x_0 can also be a periodic orbit, as observed in [77, 85].

The approach pursued in the present thesis is directed toward nonlinear systems which undergo bifurcations, and possibly chaotic motion, as a parameter is quasistatically varied. Such systems naturally possess several, and possibly infinitely many, equilibria and periodic orbits. The approach is of particular relevance to systems for which the model possesses a high degree of uncertainty. Often, an engineering system is designed to perform well, and to be stable, for a large range of parameter values. However, technological demands are pushing systems to the limits of their performance, and many engineering systems are being operated under conditions which may be viewed as 'stressed.' It is this stressed operation which gives rise to nonlinear dynamic phenomena, such as bifurcations leading, in some cases, to chaos. We take an approach which is in mathematical synergy with this description.

We consider nonlinear systems depending, for simplicity, on a single bifurcation parameter. For the 'usual' values of the parameter, the system operates at a stable equilibrium, and perturbations away from this mode of operation tend to be attenuated (stability). As the parameter is varied, the equilibrium loses stability at a bifurcation point, giving rise to new equilibria or periodic orbits, perhaps. If any of the bifurcated solutions is stable, the system may operate at such a solution. For greater variations of the parameter, these bifurcated solutions may also lose stability, and so on. There are several scenarios by which

successive bifurcations can result in a chaotic invariant set; these are discussed extensively in the chaos literature. What is important about these scenarios from a control of chaos perspective, however, is that the appearance of chaos depends heavily on various aspects of the succession of bifurcations. Suppose a particular control significantly reduces the amplitude of a bifurcated solution, or significantly enhances its stability, over a nontrivial parameter range. Then, one might expect that the occurrence of chaos might be 'delayed' to even greater variations in the parameter, or might be extinguished completely.

This work differs from previous techniques in another respect, related to nonlinear model uncertainty. Under model uncertainty, a nonlinear static state feedback controller designed relative to a given equilibrium will influence not only the stability, but also the location, of this and other system equilibria. To circumvent this difficulty, we employ a form of dynamic feedback which exactly preserves all system equilibria. This uses washout filters in a way which retains sufficient freedom to stabilize bifurcations, and to delay their occurrence if desired (see [58]). Besides preserving system equilibria, the incorporation of washout filters in the feedback control facilitates the design of a control which does not depend on the bifurcation parameter. This is also important to achieving a control which is effective over a range of parameter values, instead of at one specific parameter value.

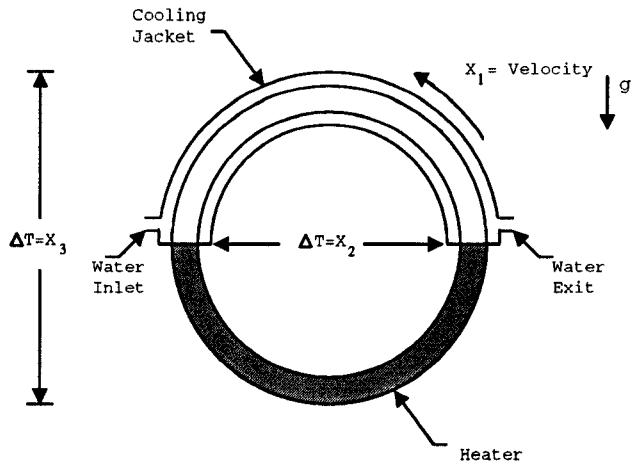

Figure 3.1: Schematic description of the experimental apparatus

3.2 Thermal Convection Loop: Homoclinic & Heteroclinic Orbits

Singer, Wang and Bau [93] study a thermal convection loop using a combination of experimentation, modeling, and simulation. The analytical model used in [93] is given by the third order system

$$\dot{x}_1 = -px_1 + px_2, \tag{3.1}$$

$$\dot{x}_2 = -x_1x_3 - x_2, \tag{3.2}$$

$$\dot{x}_3 = x_1x_2 - x_3 - R. \tag{3.3}$$

where $x_i, i = 1,2,3$, are real, and p and R are positive parameters. The experiment studied in [93] involves thermal convection in a toroidal vertical loop heated from below and cooled from above as depicted in Figure 3.1. The variables x_1, x_2, x_3 correspond, respectively, to the cross-sectionally averaged velocity in the loop, the temperature difference along the horizontal direction (side to side), and the temperature difference along the vertical direction (top to bottom). The

parameter R is the Rayleigh number, which is proportional to the net heating rate, and p denotes the Prandtl number. It is observed experimentally that, as the heating rate increases, the fluid flow in the loop goes through transitions. For a low heating rate, the fluid is in the no-motion state. As the heating rate increases, a state of steady convection arises (clockwise or counterclockwise). Further increases in the heating rate result in temporally oscillatory, and, eventually, chaotic motion of the fluid.

The transitions above are also reflected by the model (3.1)-(3.3). In particular, it is found that a invariant chaotic set is born through a pair of blue sky catastrophes [97] (*homoclinic connection*). But initially this chaotic set is not attracting, which is responsible for the *transient chaotic* motion in the system for a range of parameters. This invariant chaotic set becomes an attractor through *heteroclinic* connections ("crisis") at parameter R varies. This is the beginning of chaotic motion in the system. In the thesis, we note that birth of the homoclinic orbits, which may be viewed as being 'caused' by the subcriticality of the Hopf bifurcations, are important to the appearance of the transient chaotic and chaotic motions of the model studied here. (The model also exhibits chaotic behavior in other, distant parameter ranges arising from period doubling cascades.) In this thesis an array of feedback controllers will be designed to achieve the goal of taming chaos as well as other types stability objectives for this system. The washout filter-aided bifurcation control approach will be the main tool for control design.

To facilitate discussion of this model, set $p = 4.0$ and view R as the bifurcation parameter. A bifurcation diagram related to this model is given in Fig. 3.2. In this diagram, a solid line represents a stable equilibrium, a dashed line rep-

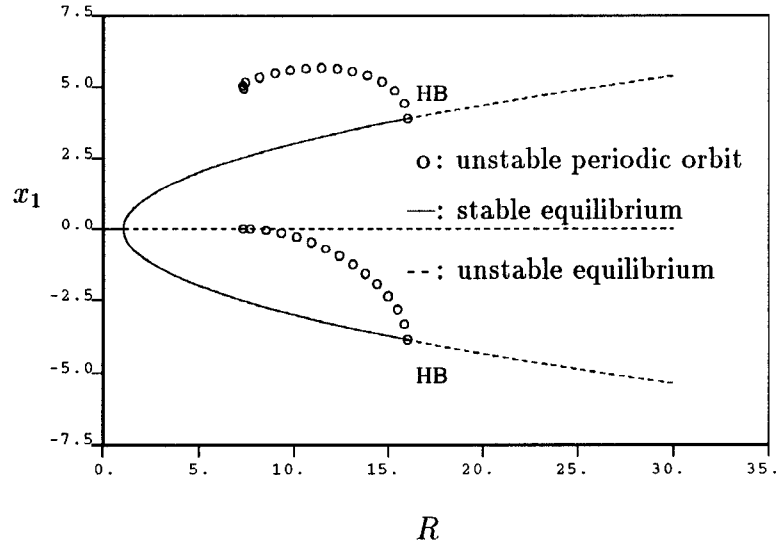

Figure 3.2: Bifurcation diagram for open loop system

resents an unstable equilibrium, and an open circle represents the maximum amplitude of an unstable periodic orbit of (3.1)-(3.3). The bifurcation diagram is obtained by employing the package AUTO [35]. The model (3.1)-(3.3) possesses symmetry, in that replacing (x_1, x_2, x_3) with $(-x_1, -x_2, x_3)$ results in the same set of equations. This symmetry is reflected in the bifurcation diagram of Fig. 3.2.

For $R \leq 1.0$ the system (3.1)-(3.3) has a single, globally attracting, equilibrium point. This equilibrium, given by $x_1 = x_2 = 0, x_3 = -R$, corresponds to the *no-motion state*. At $R = 1.0$ two additional equilibrium points appear through a pitchfork bifurcation. These equilibria, which are present for all $R > 1.0$, are given by $(x_1 = x_2 = \pm\sqrt{R-1}, x_3 = -1.0)$. Denote these equilibria by C_+ and C_-, respectively. These two equilibrium points represent the states of steady convection in the counterclockwise or clockwise directions, respectively. The no-motion equilibrium state $(0, 0, -R)$ loses its stability at the pitchfork bifurcation

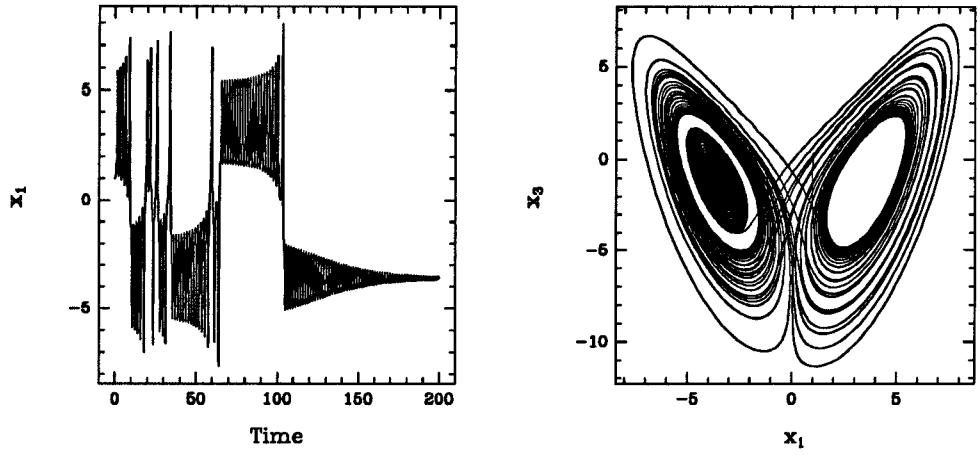

(a) (b)

Figure 3.3: A transient chaotic orbit of open loop system for $R = 14$

point, i.e., at $R = 1.0$. The convective equilibria $(\pm\sqrt{R-1}, \pm\sqrt{R-1}, -1.0)$ lose their stability in Hopf bifurcations occurring at $R = p(p+4)/(p-2) = 16.0$, as depicted in Fig. 3.2. The bifurcation diagram of Fig. 3.2 illustrates that the Hopf bifurcations at the convective equilibria result in *unstable* periodic solutions, i.e., these bifurcations are subcritical. Moreover, Fig. 3.2 also illustrates the disappearance of the unstable periodic orbit in a blue sky catastrophe [97] at the approximate value $R = 7.3198$. Not discernible from Fig. 3.2 is the fact that the model (3.1)-(3.3) admits erratic behavior for a large range of values of R. This erratic behavior may or may not be chaotic. To be more precise, one observes trajectories which appear chaotic for a long time interval, after which they settle to an equilibrium. One also observes trajectories which are chaotic in the usual sense. The former type of behavior is often referred to as "transient chaos." Transient chaos is observed in simulations of (3.1)-(3.3) for parameter values $7.3198 < R < 15.9$, for *some* initial conditions. (Extensive simulation

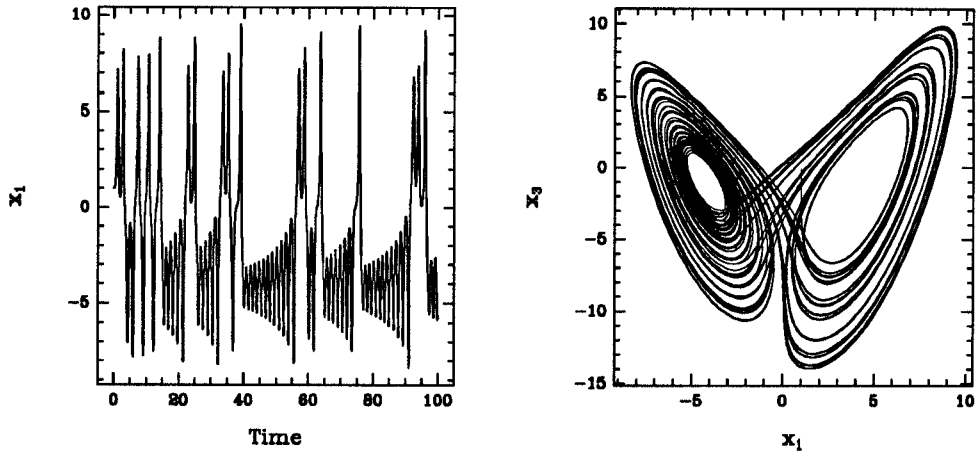

(a) (b)

Figure 3.4: A chaotic orbit of open loop system for $R = 19$

shows that initial conditions resulting in transient chaos are more common for larger values of R in this interval. See Fig. 3.3 for a typical transient chaotic trajectory of the system at $R = 14$.) At approximately $R = 15.9$ the transient chaos is converted to a chaotic attractor by a crisis. Thus for the relatively narrow range $15.9 < R < 16$, there are three possible attractors, namely C_+, C_- and a chaotic attractor, while for $R > 16$, typical trajectories of the system (3.1)-(3.3) are chaotic. Figure 3.4 shows a typical chaotic trajectory of the system at $R = 19$.

The foregoing is a necessarily brief description of the qualitative behavior of (3.1)-(3.3) and its dependence on the parameter R. There are, however, intricate details associated with the various behaviors and their bifurcations. For instance, there are several stable periodic orbit windows for some large values of R. Within these windows there are three kinds of bifurcations involving periodic orbits, namely, the saddle-node bifurcation, the symmetry breaking bifurcation

and the period doubling bifurcation [95]. The most noticeable periodic orbit window corresponds roughly to the parameter range $125 < R < \infty$.

Not only do Eqs. (3.1)-(3.3) resemble the Lorenz equations, but there is a simple transformation mapping the Lorenz system into (3.1)-(3.3). The Lorenz equations are

$$\dot{x} = -\sigma x + \sigma y, \tag{3.4}$$

$$\dot{y} = rx - y - xz, \tag{3.5}$$

$$\dot{z} = xy - bz, \tag{3.6}$$

where σ, r and b are three positive parameters. Equations (3.1)-(3.3) can be obtained from the Lorenz equations by the transformation

$$x_1 = x, \tag{3.7}$$

$$x_2 = y, \tag{3.8}$$

$$x_3 = z - r, \tag{3.9}$$

with the identifications $R = r, p = \sigma$ and $b = 1$. Hence, studies of the Lorenz equations have a direct bearing on the system (3.1)-(3.3). We should note that the homoclinic orbits at $R = 7.3198$, which may be viewed as being 'caused' by the subcriticality of the Hopf bifurcations, are important to the appearance of the transient chaotic and chaotic motions of the model studied here. Indeed, the transient chaos occurring near the homoclinic bifurcation results from a Sil'nikov-type bifurcation [92], [95]. (The model also exhibits chaotic behavior in other, distant parameter ranges arising from period doubling cascades.) Before pursuing the design of feedback control laws for the system above, it is necessary to briefly summarize results on bifurcation control.

3.3 Bifurcation Control Laws

Consider a one-parameter family of nonlinear autonomous control systems

$$\dot{x} = f_\mu(x, u). \tag{3.10}$$

where $x \in \mathbb{R}^n$ is the state vector, $\mu \in \mathbb{R}$ is the system parameter, f_μ is a smooth map from $\mathbb{R}^n \times \mathbb{R}$ to $\mathbb{R}^n$ and u is a scalar input. Local bifurcation control deals with the design of smooth control laws $u = u(x)$ which stabilize a bifurcation occurring in the one-parameter family of systems (3.10). These control laws exist generically, even if the critical eigenvalues of the linearized system at the equilibrium of interest are uncontrollable. The direct state feedback control designs of [2] result in transforming a subcritical (unstable) Hopf bifurcation to a supercritical, and hence stable, bifurcation. This was extended to stabilization of Hopf bifurcations using dynamic feedback through washout filters in [59]. The washout filter-aided feedback control law developed in [58], [59] has many desirable features. The control law does not require an accurate knowledge of the system equilibria and it exactly preserves all system equilibria. Also the incorporation of washout filters in the feedback control facilitates the design of a control which does not depend on the bifurcation parameter. This is important to achieving a control which is effective over a range of parameter values.

3.3.1 Hopf Bifurcation Formulae

In this subsection, a stability criterion for Hopf bifurcation derived in [51], [2] is briefly reviewed. The criterion is based on the Taylor series expansion of the vector field and the eigenvector computations. No center manifold transformation or normal form transformation are necessary.

Consider a nonlinear autonomous system

$$\dot{x} = f_\mu(x), \tag{3.11}$$

where $x \in \mathbb{R}^n$ is the state vector, $\mu \in \mathbb{R}$ is the system parameter, $f : \mathbb{R}^n \to \mathbb{R}^n$ is sufficiently smooth in $x\mu$ and $f_\mu(x_{e,\mu}) = 0$, i.e., $x_{e,\mu}$ is an equilibrium point of (3.11) at system parameter μ. Suppose for $\mu = \mu_c$ the following hypothesis holds:

(H) The Jacobian matrix $D_x f_{\mu_c}(x_{e,\mu_c}, 0)$ has a simple pair of pure imaginary eigenvalues $\lambda_1(\mu_c) = j\omega_c$ and $\lambda_2(\mu_c) = -j\omega_c$ with $\omega_c \neq 0$, the transversality condition $\frac{\partial \mathrm{Re}[\lambda(\mu_c)]}{\partial \mu} \neq 0$ is satisfied, and all the remaining eigenvalues are in the open left half complex plane.

The Hopf Bifurcation Theorem [47], [65] asserts the existence of a one-parameter family $p_\epsilon, 0 < \epsilon \leq \epsilon_0$ of nonconstant periodic solutions of system (3.11) emerging from $x = x_{e,\mu_c}$ at the parameter value μ_c for ϵ_0 sufficiently small. The periodic solution $p_\epsilon(t)$ occurring at parameter values $\mu(\epsilon)$ have period near $2\pi{\omega_c}^{-1}$. Exactly one of the characteristic exponents of p_ϵ governs the asymptotic stability and is given by a real, smooth and even function

$$\beta(\epsilon) = \beta_2\epsilon^2 + \beta_4\epsilon^4 + \cdots. \tag{3.12}$$

That is, p_ϵ is orbitally asymptotically stable if $\beta(\epsilon) < 0$ but is unstable if $\beta(\epsilon) > 0$. Generically the local stability of the bifurcated periodic solutions p_ϵ is typically decided by the sign of the coefficient β_2. Note the sign of β_2 also determines the stability of the critical equilibrium point x_{e,μ_c}. Therefore, a feedback control law $u = u(x)$ which renders $\beta_2 < 0$ will stabilize both the Hopf bifurcation point and the bifurcated periodic solutions. An algorithm for computing the "stability coefficient" β_2 is given as follows [2].

Step 1. Express (3.11) in the series form

$$\begin{aligned}\dot{\hat{x}} &= A_0\hat{x} + Q_0(\hat{x},\hat{x}) + C_0(\hat{x},\hat{x},\hat{x}) + \cdots \\ &\quad +\hat{\mu}(A_1\hat{x} + Q_1(\hat{x},\hat{x}) + \cdots) + \hat{\mu}^2 A_2\hat{x} + \cdots, \end{aligned} \tag{3.13}$$

where $\hat{x} = x - x_{e,\mu_c}$, $\hat{\mu} = \mu - \mu_c$, $Q_i(\hat{x},\hat{x})$ and $C_i(\hat{x},\hat{x},\hat{x})$ are the second order (in $\hat{x}$) terms and third order (in $\hat{x}$) terms generated by a vector valued symmetric bilinear form $Q_i(x,y)$ and a vector valued symmetric trilinear form $C_i(x,y,z)$ respectly. With proper rearranging the order of state variables if necessary, let r be the right eigenvector of A_0 with respect to eigenvalue $j\omega_c$ with the first component of r equal to 1. Let l be the left eigenvector of A_0 corresponding to the eigenvalue $j\omega_c$, normalized such that $lr = 1$.

Step 2. Solve the equations

$$A_0 a = -\frac{1}{2}Q_0(r,\bar{r}), \tag{3.14}$$

$$(2j\omega_c I - A_0)b = \frac{1}{2}Q_0(r,r) \tag{3.15}$$

for a and b.

Step 3. The stability coefficient β_2 is given by

$$\beta_2 = 2\mathrm{Re}\{2lQ_0(r,a) + lQ_0(\bar{r},b) + \frac{3}{4}lC_0(r,r,\bar{r})\}. \tag{3.16}$$

3.3.2 Stabilization of Hopf Bifurcations

Consider control system (3.10). Equation (3.10) is the natural extension of Eq. (3.11) to allow an additional, smooth dependence on a scalar control input u. Assume that hypothesis (H) of Section 3.3.1 holds for $u = 0$ with μ_c a critical value of μ and x_{e,μ_c} the corresponding nominal equilibrium. Set $\mu = \mu_c$. Rewrite

(3.10) in the series form (here $\hat{x} := x - x_{e,\mu_c}$)

$$\dot{\hat{x}} = A_0\hat{x} + u\gamma + uA_1\hat{x} + Q_0(\hat{x},\hat{x}) \tag{3.17}$$

$$+u^2A_2\hat{x} + uQ_1(\hat{x},\hat{x}) + C_0(\hat{x},\hat{x},\hat{x}) + \cdots. \tag{3.18}$$

Assume a control of the form

$$u = \hat{x}^T Q_u \hat{x} + C_u(\hat{x},\hat{x},\hat{x}), \tag{3.19}$$

where Q_u is a real symmetric $n \times n$ matrix and C_u is a cubic form generated by a scalar-valued symmetric trilinear form. No quartic or higher order terms are included in the feedback since it is clear from the formula (3.16) that these terms do not affect β_2. Applying the algorithm in Section 3.3.1 to the closed-loop system, upon application of the control (3.19) we obtain the closed-loop stability coefficient

$$\beta_2^* = \beta_2 + 2\mathrm{Re}\Delta \tag{3.20}$$

where

$$\begin{aligned}\Delta &= 2l[r^TQ_ua^*\gamma - Q_0(r,\frac{1}{2}(r^TQ_u\bar{r})A_0^{-1}\gamma)] \\ &\quad +l[\bar{r}^TQ_ub^*\gamma + Q_0(\bar{r},\frac{1}{2}(r^TQ_ur)(2j\omega_cI - A_0)^{-1}\gamma)] \\ &\quad +\frac{3}{4}lC_u(r,r,\bar{r})\gamma + \frac{1}{4}l[2(r^TQ_u\bar{r})A_1r + (r^TQ_ur)A_1\bar{r}]\end{aligned} \tag{3.21}$$

and

$$a^* = -\frac{1}{2}A_0^{-1}Q_0(r,\bar{r}) - \frac{1}{2}(r^TQ_ur)A_0^{-1}\gamma \tag{3.22}$$

$$b^* = \frac{1}{2}(2j\omega_cI - A_0)^{-1}Q_0(r,r) + \frac{1}{2}(2j\omega_cI - A_0)^{-1}(r^TQ_ur)\gamma. \tag{3.23}$$

From Eq. (3.20), it is clear that stability of the Hopf bifurcation point and of the local bifurcated periodic solution p_ϵ can be achieved if $\mathrm{Re}\Delta$ can be assigned by feedback of the form (3.19). To further analyze the stabilizability, two cases are discussed separately.

Linearly controllable critical mode

From the well known Popov-Belevitch-Hautus(PBH) test [55], controllability of the critical mode is equivalent to the requirement $l\gamma \neq 0$. By setting $Q_u = 0$ in the control law (3.19), Eq. (3.21) reduces to

$$\Delta = \frac{3}{4} C_u(r, r, \bar{r}) l\gamma. \tag{3.24}$$

Since the coefficients of $C_u(x, y, z)$ can be arbitrarily assigned, the value of Δ can be assigned arbitrarily in the complex plane. Thus, we have the following result [2].

Theorem 3.1 *Suppose the system (3.10) satisfies hypothesis (H) and the critical mode is linearly controllable ($l\gamma \neq 0$). Then there exists a purely nonlinear (cubic) feedback $u(\hat{x})$ of the form (3.19) which stabilizes the equilibrium point at criticality and the periodic solution emerging from that equilibrium for parameter values μ near the critical parameter value μ_c.*

Linearly uncontrollable critical mode

In this case $l\gamma = 0$, and Eq. (3.21) becomes

$$\begin{aligned} \Delta &= -2lQ_0(4, \frac{1}{2}(r^T Q_u \bar{r}) A_0^{-1}\gamma) + lQ_0(\bar{r}, \frac{1}{2}(r^T Q_u r)(2j\omega_c I - A_0)^{-1}\gamma) \\ &\quad + \frac{1}{4} l[2(r^T Q_u \bar{r}) A_1 r + (r^T Q_u r) Q_1 \bar{r}]. \end{aligned} \tag{3.25}$$

Note that only the quadratic terms in the feedback influence Δ. Require the (real) matrix Q_u to be such that [2]

$$\text{Im } Q_u r = 0 \quad \text{and} \quad \text{Re } Q_u r \neq 0. \tag{3.26}$$

Letting $\rho = (\text{Re } r)^T Q_u (\text{Re } r)$, we have

$$\begin{aligned}\Delta &= \rho\{-2lQ_0(r, \frac{1}{2}A_0^{-1}\gamma) + lQ_0(\bar{r}, \frac{1}{2}(2j\omega_c I - A_0)^{-1}\gamma) \\ &\quad + \frac{1}{4}l[2A_1 r + A_1\bar{r}]\}. \end{aligned} \tag{3.27}$$

A sufficient condition for stabilizability is as follows [3].

Theorem 3.2 *Suppose the system (3.10) satisfies hypothesis (H) and the critical mode is linearly uncontrollable ($l\gamma = 0$). Then there is a quadratic feedback $u(\hat{x})$ with $u(0) = 0$ which stabilizes the Hopf bifurcation point (the critical equilibrium point) and the periodic solutions emerging from that bifurcation point for the parameter values μ near μ_c, provided that*

$$\begin{aligned}&\text{Re}\{-2lQ_0(r, \frac{1}{2}A_0^{-1}\gamma) + lQ_0(\bar{r}, \frac{1}{2}(j\omega_c I - A_0)^{-1}\gamma) \\ &+ \frac{1}{4}l[2A_1 r + A_1\bar{r}]\} \neq 0. \end{aligned} \tag{3.28}$$

There are several concerns about using direct state feedback control as in the foregoing development. Usually the argument of u is $\hat{x} = x - x_{e,\mu_c}$, but this limits the control to one parameter value μ_c since $f_\mu(x_{e,\mu}, u(x - x_{e,\mu_c}))$ does not necessarily vanish for $\mu \neq \mu_c$. Here $x_{e,\mu}$ is an equilibrium point of $f_\mu(x_{e,\mu}, 0)$. Another option is to take the argument of the control function to be $\hat{x}_\mu = x - x_{e,\mu}$. Clearly this requires knowledge of the whole branch of equilibria within the neighborhood of x_{e,μ_c} of interest, and, more severely, requires the control u to depend on the parameter μ. Even if $x_{e,\mu}$ can be determined accurately, if the system has multiple equilibrium branches, i.e., there is at least one equilibrium point $x'_{e,\mu} \neq x_{e,\mu}$, the control above still does not preserve other branches such as $x'_{e,\mu}$. These concerns motivate the employment of the outputs of washout filters as the arguments of the control u [58, 59].

3.3.3 Control of Hopf Bifurcations through Washout Filters

In Eq. (3.10), for each system state variable x_i, $i = 1, \ldots, n$, introduce a washout filter governed by the dynamic equation

$$\dot{z}_i = x_i - d_i z_i \tag{3.29}$$

along with the output equation

$$y_i = x_i - d_i z_i. \tag{3.30}$$

Here, the d_i are positive parameters (this corresponds to using stable washout filters). In this formulation, n washout filters, one for each system state, are present. In fact, the actual number of washout filters used, and hence also the resulting increase in system order, can usually be taken less than n.

The advantages of using washout filters in this way stem from the resulting properties of equilibrium preservation and automatic equilibrium (operating point) following. For instance, if $u = u(y)$ with $u(0) = 0$ where y is a washout filter output (3.30), clearly y vanishes at steady state. Hence the x components of a closed loop equilibrium are identical with the corresponding components of the open loop equilibrium. Also, since Eq. (3.30) can always be written as

$$y_i = x_i - d_i z_i = (x_i - x_{i_{e,\mu}}) - d_i(z_i - z_{i_{e,\mu}}), \tag{3.31}$$

the control function $u = u(y)$ is guaranteed to center at the correct operating point. Moreover it is shown in [59] that, at a Hopf bifurcation point, the extended system (3.10) and (3.29) has the same stability coefficient β_2 as that of the original system (3.10).

It is well known that only the quadratic and cubic terms occurring in a nonlinear system undergoing a Hopf bifurcation influence the value of β_2. Thus only the linear, quadratic and cubic terms in an applied control u have potential for influencing β_2. Now assume any linear feedback, which may be used to modify the critical parameter value μ_c, is already reflected in the nominal system (3.10) and (3.29). Then the feedback control u may be assumed to be of the form

$$u = y^T Q_u y + C_u(y, y, y), \tag{3.32}$$

where y is the vector of washout filter outputs $y_i = x_i - d_i z_i$, Q_u is a real symmetric $n \times n$ matrix and C_u is a cubic form generated by a scalar-valued symmetric trilinear form. Such a control law is independent of the equilibrium points, and, because of its nonlinearity, preserves the linear stability characteristics of the original system.

In the following, we only briefly summarize the results for the situation that the critical eigenvalues of the linearized system at the equilibrium of interest are controllable, which is the case for the convection loop dynamics to be considered in the next section. That is, $l\gamma \neq 0$. As in Section 3.3.2, it is shown in [59] that a cubic stabilization feedback exists. That is Q_u can be set to 0 in Eq. (3.32). For simplicity, let the washout filter parameters d_i all be given by a common value, say $d > 0$. The closed-loop stability coefficient β_2^* of the overall system (3.10), (3.29), (3.30) and (3.32) (with $Q_u = 0$) is given by [59]:

$$\beta_2^* = \beta_2 + 2\mathrm{Re}\Delta, \tag{3.33}$$

where β_2 is the stability coefficient of the original system (3.10) or the extended system (3.10), (3.29) and Δ is given by

$$\Delta = \frac{3}{4}\frac{\omega_c^3(\omega_c + jd)}{(d^2 + \omega_c^2)^2} C_u(r, r, \bar{r}) l\gamma. \tag{3.34}$$

where r, l, γ, d and ω_c are as above. From this we see the control can be any cubic function $C_u(y, y, y)$ resulting in $Re\Delta$ sufficiently negative to ensure $\beta_2^* < 0$. Such a control stabilizes the Hopf bifurcation point and the periodic solutions emerging from the Hopf bifurcation point for a range of parameter values.

3.4 Bifurcation Control of Routes to Chaos in Convection Dynamics

In this section, we employ the bifurcation control results above to determine control laws for suppressing both the transient chaotic and chaotic motion of the system (3.1)-(3.3). In the course of seeking control laws for suppression of chaos, we shall also employ feedback to achieve other, subsidiary goals. For instance, in the next subsection we consider use of feedback to delay to higher values of the Rayleigh number the occurrence of the Hopf bifurcations from the convective equilibria $C_\pm$. This addresses a question which arises rather naturally in the context of using feedback to modify the phase portrait of system (3.1)-(3.3) in useful ways. The control laws developed for achieving this delay in Hopf bifurcation parameter values have a feature which occurs throughout this chapter: they do not result in any change in the set of equilibria, even in the presence of model uncertainty. This is achieved using dynamic feedback incorporating washout filters, as proposed in [59], [58] and discussed in the foregoing section.

3.4.1 Delaying the Hopf Bifurcations

Recall that the convective equilibria $C_\pm$ lose their stability at two Hopf bifurcations occurring at $R = 16$. In this subsection, we give controllers which result

in changing this critical value of R to some prescribed value. In practice, the prescribed value would likely be greater than the nominal (open loop) value, so as to result in an increase in the range of parameter values for which the system exhibits stable steady motion.

Linearizing the model (3.1)-(3.3) at the upper equilibrium C_+ of Fig. 3.2, we find that, for $R = 16$, the Jacobian matrix has a pair of imaginary eigenvalues $\pm i\omega_c$ where $\omega_c = 4.47214$ (recall that $p = 4$). Next we present a feedback control scheme which allows one to modify the critical value of R at which the Hopf bifurcations occur, and to do so without modifying the equilibria of (3.1)-(3.3). The state variable x_3 is readily observable.

A *linear washout filter aided feedback* with measurement of x_3 is a dynamic feedback described as follows. The closed loop system is given by

$$\dot{x}_1 = -px_1 + px_2, \tag{3.35}$$

$$\dot{x}_2 = -x_1x_3 - x_2, \tag{3.36}$$

$$\dot{x}_3 = x_1x_2 - x_3 - R + u, \tag{3.37}$$

$$\dot{x}_4 = x_3 - dx_4, \tag{3.38}$$

where x_4 is the washout filter state, and where the control u is of the form

$$u = -k_l y, \tag{3.39}$$

with y an output variable, given by

$$y := x_3 - dx_4. \tag{3.40}$$

Here, k_l is a scalar (linear) feedback gain.

This control preserves the symmetry inherent in the model (3.1)-(3.3). Thus, in discussing the effects of the controller above, remarks specific to the upper equilibrium branch C_+ apply also to the lower branch C_-.

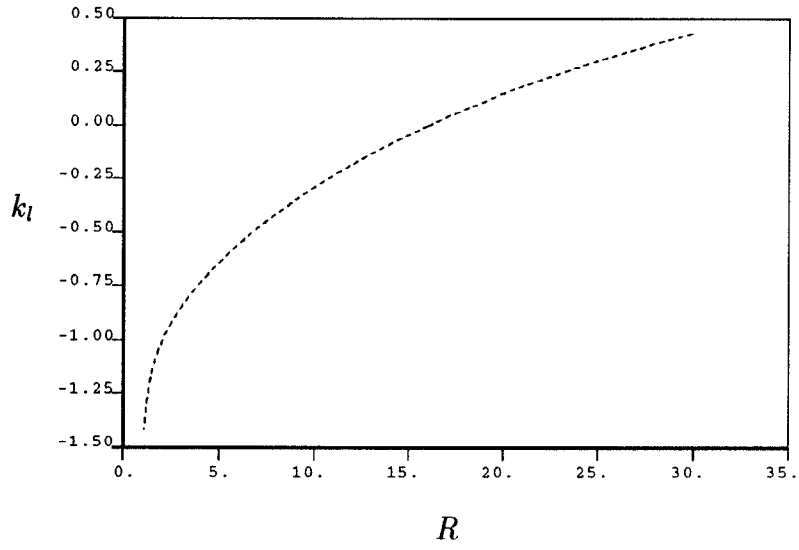

Figure 3.5: Two-parameter curve of Hopf bifurcation points for linear 'delaying' control

The control above is a dynamic feedback control. By adjusting the linear control gain k_l one can delay the Hopf bifurcations to occur at any desired parameter value. The relationship between the critical parameter value R and the control gain k_l can be determined by finding the conditions under which the Jacobian of the overall system (3.35) - (3.40) possesses a pair of pure imaginary eigenvalues. This relationship translates to the conditions

$$\begin{aligned}
&(Rd - 2p + 2Rp + dp)^2 \\
&+ (2 + d + k_l + p)^2(-2dp + 2Rdp) \\
&- (2 + d + k_l + p)(Rd - 2p + 2Rp \\
&+ dp)(R + 2d + k_l + p + dp + k_l p) = 0,
\end{aligned} \tag{3.41}$$

$$k_l + p + d + 2 > 0, \text{ and } R > 1 \tag{3.42}$$

In the case $p = 4.0$ and $d = 0.5$, these conditions are tantamount to the

restriction

$$-1.5 < k_l < 2 \tag{3.43}$$

on the gain k_l. To *delay* occurrence of the Hopf bifurcations, however, one must further restrict k_l to be positive. Indeed, negative values of k_l in the interval $-1.5 < k_l < 2$ result in moving the Hopf bifurcations to smaller values of R. Figure 3.5 shows the 2-parameter (k_l and R) curve of the Hopf bifurcation points, i.e., the relationship between k_l and critical parameter value R. Figures 3.6(a) and 3.6(b) depict the bifurcation diagrams for the closed loop system with (a) $k_l = 0.182538$ and (b) $k_l = -0.234191$, respectively. In Figure 3.6(a), the Hopf bifurcations are delayed to $R = 21$, while in Figure 3.6(b), the Hopf bifurcations are moved ahead to $R = 11$.

The foregoing discussion has resulted in linear, dynamic feedback control laws which can be tuned to result in moving the Hopf bifurcation points to any desired value of $R > 1$. These control laws also ensure asymptotic stability of the convective equilibria for all values of R up to the desired critical value. Despite this positive conclusion, the closed loop system incorporating the control laws given above still exhibits chaotic and transient chaotic behavior. This chaotic behavior is delayed to greater values of R if $0 < k_l < 2$, and moved ahead to lesser values if $-1.5 < k_l < 0$.

From the discussion above it is clear that linear feedback can stabilize the convective equilibria for arbitrary ranges of the parameter. Also as shown below, further increases in the control gain result in the annihilation of the Hopf bifurcations. These, however, do not imply that such a feedback can suppress chaos in the system. The transient chaos and chaos which occur due to the presence of homoclinic orbits in the open loop system can be suppressed by this type

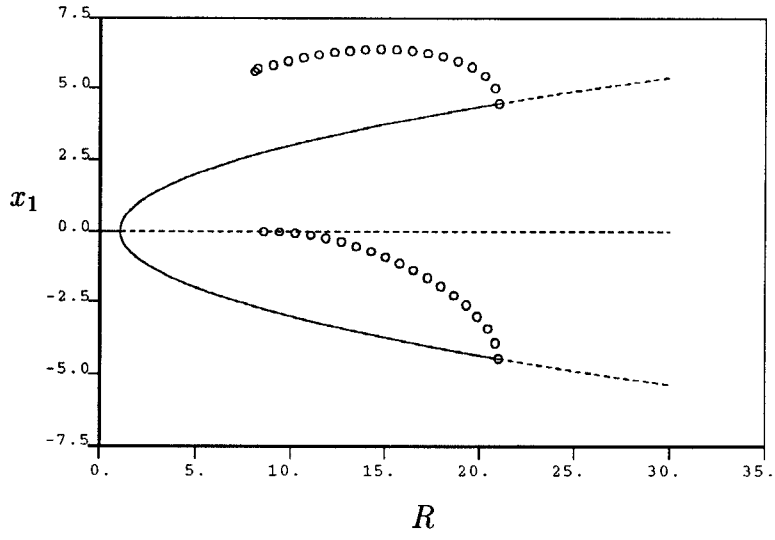

(a)

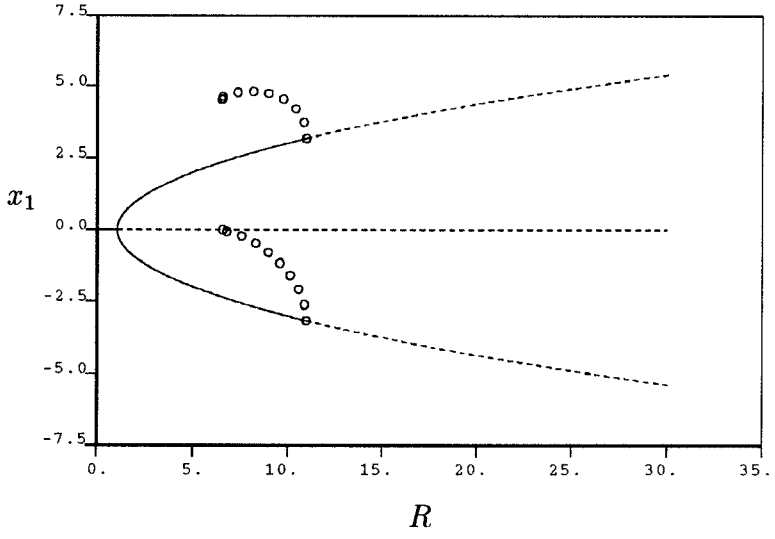

(b)

Figure 3.6: Bifurcation diagrams for linear 'delaying' control with (a) $k_l = 0.182538$ (b) $k_l = -0.234191$

of linear dynamic feedback with a higher feedback gain. Specifically, for gains $k_l > 2$ and for $p = 4, d = 0.5$, it can be shown that both the upper and lower convective equilibria are rendered asymptotically stable, and that the system no longer exhibits chaos or transient chaos that arise through the homoclinic orbits and loss of stability of the convective equilibria. However, the chaotic motion in the open loop system which results from period doubling cascades persists for the closed loop system with linear feedback. Moreover, for large values of R (e.g. $R > 275$), besides the two stable convective equilibria as attractors, there are large amplitude stable period orbits.

We proceed to investigate two alternatives to linear feedback of the type considered above. First, a nonlinear feedback control law can be designed to stabilize the Hopf bifurcations and introduce a small amplitude stable limit cycle which surrounds the equilibrium for parameter values at which it is unstable. Second, one can employ a combined linear-plus-nonlinear feedback to suppress chaos in the closed loop system. The linear part of the feedback is tuned to delay the Hopf bifurcations to a desired value of R, and the nonlinear part of the feedback is chosen to stabilize the Hopf bifurcations occurring in the closed loop system. The linear-plus-nonlinear feedback control alternative is the more versatile of these.

Before proceeding to issues of nonlinear control design, we remark that the control introduced in the foregoing does not affect the stability of the nominal equilibrium branch, $(0, 0, -R, -R/d)$. This is easy to prove by examining the associated characteristic polynomial

$$\begin{aligned} D_0(s) &= s^4 + (2 + d + k_l + p)s^3 + (1 + 2d + k_l + 2p + dp + k_l p - pR)s^2 \\ &\quad + (d + p + 2dp + k_l p - pR - dpR - k_l pR)s + dp - dpR. \end{aligned} \tag{3.44}$$

Clearly for $R \geq 1$, $D_0(s)$ is not a Hurwitz polynomial, i.e., $(0, 0, -R, -R/d)$ is unstable for $R \geq 1$. This is the same as in the open loop case.

3.4.2 Stabilizing the Hopf Bifurcations

Suppose a dynamic linear feedback has been introduced as in the foregoing subsection, resulting in positioning the Hopf bifurcations to a desired value of R. One result of such a control is to affect the bifurcated periodic solutions which emerge at the two Hopf bifurcations. Recall that these bifurcations are subcritical for the open loop system (see Fig. 3.2). The subcriticality of the Hopf bifurcations is crucial to the appearance of transient chaos and chaos in the model for various values of R. Thus the question arises as to whether or not the feedback controller of the previous subsection can be modified to result in stabilization of the Hopf bifurcations. Next, we summarize some positive results in this direction.

From formulae (3.33) and (3.34) it can be seen that any cubic function $C_u(y, y, y)$ such that $Re\triangle$ is sufficiently negative to ensure $\beta_2^* < 0$ will serve to stabilize the Hopf bifurcations. In other words, there is a family of stabilizing, purely cubic nonlinear controllers. We now choose the simplest such stabilizing control law. The closed loop system again takes the form (3.35)-(3.40), except that now the controller is

$$u = -k_n y^3. \tag{3.45}$$

Here, k_n is the nonlinear feedback gain.

Again this control preserves the symmetry inherent in the model (3.1)-(3.3). Thus, in discussing the effects of the controller above, remarks specific to the Hopf bifurcation associated with the upper equilibrium branch C_+ apply also to

that of the lower branch C_-.

To illustrate the utility of such a nonlinear control law, we state a simple result obtained using formulae (3.33) and (3.34) for β_2^* in the case $p = 4.0$ and $d = 0.5$:

$$\beta_2^* = \beta_2 - 2.42505 k_n. \tag{3.46}$$

The open loop quantity β_2 can be computed using either a known algorithm (e.g., [2]) or the software package BIFOR2 [47]. Using BIFOR2 we obtain $\beta_2 = 0.02027 \pm 0.001087$. Thus, any choice of control law (3.45) with $k_n > 0.009$ stabilizes the Hopf bifurcations occurring at $R = 16$. This is a local result. To assess the degree to which this is reflected in the global dynamics of the system, one resorts to extensive computation. Figure 3.7 shows the bifurcation diagram for the closed loop system with $k_n = 0.009$. Solid circles indicate stable limit cycles. The maximum amplitude of a stable limit cycle is given by a solid circle. The periodic orbits emerging from the Hopf bifurcation points themselves undergo further bifurcations. In the closed loop system, the stable periodic orbits emerging from the Hopf bifurcation points lose stability through cyclic fold bifurcations (CFB) [97]. The resulting unstable periodic orbits regain their stability at the secondary Hopf bifurcations (or Hopf bifurcations involving periodic orbits). In the interval between the cyclic fold and secondary Hopf bifurcations, the Ruelle-Takens route to chaos from the secondary Hopf bifurcations takes place. Simulations suggest that for $k_n = 0.009$, this interval in parameter space is the only range of parameter values where chaos is present. Simulations along with application of the bifurcation analysis tool AUTO [35] indicate that slightly larger values of the gain k_n result not only in annihilation of the Ruelle-Takens route to chaos, but also in a reduced amplitude of the stable limit cycles. This

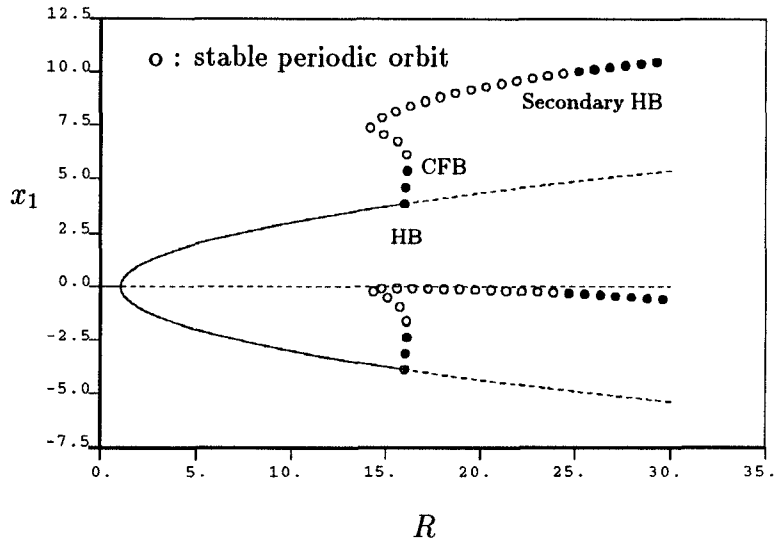

Figure 3.7: Bifurcation diagram for nonlinear 'stabilizing' control with $k_n = 0.009$

is illustrated in Figure 3.8, which shows superimposed bifurcation diagrams for the closed loop system with various control gains k_n. Figure 3.9 shows a typical system trajectory for the closed-loop system with $k_n = 2.5$ at $R = 19$.

With this type of control, transient chaos is successfully suppressed, and the previous chaotic trajectories are replaced by small amplitude stable limit cycles near the convective equilibria. Moreover, extensive simulations demonstrate that the periodic orbit windows cease to exist, as does the chaos arising from the period doubling bifurcations associated with these windows.

We conclude this subsection with a few comments on the Ruelle-Takens route to chaos and our proposed control. By taking the control gain k_n near 0.009, we in fact transfer the chaos scenario associated with the original system to a new one, namely, the Ruelle-Takens route to chaos. More significantly, slight increases in k_n result in annihilation of this route to chaos. Thus, the proposed

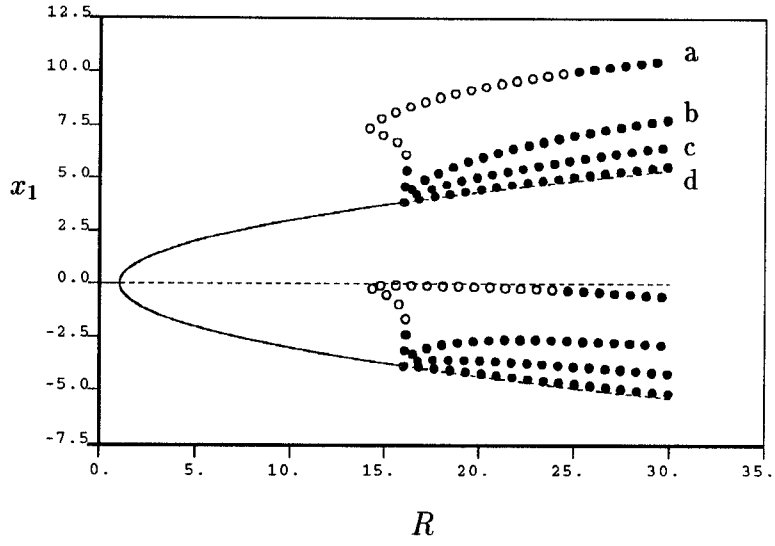

Figure 3.8: Superimposed bifurcation diagrams for nonlinear 'stabilizing' control with different control gains k_n: a. 0.009, b. 0.025, c. 0.1, d. 2.5

control may also be a candidate for the control of the Ruelle-Takens route to chaos in systems with dimension greater than three. The effect of transferring between different chaos scenarios is also an interesting subject.

3.4.3 Delaying and Stabilizing the Hopf Bifurcations

As shown in the previous subsections, a linear feedback control can be used to delay the Hopf bifurcations and a nonlinear one can be employed to stabilize the Hopf bifurcations. The linear feedback control is only effective to a limited extent in suppressing chaos. The nonlinear control, on the other hand, is very effective in suppressing chaos without affecting the linear stability of the original system. However, the linear feedback does increase the stability margin of the steady convective equilibria. Thus a natural extension to the control laws above is a combined linear-plus-nonlinear feedback control. The linear part of the

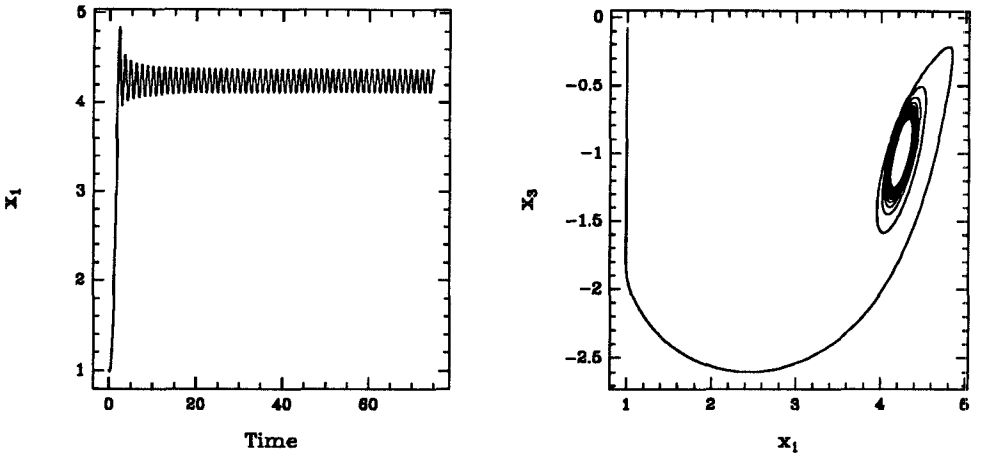

(a) (b)

Figure 3.9: A trajectory of closed loop system under nonlinear 'stabilizing' control with $k_n = 2.5$ for $R = 19$

feedback is chosen to delay the Hopf bifurcations to a desired value of R, and the nonlinear part of the feedback is chosen to stabilize the Hopf bifurcations occurring in the closed loop system. Again choosing the simplest such control laws, the closed loop system takes the form (3.35)-(3.40), except that now the controller is

$$u = -k_l y - k_n y^3. \tag{3.47}$$

The control can be designed in two stages. In the first stage, adjustment of k_l is used to delay the parameter value at which the Hopf bifurcations occur to an acceptable value. In the second stage, k_n is adjusted to stabilize the Hopf bifurcation points and the bifurcated periodic solutions resulting from the Hopf bifurcations. Figure 3.10 shows a bifurcation diagram of the closed loop system with one such linear-plus-nonlinear feedback control. Note that the control law (3.47) effects both a delay in the occurrence of the Hopf bifurcations, and

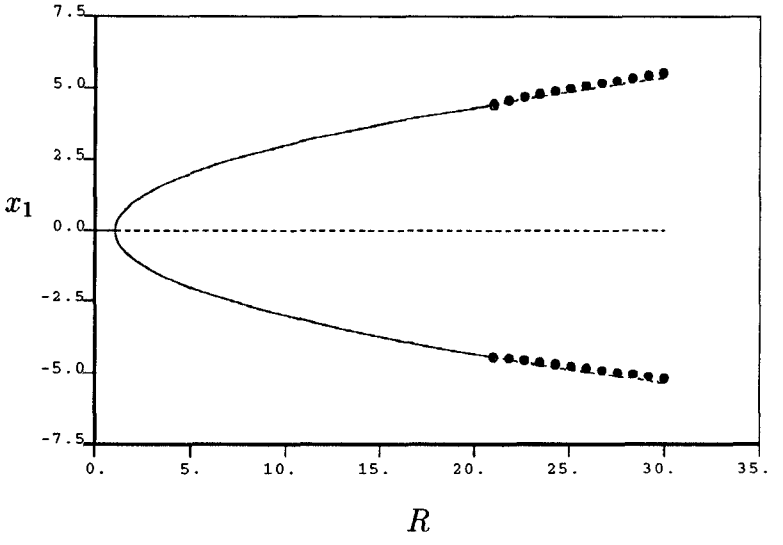

Figure 3.10: Bifurcation diagram for linear-plus-nonlinear control with $k_l = 0.182538$ and $k_n = 2.5$

stabilization of these bifurcations.

With this type of control, both transient chaos and chaos are successfully suppressed. The linear component in the control allows one to have control of the stability margin of the steady convective equilibria. The nonlinear term in the control not only stabilizes the Hopf bifurcations but also removes the periodic orbits windows. Thus one expects a significantly improved transient response of the system than that achieved using linear feedback alone.

So far all the proposed control approaches preserve the "symmetry" of the system because of the way the control is introduced. Only the asymmetric component x_3 of the states is used in constructing washout filters and controllers. This results in identical control action for the upper and lower equilibrium branches. The two Hopf bifurcations (upper branch and lower branch respectively) are relocated and/or stabilized in unison and the resulting stable

convective equilibria and/or the stable limit cycles coexist, each with its respective basin.

Surely these approaches are very effective to relocate or suppress chaos, but for a given initial condition it is not very clear beforehand to which convective equilibrium or limit cycle the trajectory converges. It may be desirable not only to suppress chaos but also to be able to direct a trajectory to the neighborhood of a specified equilibrium. This motivates the design of another class of controllers, which imparts preference for one equilibrium over another. This is the subject of the next subsection.

3.4.4 Targeting Control

We now carry out the design of control laws to "target" a particular equilibrium of the system. That is, other equilibria or periodic orbits surrounding them are rendered unstable, while the target equilibrium, or a periodic orbit surrounding it, is stabilized. This is achieved by using the readily observable symmetric component x_2 of the state vector in constructing the controllers. A linear feedback is employed to increase the stability margin of one convective equilibrium and at the same time to decrease that of another convective equilibrium. A pure nonlinear feedback, on the other hand, is designed to stabilize the Hopf bifurcation of one equilibrium branch, leaving the linear stability of the original system and the stability of the other Hopf bifurcation unchanged. As in the case of the symmetry preserving control laws in the previous subsections, one can employ a combined linear-plus-nonlinear feedback approach to achieve other more flexible types of stability.

Targeting an Equilibrium Recall that the convective equilibria $C_{\pm}$ lose their

stability at Hopf bifurcations occurring at $R = 16$. In Section 3.4.1, a linear feedback control is employed to modify the critical value of R at which *both* the Hopf bifurcations occur. Here, we give controllers which result in changing the critical value of R to two different values for the C_+ branch and the C_- branch respectively. In other words, while the critical value of R at which the Hopf bifurcation associated with the C_+ (C_-) branch occurs is modified to a larger value of R, the critical value of R associated with the C_- (C_+) branch is modified to a lesser value of R. In doing so, the stability margin of one equilibrium is increased while that of the other is decreased. Hence, one equilibrium is preferred to the other ("targeted").

A linear washout filter aided feedback with measurement of x_2 is a dynamic feedback. The state variable x_2 is readily measurable. The closed loop system is given by

$$\dot{x}_1 = -px_1 + px_2, \tag{3.48}$$

$$\dot{x}_2 = -x_1x_3 - x_2, \tag{3.49}$$

$$\dot{x}_3 = x_1x_2 - x_3 - R + u, \tag{3.50}$$

$$\dot{x}_4 = x_2 - dx_4, \tag{3.51}$$

where the x_4 is the washout filter state, and where the control u takes the form

$$u = k_l y, \tag{3.52}$$

with y an output variable, given by

$$y := x_2 - dx_4. \tag{3.53}$$

Here, k_l is a scalar (linear) feedback gain.

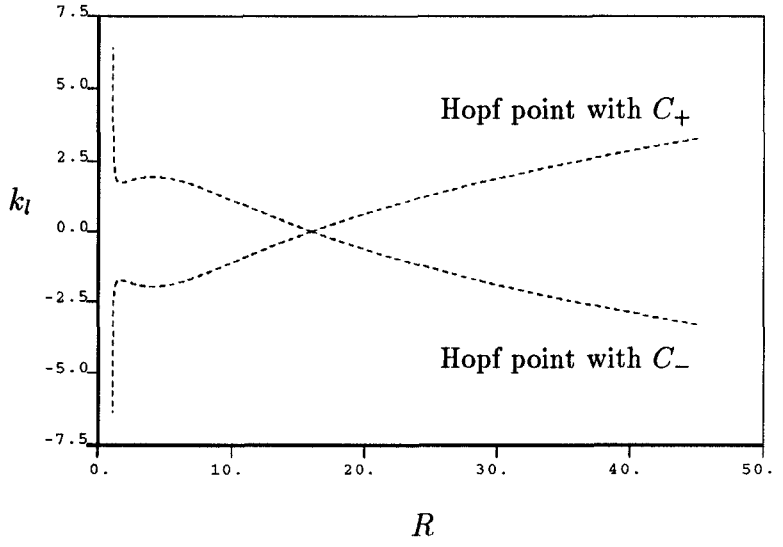

Figure 3.11: Two-parameter curves of Hopf bifurcation points for linear 'targeting' control

The control does not preserve the symmetry inherent in the model (3.1)-(3.3), though it does preserve the (symmetric) equilibrium structure of (3.1)-(3.3). However, the closed loop system (3.48)-(3.53) possesses symmetry involving the control gain k_l. That is, replacing (x_1, x_2, x_3, x_4) and k_l with $(-x_1, -x_2, x_3, -x_4)$ and $-k_l$, respectively, results in the same set of equations. Thus, the sign of k_l alone determines which equilibrium is stabilized. The effect of positive k_l on the system is opposite to that of negative of k_l. This can also be seen from the characteristic polynomials evaluated at C_+ and C_-. For positive (negative) k_l the stability margin of C_+ (C_-) is increased in the parameter space and that of C_- (C_+) is decreased.

Figure 3.11 illustrates the 2-parameter (k_l and R) curves of the Hopf bifurcation points, i.e., the relationship between k_l and the critical values of R at which the Hopf bifurcations occur. Figure 3.12 shows a bifurcation diagram of

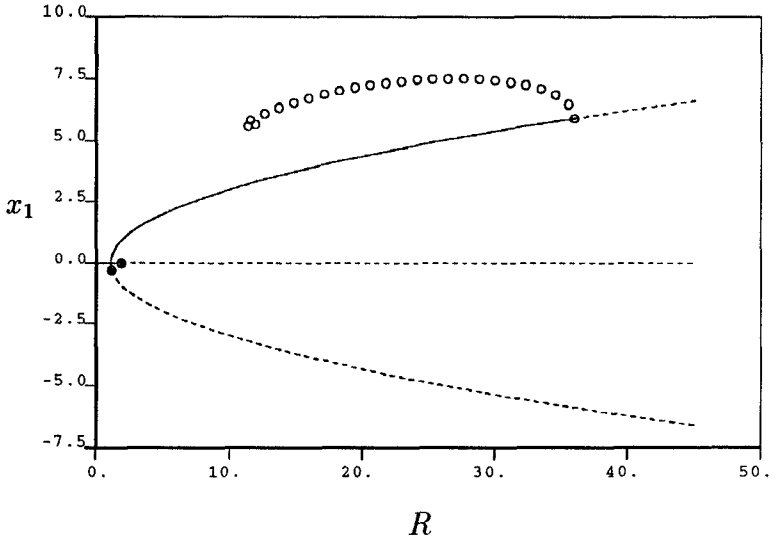

Figure 3.12: Bifurcation diagram for linear 'targeting' control with $k_l = 2.5$

the closed loop system for $k_l = 2.5$. It can be seen that C_+ is rendered stable up to $R = 36.0043$, and C_- is unstable for $R > 1.08538$. In the interval $1.08538 < R < 36.0043$, C_+ is stable and C_- is unstable. Hence typical system trajectories converge to C_+. Also note that the Hopf bifurcation at $R = 36.0043$ is still subcritical, while the Hopf bifurcation at $R = 1.08538$ is rendered supercritical. Switching the sign of k_l, say, $k_l = -2.5$, the situation is reversed: C_- is rendered stable in the same interval. So by reversing the sign of k_l one can switch the asymptotic behavior of the system from one equilibrium to another.

The relationship between k_l and the critical values of R at which the Hopf bifurcations occur is quantified by the conditions

$$\begin{aligned}
&(-2p + dp + k_l p\sqrt{R-1} + dR + 2pR)^2 + (2dpR - 2dp)(2 + d + p)^2 \\
&-(2d + p + dp + k_l\sqrt{R-1} + R)(-2p + dp \\
&+ k_l p\sqrt{R-1} + dR + 2pR)(2 + d + p) = 0,
\end{aligned} \tag{3.54}$$

$$-2p + dp + k_l p\sqrt{R-1} + dR + 2pR > 0, \quad \text{and} \quad R > 1. \tag{3.55}$$

Simulation evidence suggests that for some choices of k_l there are further bifurcations involving periodic orbits even for moderate values of R. (Recall that the open loop system as well as the closed loop with a linear feedback delaying Hopf bifurcations also experience bifurcations involving periodic orbits for some larger values of R.) However, simulations also suggest that for $|k_l| \leq 2.5$, such bifurcations are unlikely to occur. This in turn limits the ability of the proposed control to modify the critical values of R, therefore the ability to affect the stability margin of $C_{\pm}$. One way to accommodate this limitation is to apply a control strategy that combines the Hopf bifurcation delaying control and the targeting control discussed here. The presence of these 'unwelcome' bifurcations of periodic orbits signals the need for caution in applying linear control. Moreover, the closed loop system incorporating the control laws given above still exhibits chaotic and transient chaotic behavior. This chaotic (and transient chaotic) behavior is delayed to greater values of R. Also the chaotic (and transient chaotic) trajectories tend to spend more time around the preferred equilibrium. Next, we present a nonlinear feedback control which not only suppresses chaos but also targets a periodic orbit in the vicinity of a given equilibrium.

Before proceeding to issues of nonlinear control design, we again remark that the control introduced in the foregoing does not affect the stability of the nominal equilibrium branch, i.e., the $(0, 0, -R, 0)$ branch. This is easy to verify by examing the associated characteristic polynomial.

Targeting the Vicinity of an Equilibrium In Section 3.4.2 a nonlinear dynamic feedback is designed to stabilize the Hopf bifurcations and the resulting closed loop system shows no chaotic behavior. In the previously chaotic region,

two stable small amplitude periodic orbits coexist. Here we employ a similar type of nonlinear feedback but with the goal of introducing only one of these two periodic orbits. That is, one periodic orbit is rendered unstable, while a stable periodic orbit is introduced near the targeted equilibrium. This is achieved by stabilizing the Hopf bifurcation of one equilibrium branch, while not affecting the linear stability of the original system and the stability of the other Hopf bifurcation.

Using the bifurcation control techniques of Section 3.3, one can again show that there is a family of stabilizing, purely cubic nonlinear controllers. With the simplest such control law, the closed loop system again takes the form (3.48)-(3.53), except that now the controller is

$$u = k_n y^3. \tag{3.56}$$

Here, as before, k_n denotes a scalar (nonlinear) feedback gain.

Applying the Hopf bifurcation formulae (3.33) and (3.34) to the Hopf bifurcation associated with C_+ at $R = 16$, we find

$$\beta_2^* = \beta_2 - 0.35291 k_n. \tag{3.57}$$

For the Hopf bifurcation associated with C_-, we have

$$\beta_2^* = \beta_2 + 0.35291 k_n. \tag{3.58}$$

Recall that $\beta_2 = 0.02027 \pm 0.001087$.

Again one can see that the sign of k_n can be used for switching between the equilibria (actually, between periodic orbits in their vicinity). Also for $k_n > 0.06233$, the control $u = k_n y^3$ is a stabilizing control for the Hopf bifurcation associated with C_+. For $k_n < -0.06233$ the control u stabilizes the Hopf

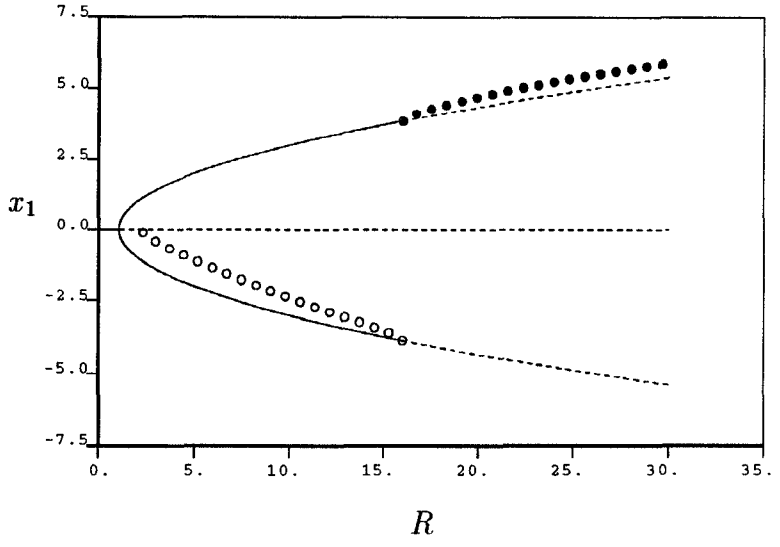

Figure 3.13: Bifurcation diagram for nonlinear 'targeting' control with $k_n = 2.5$

bifurcation associated with C_-. By changing the sign of k_n one can switch the asymptotic behavior of the system from one periodic orbit to another. These are local results. Bifurcation analysis and simulation evidence indicate that larger values of $|k_n|$ increase the stability margin in parameter space and also ensure a smaller amplitude of the periodic orbits. Figure 3.13 shows a bifurcation diagram of the closed loop system with $k_n = 2.5$. Note that the Hopf bifurcation point as well as the bifurcated periodic solutions associated with C_+ are stabilized while those associated with C_- are rendered unstable.

From a stability point of view, this approach results in the system preferring one periodic orbit to another. However, simulations show that though chaos is no longer present, the domain of attraction of the preferred (targeted) periodic orbit is not the whole space. Although one might hope that generally trajectories of the closed loop system converge to the preferred period orbit (the only attractor), simulations indicate that some trajectories diverge to infinity. The stable

manifold of the nominal saddle equilibrium separates the domains of attraction for the target periodic orbit and infinity. In the closed loop system, even the stable convective equilibrium for which the associated Hopf bifurcation is still subcritical has its domain of attraction significantly reduced as compared with the case for the open loop system. These undesirable effects can, fortunately, be circumvented by the scheme described next. This scheme is basically the same as that used in [77], except that in [77] linearization and pole placement are employed.

Define a neighborhood $D(C_{\pm}, \epsilon)$ around C_+ or C_-. The neighborhood D can be of any shape, e.g., a ball. Denote ϵ the minimum distance from the points on the boundary of D to $C_{\pm}$. The size of D can be changed by adjusting ϵ. Now suppose the target periodic orbit is near C_+, i.e., the objective is such that for almost all initial conditions in the basin of the chaotic attractor, the dynamics of the system converges to the desired periodic orbit surrounding C_+. Continue to use the nonlinear control function (3.56). However, activate the control only if a trajectory from any given initial condition reaches D. Usually the trajectory is locked onto the desired attractor. In case the trajectory does wonder away from D, then deactivate the control and wait for the trajectory to enter D again. The ergodic nature of the chaotic dynamics ensures that the state trajectory eventually enters into this neighborhood. A typical trajectory experiences a chaotic transient. This may prove to be undesirable in some cases. Again, by switching the control, i.e., the sign of k_n we can switch the system dynamics from one periodic orbit to another.

Let us conclude this section with some remarks on the relationship among the various controllers presented. First, note that linear feedback and nonlinear

feedback are presented separately in this subsection. However, they may be combined to yield a controller of the form $u = k_l y + k_n y^3$ which introduces further freedom in the achievable dynamical structure of the system and its limit sets. Moreover, one can also combine the targeting control results of the current subsection with control laws for delaying bifurcations and those for stabilizing bifurcations presented in previous subsections. In general, these control laws illustrate how the bifurcation control approach may be employed to yield various stability goals related to the bifurcations displayed by a given system, without modifying its equilibrium structure.

3.5 Concluding Remarks

Using bifurcation control ideas, control laws have been systematically designed for the suppression of both transient chaotic and chaotic motion in a thermal convection system model. The control laws exactly preserve all the equilibrium branches of the system, and can be designed to simultaneously stabilize *both* convective equilibrium branches. This stabilization can take one of two forms. One can literally stabilize the equilibria using linear dynamic feedback. But the closed loop system can still exhibit transient chaotic and chaotic motion for some value (larger) of the Rayleigh number R due to bifurcations of periodic orbits. Alternatively, it is possible to re-locate the Hopf bifurcations to occur at higher values of the Rayleigh number R, and then employ nonlinear control to ensure stability of these bifurcations. In this way, a small amplitude stable limit cycle is introduced which surrounds the equilibrium for parameter values at which it is unstable. Simulations show that this control scheme is effective

in suppressing chaos for any parameter range. For some parameter ranges the choice between linear feedback and linear-plus-nonlinear feedback depends on several factors, including degree of confidence in the model and available net gain. However, both types of feedback are related in their structure, especially in their incorporation of washout filters and preservation of model symmetry. Other controllers are also designed so that in addition to the goal of taming chaos, one can "target" a particular equilibrium or its vicinity. That is, other equilibria or periodic orbits are rendered unstable, while the target equilibrium or periodic orbit is stabilized. By changing the signs of the controllers, one can switch the asymptotic behavior of the system from one equilibrium or periodic orbit to another.

Although this chapter has focused on a particular model with a particular set of bifurcations, the approach itself may be viewed in the following general terms. Design of feedback control laws directed at primary bifurcations in a succession of bifurcations leading to chaos is a viable technique for the taming of chaos. Chaos can be suppressed, relocated in parameter and state space, and its type may be changed. Moreover, this can be achieved in a robust fashion, maintaining the positions of system equilibria even in the presence of model uncertainty. The resulting controllers do not depend on the bifurcation parameter and are effective over a range of parameter values.

Chapter 4

Stabilization of Period Doubling Bifurcations and Implications for Control of Chaos

The stabilization of period doubling bifurcations for discrete-time nonlinear systems is investigated. Both static and dynamic feedback controllers are studied. It is shown that generically such bifurcations can be stabilized using smooth feedback, even if the linearized system is uncontrollable at criticality. In the course of the analysis, expressions are derived for bifurcation stability coefficients of general n-dimensional systems undergoing period doubling bifurcation. A connection is determined between control of the amplitude of a period doubled orbit and the elimination of a period doubling cascade to chaos. For illustration, the results are applied to the Hénon system.

4.1 Introduction

There are many examples of dynamical system models which undergo a cascade of period doubling bifurcations, resulting in chaotic motion [97], [46]. The scenario involves a dynamical system depending on a real parameter μ. For a range of values of this parameter, the system possesses a periodic orbit. For a certain, critical value of μ, the periodic orbit undergoes a period doubling bifurcation. This means that another periodic orbit, initially of exactly twice the period of the given orbit, emerges from the original orbit. The bifurcated orbit then undergoes another period doubling bifurcation. This sequence of period doublings continues in a cascade, resulting in a chaotic invariant set. This chaotic invariant set is often also a strange attractor, i.e., it is asymptotically stable, in which case the system can be expected to display chaotic motion.

The purpose of this chapter is to give a technique for the design of feedback control laws which allow one to control the degree of stability, and the amplitude, of a given period doubled orbit. We prove that if this degree of stability can be made sufficiently large, then the cascade of period doublings to chaos is eliminated. We employ notation analogous to our previous work on local stabilization of bifurcations from equilibria of differential systems [2], [3]. We also consider the possibility of robustly stabilizing period doubling bifurcations and the associated route to chaos, in a sense analogous to that of Chapter 3. That is, the control is designed using a dynamic state feedback which ensures that low frequency orbits of the system are retained in the closed loop system, with only the transient dynamics and higher frequency orbits modified. In Chapter 3, this is accomplished using washout filters in the feedback. Here, a similar technique is found to be useful.

To facilitate the design of stabilizing feedback for period doubling bifurcations, we seek general yet simple formulae for determining the stability characteristics of period doubling bifurcations. Previous results have been obtained using center manifold reduction and coordinate transformations. For example, the paper [80] uses such methods in the calculation of stability characteristics of period doubling bifurcations. This approach results in calculations which are not readily useful as a basis for stabilizing control design. The general bifurcation calculations presented in this chapter form the basis for our control design results. The results are then applied to the period doubling route to chaos in the Hénon system. The control law used in that example preserves all system equilibria even in the face of model uncertainty.

4.2 Bifurcation Formulae for Period Doubling

Consider a discrete-time nonlinear system

$$x_{k+1} = f_\mu(x_k) \tag{4.1}$$

where $x_k \in \mathbb{R}^n$ for each integer k, and $\mu \in \mathbb{R}$ is the bifurcation parameter. Suppose that the origin is an equilibrium point of (4.1) for $\mu = 0$, i.e., $f_0(0) = 0$. Since μ is a real parameter, there are three generic bifurcations for (4.1). These are the the fold bifurcation, the period doubling bifurcation, and the Neimark-Sacker-Moser bifurcation.

In this work, we focus on the period doubling bifurcation. In designing stabilizing control laws for the period doubling bifurcation, it is useful to have a framework for the analysis of these bifurcations and, specifically, their stability. We pursue such a framework next. The approach used below and the formulae we

obtain do not involve transformations of variable or center manifold reduction, and are applicable directly to system (4.1). This approach is an instance of the Projection Method [53].

Expanding the map of (4.1) in a Taylor series, we have

$$f_\mu(x) = A(\mu)x + Q(x,x) + C(x,x,x) + \cdots \tag{4.2}$$

To determine conditions for a period doubling bifurcation, consider without loss of generality the case in which (4.1) possesses a period-1 orbit (fixed point) at the origin for $\mu = 0$. We seek conditions under which a period-2 orbit bifurcates from $x = 0$ at $\mu = 0$.

The hypotheses associated with the occurrence of a period doubling bifurcation for Eq. (4.1) from the period-1 orbit 0 are as follows. Let an eigenvalue $\lambda_1(\mu)$ of the linearization of (4.1) be such that:

$$\lambda_1(0) = -1,$$

$$\text{and} \quad |\lambda_i(0)| < 1 \quad \text{for} \quad i = 2, \ldots, n.$$

Let $\ell :=$ the left eigenvector of A associated with the eigenvalue -1, and $r :=$ the right eigenvector of A associated with the eigenvalue -1.

Period doubling bifurcation from the period-1 orbit 0 can now be analyzed. First, repeating (4.1), we have

$$x_{k+1} = A(\mu)x_k + Q(x_k, x_k) + C(x_k, x_k, x_k) + \ldots \tag{4.3}$$

Next, applying the recursion above to x_{k+1}, we have

$$\begin{aligned} x_{k+2} \;=\; & A^2(\mu)x_k + A(\mu)Q(x_k,x_k) + A(\mu)C(x_k,x_k,x_k) + \ldots \\ & + Q(A(\mu)x_k + Q(x_k,x_k) + \ldots,\; A(\mu)x_k + Q(x_k,x_k) + \ldots) \\ & + C(A(\mu)x_k + Q(x_k,x_k) + \ldots,\; \ldots,\; \ldots) + \ldots \end{aligned}$$

A period-2 orbit x, if one exists, must satisfy

$$\begin{aligned} 0 &= (A^2(\mu) - I)x + A(\mu)Q(x,x) + A(\mu)C(x,x,x) + \dots \\ &\quad + Q(A(\mu)x + Q(x,x) + \dots,\ A(\mu)x + Q(x,x) + \dots) \\ &\quad + C(A(\mu)x + Q(x,x) + \dots,\ \dots,\ \dots) + \dots \\ &=: \tilde{A}(\mu)x + \tilde{Q}(x,x) + \tilde{C}(x,x,x) + \dots \end{aligned}$$

where

$$\begin{aligned} \tilde{A}(\mu) &:= A^2(\mu) - I \\ \tilde{Q}(x,x) &:= A(0)Q(x,x) + Q(A(0)x, A(0)x) \\ \tilde{C}(x,x,x) &:= A(0)C(x,x,x) + 2Q(A(0)x,\ Q(x,x)) + C(A(0)x, A(0)x, A(0)x) \end{aligned}$$

Since

$$A(0)r = -r, \quad \ell A(0) = -\ell$$

we have

$$A^2(0)r = r, \quad \ell A^2(0) = \ell$$

$$\Rightarrow (A^2(0) - I)r = 0, \quad \ell(A^2(0) - I) = 0$$

Thus, $\tilde{A}(0)$ possesses a zero eigenvalue, which is seen also to be simple, by the Spectral Mapping Theorem. Also by this theorem we find that $\frac{d}{d\mu}\lambda_1(\tilde{A}(\mu))|_{\mu=0}$ is nonzero if $\frac{d}{d\mu}\lambda_1(A(\mu))|_{\mu=0} \neq 0$. This latter condition is therefore taken as a further condition for period doubling bifurcation, and, together with the previous conditions, the foregoing is a sketch of a proof for a theorem on period doubling bifurcation.

We have shown, by reducing the problem to one of standard stationary bifurcation analysis, that the system (4.1) possesses a nontrivial period doubled orbit $x(\epsilon)$ emanating from $x = 0$ for $\mu = \mu(\epsilon)$ near 0.

To determine the stability of the period doubled orbit, we obtain formulae for bifurcation stability coefficients. These are simply coefficients in the Taylor expansions in an amplitude parameter ϵ of the critical eigenvalue of the period doubled orbit. Let this eigenvalue be given by

$$\beta(\epsilon) = \beta_1\epsilon + \beta_2\epsilon^2 + \cdots \tag{4.4}$$

Then, using formulae obtained in [3] for stationary bifurcation stability coefficients, we find:

$$\begin{aligned}
\beta_1 &= \ell\tilde{Q}(r,r) \\
&= \ell[A(0)Q(r,r) + Q(A(0)r, A(0)r)] \\
&= -\ell Q(r,r) + \ell Q(-r,-r) \\
&= -\ell Q(r,r) + \ell Q(r,r) \\
&= 0.
\end{aligned}$$

Thus, $\beta_1 = 0$. As for β_2, we have:

$$\beta_2 = 2\ell[\tilde{C}(r,r,r) - 2\tilde{Q}(r, \tilde{A}^-\tilde{Q}(r,r))] \tag{4.5}$$

Here

$$\tilde{A}^- := (\tilde{A}^T\tilde{A} + \ell^T\ell)^{-1}\tilde{A}^T$$

This analysis shows that $\beta_1 = 0$ and that, *generically* $\beta_2 \neq 0$. Hence, we have that if $\lambda_1(0) = -1$, $\lambda_1'(0) \neq 0$, $\beta_2 \neq 0$, then there is a pitchfork bifurcation for the sped-up system, giving two period-2 orbits occurring either supercritically or subcritically. For the original system, this means there is a *single* period doubled orbit occurring either supercritically or subcritically. Whether the period

doubled orbit is supercritical or subcritical is determined by the sign of β_2. The period doubled orbit is supercritical if $\beta_2 < 0$ but is subcritical if $\beta_2 > 0$. The next hypothesis is invoked in the theorem below.

(P) The map f of Eq. (4.1) is sufficiently smooth and has a fixed point at $x = 0$ for all μ. The linearization of (4.1) possess an eigenvalue $\lambda_1(\mu)$ with $\lambda_1(0) = -1$ and $\lambda_1'(0) \neq 0$. All remaining eigenvalues have magnitude less than unity.

Theorem 4.1 *(Period Doubling Bifurcation Theorem) If (P) holds, then a period doubled orbit bifurcates from the origin at $\mu = 0$. The period doubled orbit is supercritical and stable if $\beta_2 < 0$ but is subcritical and unstable if $\beta_2 > 0$.*

The computations above can be carried out readily for nonlinear systems of any finite order, given in discrete-time form. Another approach (see, e.g., [45]) uses center manifold reduction and focuses on the one-dimensional case. Next we establish a connection between the results obtained above and following theorem quoted from Guckenheimer and Holmes [45, Theorem 3.5.1].

Theorem 4.2 [45, Theorem 3.5.1] *Let $f_\mu : \mathbb{R} \to \mathbb{R}$ be a one-parameter family of mappings such that f_{μ_0} has a fixed point x_0 with eigenvalue -1. Assume*

(F1) $\left(\dfrac{\partial f}{\partial \mu}\dfrac{\partial^2 f}{\partial x^2} + 2\dfrac{\partial^2 f}{\partial x \partial \mu}\right) = \dfrac{\partial f}{\partial \mu}\dfrac{\partial^2 f}{\partial x^2} - \left(\dfrac{\partial f}{\partial x} - 1\right)\dfrac{\partial^2 f}{\partial x \partial \mu} \neq 0$ *at* (x_0, μ_0);

(F2) $a = \left(\dfrac{1}{2}\left(\dfrac{\partial^2 f}{\partial x^2}\right)^2 + \dfrac{1}{3}\left(\dfrac{\partial^3 f}{\partial x^3}\right)\right) \neq 0$ *at* (x_0, μ_0).

Then there is a smooth curve of fixed points of f_μ passing through (x_0, μ_0), the stability of which changes at (x_0, μ_0). There is also a smooth curve γ passing through (x_0, μ_0) so that $\gamma - \{(x_0, \mu_0)\}$ is a union of hyperbolic period 2 orbits. The curve γ has quadratic tangency with the line $\mathbb{R} \times \{\mu_0\}$ at (x_0, μ_0).

Here the quantity (F1) is the μ-derivative of $\partial f_\mu / \partial x$ along the curve of fixed points. In (F2) the sign of a determines the stability and direction of bifurcation of the orbits of period 2. If a is positive, the orbits are stable; if a is negative they are unstale.

Applying Theorem 4.1 and formula (4.5) to f_μ for the one dimensional case, it is easy to see that condition $\lambda_1' \neq 0$ in hypothesis (P) is precisely condition (F1) in Theorem 4.2. Moreover, it is not difficult to verify that

$$\beta_2 = -2a$$

Thus, the computations and results obtained in this section for period doubling bifurcation in n-dimensional systems specialize to familiar calculations for the one-dimensional case.

4.3 Control of Period Doubling Bifurcation

We now consider the control of a period doubling bifurcation. Suppose we are given a discrete-time one-parameter family of nonlinear systems

$$x_{k+1} = f_\mu(x_k, u) \tag{4.6}$$

where $x_k \in \mathbb{R}^n$ for each integer k, u is a scalar control input, $\mu \in \mathbb{R}$ is the bifurcation parameter, and the vector field f_μ is sufficiently smooth. In the sequel the system

$$x_{k+1} = f_0(x_k, u) \tag{4.7}$$

which is simply (4.6) with $\mu = 0$, will also be of interest.

The goal of this section is develop control laws $u(x_k)$ which stabilize a period doubling bifurcation occurring in (4.6). By stabilizing the bifurcation, regular

behavior can often be ensured over a wide range of parameter values. Note that we allow arbitrary dependence of the system equations on the control u. However, in some applications, it happens that the system equations involve the parameter μ and the control u only through the sum $u + \mu$. In such cases, one naturally asks if it is instead possible to select a parameter value $\bar{\mu}$ for which the system is stable, and simply take the control to be a constant which adjusts for changes in the value of μ. A serious argument against such an approach is that it would require precise knowledge of the current value of the parameter μ and of the system dynamics (4.6). In practice, we are often confronted with uncertain models. By instead employing a feedback control of the type we seek here, a degree of *robustness* to model uncertainty is achieved. Moreover, the control energy spent in the feedback control methodology is small for initial conditions near the desired fixed point or periodic orbit, while the adjust-as-you-go approach would involve large control effort even for small excursions from the desired solution.

The following hypothesis is invoked in the synthesis of feedback controls $u = u(x_k)$ achieving certain stability properties for each of the descriptions (4.6) and (4.7).

(**P′**) Eq. (4.6) has a period-1 orbit at the origin when $u \equiv 0$. Furthermore, the linearization of the uncontrolled version of (4.6) at $x = 0$ possesses a simple eigenvalue $\lambda_1(\mu)$ with $\lambda_1(0) = -1$, $\lambda_1'(0) \neq 0$. The remaining eigenvalues $\lambda_2(0), \ldots, \lambda_n(0)$ have magnitude less than unity.

By Theorem 4.1, hypothesis (P′) implies a period doubling bifurcation for the uncontrolled version of Eq. (4.6). Two stabilization problems are addressed by the results of this section. One of these pertains to Eq. (4.6) and the other

to Eq. (4.7). For Eq. (4.6), the goal is to ensure local asymptotic stability and sufficient stability margin of the bifurcated period doubled orbit. This will be referred to as the *local period doubling bifurcation control problem.* For the description (4.7), the same control laws solve the *local feedback stabilization problem* for the period-1 orbit 0.

Rewrite Eq. (4.6) by expanding the vector field in a Taylor series:

$$\begin{aligned} x_{k+1} &= f_\mu(x_k, u) \\ &= Ax_k + \mu L_1 x_k + u\check{L}_1 x_k + ub + Q(x_k, x_k) \\ &\quad +\mu^2 L_2 x_k + \mu Q_1(x_k, x_k) + u\check{Q}_1(x_k, x_k) \\ &\quad +C(x_k, x_k, x_k) + \ldots \end{aligned}$$

Take the control u to be of the form

$$u(x_k) = x_k^T Q_u x_k + C_u(x_k, x_k, x_k)$$

where Q_u is a real symmetric $n \times n$ matrix and $C_u(x, x, x)$ is a cubic form generated by a scalar valued symmetric trilinear form $C_u(x, y, z)$. Note that $u(x_k)$ contains no constant terms or terms linear in x_k. A constant term would physically represent a continuous expenditure of control energy. Also, the absence of a linear term in the feedback ensures that the left and right eigenvectors corresponding to the critical eigenvalue -1 (also those of the zero eigenvalue of the sped-up system), and the value of μ at criticality, will be unaffected by the feedback control. Further discussion on nonlinear vs. linear feedback control of bifurcating systems can be found in [3]. It suffices to note here that this work may be viewed as belonging to the general approach in which local calculations are employed near equilibrium points to achieve the controls containing linear

and nonlinear terms. The linear terms is used to modify the location of the bifurcation, while the nonlinear terms are used to modify the stability properties. This general approach was also used in Chapter 3.

The closed loop dynamics with a feedback of this form are given as follows (starred quantities below denote values after feedback):

$$\begin{aligned} x_{k+1} &= Ax_k + Q^*(x_k, x_k) + C^*(x_k, x_k, x_k) \\ &\quad +\mu L_1 x_k + \mu^2 L_2 x_k + \dots \end{aligned}$$

where

$$\begin{aligned} Q^*(x,x) &= (x^T Q_u x)b + Q(x,x) \\ C^*(x,x,x) &= C_u(x,y,z)b + C(x,x,x) + (x^T Q_u x)\check{L}_1 x \end{aligned}$$

Symmetric bilinear and trilinear forms $Q^*(x,y)$, $C^*(x,y,z)$ generating the quadratic and cubic forms $Q^*(x,x)$ and $C^*(x,x,x)$, respectively, are now chosen:

$$\begin{aligned} Q^*(x,y) &= (x^T Q_u y)b + Q(x,y) \\ C^*(x,y,z) &= C_u(x,y,z)b + C(x,y,z) \\ &\quad +\frac{1}{3}(x^T Q_u y)\check{L}_1 z + \frac{1}{3}(x^T Q_u z)\check{L}_1 y + \frac{1}{3}(y^T Q_u z)\check{L}_1 x \end{aligned}$$

For the sped-up system after feedback,

$$\begin{aligned} \tilde{A} &= A^2 - I \\ \tilde{Q}^*(x,y) &= AQ^*(x,y) + Q^*(Ax, Ay) \\ \tilde{C}^*(x,y,z) &= AC^*(x,y,z) + 2Q^*(Ax, Q^*(y,z)) + C^*(Ax, Ay, Az) \end{aligned}$$

Substituting $Q^*(x,y)$ and $C^*(x,y,z)$ into the expressions above gives

$$\tilde{Q}^*(x,y) = A(x^T Q_u y)b + AQ(x,y) + ((Ax)^T Q_u (Ay))b + Q(Ax, Ay)$$

$$\begin{aligned}
\tilde{C}^*(x,y,z) &= AC_u(x,y,z)b + AC(x,y,z) + A(x^TQ_uy)\check{L}_1z \\
&\quad +2(Ax)^TQ_u((y^TQ_uz)b + Q(y,z))b \\
&\quad +2Q(Ax,(y^TQ_uz)b + Q(y,z)) \\
&\quad +C_u(Ax,Ay,Az)b + C(Ax,Ay,Az) + ((Ax)^TQ_u(Ay))\check{L}_1(Az)
\end{aligned}$$

To compute β_1 and β_2 note that

$$\begin{aligned}
\tilde{Q}^*(r,r) &= (A+I)(r^TQ_ur)b + (A+I)Q(r,r) \\
&= \tilde{Q}(r,r) + (A+I)(r^TQ_ur)b) \\
\tilde{C}^*(r,r,r) &= (A-I)C_u(r,r,r)b + (A-I)C(r,r,r) + A(r^TQ_ur)\check{L}_1r \\
&\quad -2r^TQ_u((r^TQ_ur)b + Q(r,r))b \\
&\quad -2Q(r,(r^TQ_ur)b) - 2Q(r,Q(r,r)) \\
&\quad -(r^TQ_ur)\check{L}_1r \\
&= \check{C}(r,r,r) + (A-I)C_u(r,r,r)b + A(r^TQ_ur)\check{L}_1r \\
&\quad -2r^TQ_u((r^TQ_ur)b + Q(r,r))b \\
&\quad -2Q(r,(r^TQ_ur)b) - (r^TQ_ur)\check{L}_1r
\end{aligned}$$

Thus after feedback, the coefficient β_1 becomes

$$\begin{aligned}
\beta_1^* &= l\tilde{Q}^*(r,r) \\
&= l[\tilde{Q}(r,r) + (A+I)(r^TQ_ur)b] \\
&= l\tilde{Q}(r,r) + (-l+l)(r^TQ_ur)b \\
&= \beta_1 + 0 \\
&= 0
\end{aligned}$$

As for β_2, we have:

$$\beta_2^* = 2l(\tilde{C}^*(r,r,r)) - 2\tilde{Q}^*(r,\tilde{A}^-\tilde{Q}^*(r,r)))$$

$$= \beta_2 + \Delta \tag{4.8}$$

where Δ is given by

$$\begin{aligned}
\Delta \;=\; & -4lC_u(r,r,r)b \\
& -4l[(r^TQ_ur)\check{L}_1r + r^TQ_u((r^TQ_ur)b + Q(r,r))b \\
& +Q(r,(r^TQ_ur)b)] \\
& +4l[Q(r,\tilde{A}^-(A+I)(r^TQ_ur)b) \\
& +(r^TQ_u\tilde{A}^-((A+I)(r^TQ_ur)b + (A+I)Q(r,r)))b] \\
& +4l[Q(r,A\tilde{A}^-(A+I)(r^TQ_ur)b) \\
& +r^TQ_u(A\tilde{A}^-((A+I)(r^TQ_ur)b + (A+I)Q(r,r)))b]
\end{aligned} \tag{4.9}$$

It remains to use Eq. (4.9) to find conditions under which β_2^* can be made negative and of some desired magnitude. This will be achieved by determining criteria under which Δ can be set to any desired value by feedback control. (See the discussion following Theorem 4.4 below for elaboration of the importance of $|\beta_2|$ to system behavior.)

The case $lb \neq 0$ deserves special consideration, since from the Popov-Belevitch-Hautus (PBH) eigenvector test for controllability of modes of linear time-invariant systems [55], the critical mode is then controllable for the linearized system. Hence a linear stabilizing feedback exists in this case. Interestingly, Eq. (4.9) shows that if $lb \neq 0$ a *cubic* stabilizing feedback also exists. To see this, simply set $Q_u = 0$ and consider the effect of the cubic terms in the feedback control. The outcome is that since Δ reduces to

$$\Delta = -4C_u(r,r,r)lb \tag{4.10}$$

and $C_u(r,r,r)$ can be assigned any real value by appropriate choice of the trilinear

form $C_u(x, y, z)$, the origin is certainly local stabilizable if $lb \neq 0$.

Theorem 4.3 *Suppose that hypothesis (P') is satisfied and that $lb \neq 0$. That is, the critical eigenvalue is controllable for the linearized system. Then there is a feedback $u(x_k)$ with $u(0) = 0$ which solves the local period doubling bifurcation control problem for Eq. (4.6) and the local smooth feedback stabilization problem for Eq. (4.7). Moreover, this can be accomplished with third order terms in $u(x_k)$, leaving the critical eigenvalue unaffected.*

Under the controllability assumption of Theorem 4.3, it is known that a *linear* feedback exists which stabilizes the origin at criticality. It is therefore natural to question the utility of results (such as Theorem 4.3) giving *nonlinear* stabilizing feedback controls. There are indeed several reasons for using nonlinear feedbacks, two of which are noted next. First, the effect of a linear feedback control designed to stabilize the linearized version of the critical system (4.7) on the one-parameter family of systems (4.6) may be difficult to determine. Indeed, at least for small feedback gains, one can expect that the bifurcation will reappear at a different value of the parameter μ. The stability of this new bifurcation is not easily determined. Hence, simply using a linear stabilizing feedback may be unacceptable if the goal is to stabilize a bifurcation and not merely to stabilize an equilibrium point for a fixed parameter value. Second, it should not be surprising that in some situations a linear feedback which locally stabilizes an equilibrium may result in globally unbounded behavior, whereas nonlinear feedbacks exist which stabilize the equilibrium both locally and globally [3]. Hence, even if stabilization, rather than bifurcation control, is the issue being studied, nonlinear feedback controls can be superior.

Next the case in which $lb = 0$ will be considered. By the PBH test, this corresponds to the critical mode being uncontrollable for the linearized system. Observe that the expression for Δ now simplifies to

$$\begin{aligned}\Delta &= -4l(r^TQ_ur)\check{L}_1r - 4lQ(r,(r^TQ_ur)b) \\ &\quad +4lQ(r,\tilde{A}^-(A+I)(r^TQ_ur)b) \\ &\quad +4lQ(r,A\tilde{A}^-(A+I)(r^TQ_ur)b) \qquad (4.11)\end{aligned}$$

Introducing the parameter $\rho := r^TQ_ur$ and recalling that Q is a bilinear form, Eq. (4.11) becomes

$$\begin{aligned}\Delta &= -4\rho\{l\check{L}_1r + lQ(r,b) - lQ(r,\tilde{A}^-(A+I)b) \\ &\quad -lQ(r,A\tilde{A}^-(A+I)b)\}. \qquad (4.12)\end{aligned}$$

The next result gives a sufficient condition for stabilizability in the case $lb = 0$. The derivation also indicates how a stabilizing feedback might be chosen. Simply choose ρ of the proper sign (depending on the sign of the expression in (4.13)) and large enough magnitude.

Theorem 4.4 *Suppose that hypothesis (P') is satisfied and that $lb = 0$. Then there is a feedback $u(x_k)$ with $u(0) = 0$ which solves the local period doubling bifurcation control problem for Eq. (4.6) and the local smooth feedback stabilization problem for Eq.(4.7), provided that*

$$\begin{aligned}0 \neq\ & l\check{L}_1r + lQ(r,b) - lQ(r,\tilde{A}^-(A+I)b) \\ & -lQ(r,A\tilde{A}^-(A+I)b). \qquad (4.13)\end{aligned}$$

Period doubling bifurcation occurs when a periodic orbit loses stability. In the period doubling route to chaos, period doubled orbits also lose stability with

slight parameter variation. If the stability of one such period doubled orbit (or the original fixed point) is enhanced sufficiently, then one would at the minimum expect a delay in the next period doubling bifurcation. Moreover, one would hope that guaranteeing a sufficient degree of stability for one period doubling bifurcation in the route to chaos might eliminate the route to chaos altogether.

For systems (4.6), feedback control laws of the form $u = u(x_k)$ are said to be *static* or *direct* control laws. The control laws developed in this section are of this type. Suppose that (4.6) is an approximate model of an actual system. In such a case, a direct state feedback designed with reference to a particular equilibrium will affect not only the stability of the equilibrium but possibly also the location of this and other system equilibria. Also precise knowledge of the equilibrium of interest is needed for not only the critical parameter value but also over a range of parameter values. This in turn often means the control law will depend on the system bifurcation parameter. Other, so-called *dynamic feedback controllers* of a special form can be employed instead which guarantee preservation of all system equilibria even under uncertainty. No accurate knowledge of the system equilibria is required. Specifically, we are extending the preceding results employing dynamic feedback through so-called *washout filters*. The results, which are presented in the next section, are similar in spirit to previous work of the authors on control of bifurcations and chaos for continuous-time systems (e.g., [101], [58]).

4.4 Control of Period Doubling Bifurcation through Washout Filters

Next, we present results on control of period doubling bifurcation through "discrete-time washout filters."

Specifically, for x_k in Eq. (4.6), the dynamics of the washout filters is given as follows:

$$z_{k+1} = x_k - (d-1)z_k \tag{4.14}$$

and the output function is defined as

$$y_k = x_k - dz_k \tag{4.15}$$

where $0 < d < 2$ corresponds to using stable washout filters. In this formulation, n washout filters, one for each system state, are present, although often fewer washout filters suffice.

The decisive property of washout filters is that they reject steady-state inputs, while passing transients inputs. To see this for (4.14)-(4.15), note at steady-state,

$$x_k = dz_k$$

the output $y_k = 0$ (ref. Eq. (4.15)) and the steady-state input signal has been washed out.

Now let the control input u be a function of y_k, $u = u(y_k)$ with $u(0) = 0$. Since y_k vanishes at steady-state, the x components of the closed loop equilibria are identical with the corresponding components of the open loop equilibria. Therefore, by incorporating washout filters in the feedback, the equilibria of the system are preserved.

As in Section 4.3, hypothesis (P′) is invoked in the synthesis of a feedback control $u = u(y_k)$ for each of the descriptions (4.6) and (4.7). Again the local period doubling bifurcation control problem for Eq. (4.6)) and the local feedback stabilization problem for Eq. (4.7) are considered.

As before, rewrite Eq. (4.6) by expanding the map in a Taylor series:

$$\begin{aligned} x_{k+1} &= f_\mu(x_k, u) \\ &= Ax_k + \mu L_1 x_k + u\check{L}_1 x_k + ub + Q(x_k, x_k) \\ &\quad +\mu^2 L_2 x_k + \mu Q_1(x_k, x_k) + u\check{Q}_1(x_k, x_k) \\ &\quad +C(x_k, x_k, x_k) + \dots \end{aligned}$$

Denote

$$\zeta_k := \begin{pmatrix} x_k \\ z_k \end{pmatrix}$$

then the *extended* system (the system with washout filters appended) becomes (barred quantities below indicate values reflecting inclusions of washout filters)

$$\begin{aligned} \zeta_{k+1} &= \bar{A}\zeta_k + \mu\bar{L}_1\zeta_k + u\bar{\check{L}}_1\zeta_k + u_k\bar{b} + \bar{Q}(\zeta_k, \zeta_k) \\ &\quad +\mu^2\bar{L}_2 x_k + \mu\bar{Q}_1(\zeta_k, \zeta_k) + u_k\bar{\check{Q}}_1(\zeta_k, \zeta_k) \\ &\quad +\bar{C}(\zeta_k, \zeta_k, \zeta_k) + \dots \end{aligned} \tag{4.16}$$

Here,

$$\bar{A} := \begin{pmatrix} A & 0 \\ I & -(d-1)I \end{pmatrix}, \qquad \bar{b} := \begin{pmatrix} b \\ 0 \end{pmatrix},$$

$$\bar{\check{L}}_1 := \begin{pmatrix} \check{L}_1 & 0 \\ 0 & 0 \end{pmatrix}, \quad \bar{Q}(\zeta_k, \zeta_k) := \begin{pmatrix} Q(x_k, x_k) \\ 0 \end{pmatrix},$$

$$\bar{C}(\zeta_k, \zeta_k, \zeta_k) := \begin{pmatrix} C(x_k, x_k, x_k) \\ 0 \end{pmatrix}.$$

Take the control u to be of the form

$$u = y_k^T Q_u y_k + C_u(y_k, y_k, y_k) \tag{4.17}$$

where Q_u is a real symmetric $n \times n$ matrix and C_u is a cubic form generated by a scalar valued symmetric trilinear form $C_u(x, y, z)$. Writing Eq. (4.17) in ζ coordinates, we have

$$u = \zeta_k^T \bar{Q}_u \zeta_k + \bar{C}_u(\zeta_k, \zeta_k, \zeta_k)$$

where

$$\bar{Q}_u := \begin{pmatrix} Q_u & -dQ_u \\ -dQ_u & d^2 Q_u \end{pmatrix},$$

$$\begin{aligned} \bar{C}_u(\zeta_k, \zeta_k, \zeta_k) &:= C_u(x_k - dz_k, x_k - dz_k, x_k - dz_k) \\ &= C_u(x_k, x_k, x_k) - 3dC_u(x_k, x_k, z_k) + 3d^2 C_u(x_k, z_k, z_k) \\ &\quad -d^3 C_u(z_k, z_k, z_k). \end{aligned}$$

In order to investigate the influence of washout filters on the stability coefficients β_1 and β_2, the eigenvectors of the extended system are expressed in terms of the eigenvectors of the original system, namely, r and l. We have that

$$\bar{l} = (l, 0) \qquad \bar{r} = \begin{pmatrix} r \\ \frac{1}{d-2} r \end{pmatrix}.$$

To see this, note that

$$\bar{l}\bar{A} = (lA, 0) = (-l, 0) = -\bar{l}$$

and

$$\bar{A}\bar{r} = \begin{pmatrix} Ar \\ r - \frac{d-1}{d-2} r \end{pmatrix} = \begin{pmatrix} -r \\ -\frac{1}{d-2} r \end{pmatrix} = -\bar{r}.$$

Thus $\bar{l}$ and $\bar{r}$ are the left and right eigenvectors of $\bar{A}$ associated with eigenvalue -1. Note that

$$\bar{l} \cdot \bar{r} = l \cdot r = 1.$$

It is easy to check that the coefficient β_1 remains zero for the closed loop system with washout filters. As for β_2, following similar arguments as in Eqs. (4.8) and (4.9), we have

$$\beta_2^* = \bar{\beta}_2 + \bar{\Delta}$$

where

$$\bar{\beta}_2 = 2\bar{l}[\bar{\tilde{C}}(\bar{r},\bar{r},\bar{r}) - 2\bar{\tilde{Q}}(\bar{r}, \bar{\tilde{A}}^{-}\bar{\tilde{Q}}(\bar{r},\bar{r}))]$$

with

$$\begin{aligned}
\bar{\tilde{A}} &= \bar{A}^2 - I \\
\bar{\tilde{Q}}(\zeta,\zeta) &= \bar{A}\bar{Q}(\zeta,\zeta) + \bar{Q}(\bar{A}\zeta,\bar{A}\zeta) \\
\bar{\tilde{C}}(\zeta,\zeta,\zeta) &= \bar{A}\bar{C}(\zeta,\zeta,\zeta) + 2\bar{Q}(\bar{A}\zeta,\bar{Q}(\zeta,\zeta)) + \bar{C}(\bar{A}\zeta,\bar{A}\zeta,\bar{A}\zeta) \\
\bar{\tilde{A}}^{-} &= \left(\bar{\tilde{A}}^T\bar{\tilde{A}} + \bar{l}^T\bar{l}\right)^{-1}\bar{\tilde{A}}^T
\end{aligned}$$

and $\bar{\Delta}$ is given by

$$\begin{aligned}
\bar{\Delta} &= -4\bar{l}\bar{C}_u(\bar{r},\bar{r},\bar{r})\bar{b} \\
&\quad -4\bar{l}[(\bar{r}^T\bar{Q}_u\bar{r})\bar{\tilde{L}}_1\bar{r} + \bar{r}^T\bar{Q}_u((\bar{r}^T\bar{Q}_u\bar{r})\bar{b} + \bar{Q}(\bar{r},\bar{r}))\bar{b} \\
&\quad +\bar{Q}(\bar{r},(\bar{r}^T\bar{Q}_u\bar{r})\bar{b})] \\
&\quad +4\bar{l}[\bar{Q}(\bar{r},\bar{\tilde{A}}^{-}(\bar{A}+I)(\bar{r}^T\bar{Q}_u\bar{r})\bar{b}) \\
&\quad +(\bar{r}^T\bar{Q}_u\bar{\tilde{A}}^{-}((\bar{A}+I)(\bar{r}^T\bar{Q}_u\bar{r})\bar{b} + (\bar{A}+I)\bar{Q}(\bar{r},\bar{r})))\bar{b}] \\
&\quad +4\bar{l}[\bar{Q}(\bar{r},\bar{A}\bar{\tilde{A}}^{-}(\bar{A}+I)(\bar{r}^T\bar{Q}_u\bar{r})\bar{b}) \\
&\quad +\bar{r}^T\bar{Q}_u(\bar{A}\bar{\tilde{A}}^{-}((\bar{A}+I)(\bar{r}^T\bar{Q}_u\bar{r})\bar{b} + (\bar{A}+I)\bar{Q}(\bar{r},\bar{r})))\bar{b}] \qquad (4.18)
\end{aligned}$$

To simplify the expression for β_2^*, we need the following lemmas. The idea is to express the quantities of the extended system in terms of those of the original system.

Lemma 4.5 *The following matrix identity holds*

$$\bar{\tilde{A}}^- = \left(\bar{\tilde{A}}^T \bar{\tilde{A}} + \bar{l}^T \bar{l}\right)^{-1} \bar{\tilde{A}}^T = \begin{pmatrix} \tilde{A}^- & 0 \\ A_{21} & A_{22} \end{pmatrix}$$

where

$$A_{21} = -\frac{1}{d^2 - 2d}(A - (d-1)I)\tilde{A}^-, \qquad A_{22} = \frac{1}{d^2 - 2d} I$$

and we use the rotation

$$\tilde{A}^- = (\tilde{A}^T \tilde{A} + l^T l)^{-1} \tilde{A}^T$$

Proof

$$\begin{aligned}
&\left(\bar{\tilde{A}}^T \bar{\tilde{A}} + \bar{l}^T \bar{l}\right) \begin{pmatrix} \tilde{A}^- & 0 \\ A_{21} & A_{22} \end{pmatrix} \\
= &\begin{pmatrix} \tilde{A}^T\tilde{A} + (A-(d-1)I)^T(A-(d-1)I) + l^T l & (d^2-2d)(A-(d-1)I)^T \\ (d^2-2d)(A-(d-1)I) & (d^2-2d)^2 I \end{pmatrix} \\
&\cdot \begin{pmatrix} \tilde{A}^- & 0 \\ -\frac{1}{d^2-2d}(A-(d-1)I)\tilde{A}^- & \frac{1}{d^2-2d} I \end{pmatrix} \\
= &\begin{pmatrix} (\tilde{A}^T\tilde{A} + l^T l)\tilde{A}^- & (A-(d-1)I)^T \\ 0 & (d^2-2d)I \end{pmatrix} \\
= &\begin{pmatrix} \tilde{A}^T & (A-(d-1)I)^T \\ 0 & (d^2-2d)I \end{pmatrix} \\
= &\ (\bar{A}^2 - I)^T \\
= &\ \bar{\tilde{A}}^T
\end{aligned}$$

Q.E.D

Lemma 4.6 *The extended system (4.16) has the same open-loop stability coefficient as the original system (4.6), that is,*

$$\bar{\beta}_2 = \beta_2$$

Proof

$$\begin{aligned}
\bar{\tilde{Q}}(\bar{r},\bar{r}) &= \bar{A}\bar{Q}(\bar{r},\bar{r}) + \bar{Q}(\bar{A}\bar{r},\bar{A}\bar{r}) \\
&= \begin{pmatrix} A & 0 \\ I & -(d-1)I \end{pmatrix} \begin{pmatrix} Q(r,r) \\ 0 \end{pmatrix} + \begin{pmatrix} Q(-r,-r) \\ 0 \end{pmatrix} \\
&= \begin{pmatrix} AQ(r,r) \\ Q(r,r) \end{pmatrix} + \begin{pmatrix} Q(r,r) \\ 0 \end{pmatrix} \\
&= \begin{pmatrix} \tilde{Q}(r,r) \\ Q(r,r) \end{pmatrix}
\end{aligned}$$

$$\begin{aligned}
\bar{\tilde{C}}(\bar{r},\bar{r},\bar{r}) &= \bar{A}\bar{C}(\bar{r},\bar{r},\bar{r}) + 2\bar{Q}(\bar{A}\bar{r},\bar{Q}(\bar{r},\bar{r})) + \bar{C}(\bar{A}\bar{r},\bar{A}\bar{r},\bar{A}\bar{r}) \\
&= \begin{pmatrix} A & 0 \\ I & -(d-1)I \end{pmatrix} \begin{pmatrix} C(r,r,r) \\ 0 \end{pmatrix} \\
&\quad +2\bar{Q}\left(-\bar{r}, \begin{pmatrix} Q(r,r) \\ 0 \end{pmatrix}\right) + \begin{pmatrix} C(-r,-r,-r) \\ 0 \end{pmatrix} \\
&= \begin{pmatrix} AC(r,r,r) \\ C(r,r,r) \end{pmatrix} + 2\begin{pmatrix} Q(-r,Q(r,r)) \\ 0 \end{pmatrix} + \begin{pmatrix} -C(r,r,r) \\ 0 \end{pmatrix} \\
&= \begin{pmatrix} AC(r,r,r) - 2Q(r,Q(r,r)) - C(r,r,r) \\ C(r,r,r) \end{pmatrix} \\
&= \begin{pmatrix} \tilde{C}(r,r,r) \\ C(r,r,r) \end{pmatrix}
\end{aligned}$$

Using Lemma 4.5, we have

$$\begin{aligned}\bar{\tilde{A}}^{-}\bar{\tilde{Q}}(\bar{r},\bar{r}) &= \begin{pmatrix} \tilde{A}^{-} & 0 \\ A_{21} & A_{22} \end{pmatrix}\begin{pmatrix} \tilde{Q}(r,r) \\ Q(r,r) \end{pmatrix} \\ &= \begin{pmatrix} \tilde{A}^{-}\tilde{Q}(r,r) \\ A_{21}\tilde{Q}(r,r)+A_{22}Q(r,r) \end{pmatrix}\end{aligned}$$

thus

$$\begin{aligned}\bar{\tilde{Q}}(\bar{r},\bar{\tilde{A}}^{-}\bar{\tilde{Q}}(\bar{r},\bar{r})) &= \bar{A}\bar{Q}(\bar{r},\bar{\tilde{A}}^{-}\bar{\tilde{Q}}(\bar{r},\bar{r}))+\bar{Q}(\bar{A}\bar{r},\bar{A}\bar{\tilde{A}}^{-}\bar{\tilde{Q}}(\bar{r},\bar{r})) \\ &= \begin{pmatrix} AQ(r,\tilde{A}^{-}\tilde{Q}(r,r)) \\ Q(r,\tilde{A}^{-}\tilde{Q}(r,r)) \end{pmatrix} \\ +\bar{Q}\left(\begin{pmatrix} Ar \\ -\frac{1}{d-2}r \end{pmatrix},\begin{pmatrix} A\tilde{A}^{-}\tilde{Q}(r,r) \\ \tilde{A}^{-}\tilde{Q}(r,r)-(d-1)(A_{21}\tilde{Q}(r,r)+A_{22}Q(r,r)) \end{pmatrix}\right) \\ &= \begin{pmatrix} AQ(r,\tilde{A}^{-}\tilde{Q}(r,r))+Q(Ar,A\tilde{A}^{-}\tilde{Q}(r,r)) \\ Q(r,\tilde{A}^{-}\tilde{Q}(r,r)) \end{pmatrix}\end{aligned}$$

Now

$$\begin{aligned}\bar{\beta}_2 &= 2\bar{l}[\bar{\tilde{C}}(\bar{r},\bar{r},\bar{r})-2\bar{\tilde{Q}}(\bar{r},\bar{\tilde{A}}^{-}\bar{\tilde{Q}}(\bar{r},\bar{r}))] \\ &= 2(l,0)\left[\begin{pmatrix} \tilde{C}(r,r,r) \\ C(r,r,r) \end{pmatrix}-2\begin{pmatrix} AQ(r,\tilde{A}^{-}\tilde{Q}(r,r))+Q(Ar,A\tilde{A}^{-}\tilde{Q}(r,r)) \\ Q(r,\tilde{A}^{-}\tilde{Q}(r,r)) \end{pmatrix}\right] \\ &= 2[l\tilde{C}(r,r,r)-2l(AQ(r,\tilde{A}^{-}\tilde{Q}(r,r))+Q(Ar,A\tilde{A}^{-}\tilde{Q}(r,r)))] \\ &= 2l[\tilde{C}(r,r,r)-2\tilde{Q}(r,\tilde{A}^{-}\tilde{Q}(r,r))] \\ &= \beta_2\end{aligned}$$

Q.E.D

As a result of Lemma 4.6, we have

$$\begin{aligned}\beta_2^{*} &= \bar{\beta}_2+\bar{\Delta} \\ &= \beta_2+\bar{\Delta}\end{aligned}$$

As before it remains to use Eq. (4.18) to find conditions under which β_2^* can be made negative and of some desired magnitude. This will be achieved by determining criteria under which $\bar{\Delta}$ can be set to any desired value by feedback control. Again some simplifications of $\bar{\Delta}$ of Eq. (4.18) are needed. Two cases are discussed separately.

The case $lb \neq 0$ corresponds to the case that the critical mode is controllable for the linearized system. We obtain a similar result to Theorem 4.3 in that a cubic feedback control law exists. To see this, note first that $\bar{l}\bar{b} = lb$ and then simply set $Q_u = 0$, now consider the effect of the cubic terms in the feedback control. The outcome is that since $\bar{\Delta}$ reduces to

$$\begin{aligned}
\bar{\Delta} &= -4\bar{C}_u(\bar{r},\bar{r},\bar{r})\bar{l}\bar{b} \\
&= -4C_u(r-\frac{d}{d-2}r, r-\frac{d}{d-2}r, r-\frac{d}{d-2}r)lb \\
&= -4\frac{8}{(2-d)^3}C_u(r,r,r)lb \\
&= \frac{8}{(2-d)^3}\Delta
\end{aligned} \tag{4.19}$$

where $\Delta = -4C_u(r,r,r)lb$ is the same as Eq. (4.10) in the static feedback design. It is easy to see that $C_u(r,r,r)$ (or Δ can be assigned any real value by appropriate choice of the trilinear form $C_u(x,y,z)$, the origin is certainly local stabilizable if $lb \neq 0$. The effect the washout filters on the stability coefficients appears as a scaling factor in Eq. (4.19). Since $0 < d < 2$ the scaling factor enables the washout filter-aided to use a smaller gain to achieve the same extent of stability.

Theorem 4.7 *Suppose that hypothesis (P') is satisfied and that $lb \neq 0$. That is, the critical eigenvalue is controllable for the linearized system. Then there is*

a washout filter-aided feedback $u(y_k)$ which solves the local period doubling bifurcation control problem for Eq. (4.6) and the local smooth feedback stabilization problem for Eq. (4.7). Moreover, this can be accomplished with third order terms in $u(y_k)$, leaving the critical eigenvalue unaffected.

Next the case in which $lb = 0$ will be considered. This corresponds to the critical mode being uncontrollable for the linearized system. Observe that the expression for $\bar{\Delta}$ now simplifies to

$$\begin{aligned}\bar{\Delta} &= -4\bar{l}(\bar{r}^T\bar{Q}_u\bar{r})\bar{\check{L}}_1\bar{r} - 4\bar{l}\bar{Q}(\bar{r},(\bar{r}^T\bar{Q}_u\bar{r})\bar{b}) \\ &\quad +4\bar{l}\bar{Q}(\bar{r},\bar{\tilde{A}}^-(\bar{A}+I)(\bar{r}^T\bar{Q}_u\bar{r})\bar{b}) \\ &\quad +4\bar{l}\bar{Q}(\bar{r},\bar{A}\bar{\tilde{A}}^-(\bar{A}+I)(\bar{r}^T\bar{Q}_u\bar{r})\bar{b}) \qquad (4.20)\end{aligned}$$

Introduce the parameter

$$\begin{aligned}\bar{\rho} &:= \bar{r}^T\bar{Q}_u\bar{r} \\ &= (r - \frac{d}{d-2}r)^T Q_u (r - \frac{d}{d-2}r) \\ &= \frac{4}{(2-d)^2} r^T Q_u r \\ &= \frac{4}{(2-d)^2}\rho\end{aligned}$$

where $\rho = r^T Q_u r$ is the same quantity used in the static feedback synthesis. Note that

$$\bar{\tilde{A}}^-(\bar{A}+I) = \begin{pmatrix} \tilde{A}^- & 0 \\ A_{21} & A_{22} \end{pmatrix}\begin{pmatrix} A+I & 0 \\ I & -(d-2)I \end{pmatrix} = \begin{pmatrix} \tilde{A}^-(A+I) & 0 \\ A'_{21} & A'_{22} \end{pmatrix}$$

$$\begin{aligned}\bar{A}\bar{\tilde{A}}^-(\bar{A}+I) &= \begin{pmatrix} A & 0 \\ I & -(d-1)I \end{pmatrix}\begin{pmatrix} \tilde{A}^-(A+I) & 0 \\ A'_{21} & A'_{22} \end{pmatrix} \\ &= \begin{pmatrix} A\tilde{A}^-(A+I) & 0 \\ A''_{21} & A''_{22} \end{pmatrix}\end{aligned}$$

Eq. (4.20) becomes

$$\begin{aligned}\bar{\Delta} &= -4\bar{\rho}\{\bar{l}\bar{\check{L}}_1\bar{r} + \bar{l}\bar{Q}(\bar{r},\bar{b}) - \bar{l}\bar{Q}(\bar{r},\bar{\tilde{A}}^{-}(\bar{A}+I)\bar{b}) \\ &\quad -\bar{l}\bar{Q}(\bar{r},\bar{A}\bar{\tilde{A}}^{-}(\bar{A}+I)\bar{b})\} \\ &= -4\frac{4}{(2-d)^2}\rho\{l\check{L}_1 r + lQ(r,b) - lQ(r,\tilde{A}^{-}(A+I)b) \\ &\quad -lQ(r,A\tilde{A}^{-}(A+I)b)\} \\ &= \frac{4}{(2-d)^2}\Delta \end{aligned} \tag{4.21}$$

where Δ is the same as Eq. (4.12) in the static feedback design. Thus we obtain a similar result to Theorem 4.4 giving a sufficient condition for stabilizability in the case $lb = 0$. The derivation again indicates how a washout filter-aided stabilizing feedback might be chosen. Simply choose ρ of the proper sign (depending on the sign of the expression in (4.22)) and large enough magnitude. The effect of washout filters again appears in the form of an advantageous scaling factor.

Theorem 4.8 *Suppose that hypothesis (P') is satisfied and that $lb = 0$. Then there is a washout filter-aided feedback $u(y_k)$ which solves the local period doubling bifurcation control problem for Eq. (4.6) and the local smooth feedback stabilization problem for Eq.(4.7), provided that*

$$\begin{aligned} 0 \neq\ & l\check{L}_1 r + lQ(r,b) - lQ(r,\tilde{A}^{-}(A+I)b) \\ & -lQ(r,A\tilde{A}^{-}(A+I)b). \end{aligned} \tag{4.22}$$

Note that the condition (4.22) is precisely the same as condition (4.13) in Theorem 4.4. The discussion following Theorem 4.4 in Section 4.3 for the implication of stabilization of period doubling to controlling chaos applys here as well. In the next section, an example is given showing the nature and advantages of washout-filter based control of period doubling bifurcation.

4.5 Hénon System: Period Doubling Route to Chaos

Consider the nonlinear *Hénon system*

$$x_{n+1} = \rho - x_n^2 + py_n \tag{4.23}$$

$$y_{n+1} = x_n \tag{4.24}$$

where p and ρ are real parameters. In the following, we fix $p = 0.3$ and view ρ as the bifurcation parameter. We present results for $\rho \in (0, 1.4)$. The software tool *Dynamics* [75] was used to assist in the calculations. Fig. 4.1 shows a bifurcation diagram of the Hénon system under these parameter settings. There is a period doubling cascade to chaos. This period doubling cascade is the focus of our control design.

In Fig. 4.1, the fixed point (x^*, y^*) of interest is given by

$$\left(\frac{p - 1 + \sqrt{(1-p)^2 + 4\rho}}{2}, \quad \frac{p - 1 + \sqrt{(1-p)^2 + 4\rho}}{2} \right)$$

and the associated Jacobian matrix is

$$J = \begin{bmatrix} -2x^* & p \\ 1 & 0 \end{bmatrix}.$$

From this we can determine the critical ρ_c at which the first period doubling takes place:

$$\rho_c = \frac{3}{4}(1-p)^2.$$

This translates to $\rho_c = 0.3675$ for the case $p = 0.3$.

Now consider the Hénon system subject to control

$$x_{n+1} = \rho - x_n^2 + py_n + u_n \tag{4.25}$$

$$y_{n+1} = x_n \tag{4.26}$$

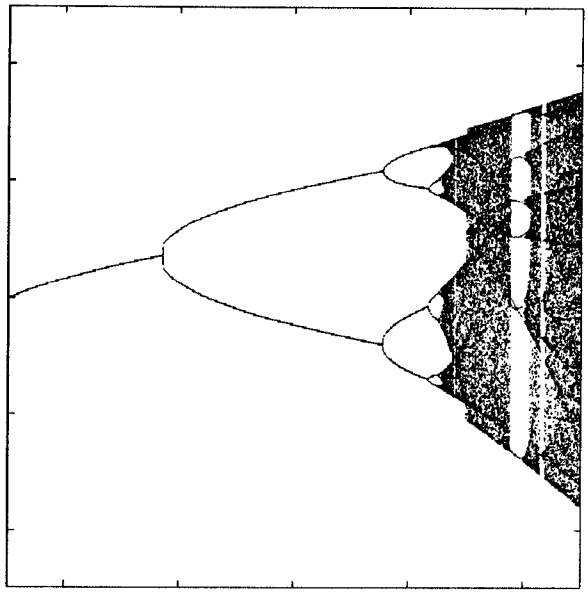

$0 \text{ - } \rho \text{ - } 1.4 \qquad -2.5 \text{ - } x \text{ - } 2.5$

Figure 4.1: Bifurcation diagram of open-loop Hénon system

where u_n is the control input. Note that this control input can be interpreted as a perturbation to the bifurcation parameter ρ. The system linearization at the fixed point (x^*, y^*) is controllable at the critical parameter value ρ_c (indeed, for all values of ρ).

There are several considerations in choosing the form of control function u_n. To apply the results of static feedback design in Section 4.3, we have to take the u_n to be of the form $u_n = u_n(x_n - x^*, y_n - y^*)$. Clearly this requires the precise knowledge of (x^*, y^*) over a range of parameter values. More severely this requires the control to depend on the parameter ρ. Also this choice of controller does not preserve the other existing fixed point of the system (4.23)-(4.24). These considerations lead to the employment of the outputs of the washout filters as the arguments to the control u_n in the following.

4.5.1 Robust Nonlinear Bifurcation Control

We employ a dynamic feedback control law which results in the overall system description

$$x_{n+1} = \rho - x_n^2 + py_n + u_n \tag{4.27}$$

$$y_{n+1} = x_n \tag{4.28}$$

$$w_{n+1} = x_n + (1-d)w_n \tag{4.29}$$

$$z_n = x_n - dw_n \tag{4.30}$$

$$u_n = k_1 z_n^3 \tag{4.31}$$

This involves the use of a discrete-time washout filter. Here, w_n is the washout filter state variable, z_n is the output function and $0 < d < 2$ is related to the washout filter time constant. Note that only one washout filter is utilized. The controller u_n (4.31) is a function of the output z_n and does not depend on knowledge of (x^*, y^*) and/or ρ.

From Theorem 4.7, the control law above ensures, locally, that the degree of stability can be made sufficiently large. Thus further period doubling bifurcation is prevented in the parameter range of interest. The period doubling route to chaos is therefore at least delayed to greater parameter values. Fig. 4.2 shows a bifurcation diagram which applies with this choice of control for $k_1 = 1.8$. Fig. 4.3 shows a time response of the Hénon system starting in a chaotic motion and settling to a period-2 orbit upon activation of the control law.

4.5.2 Robust Linear Bifurcation Control

Finally, we consider linear washout filter-aided control laws for delaying the occurrence of period doubling bifurcation in the Hénon system. The closed-loop

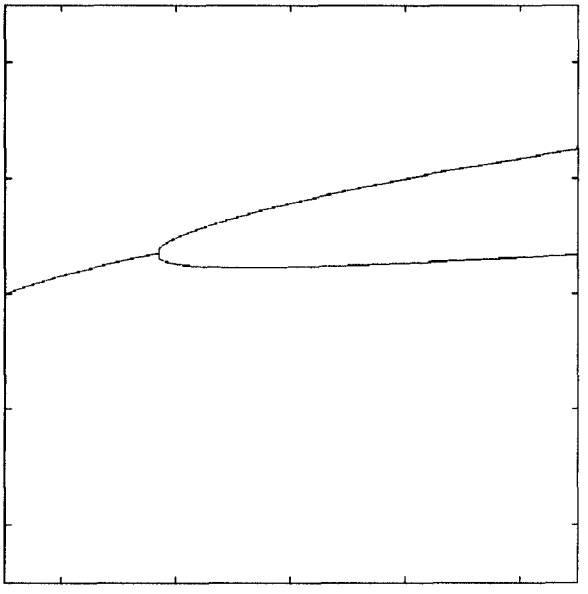

$0 \text{ - } \rho \text{ - } 1.4 \qquad -2.5 \text{ - } x \text{ - } 2.5$

Figure 4.2: Bifurcation diagram of Hénon system with dynamic cubic control: $k_1 = 1.8$

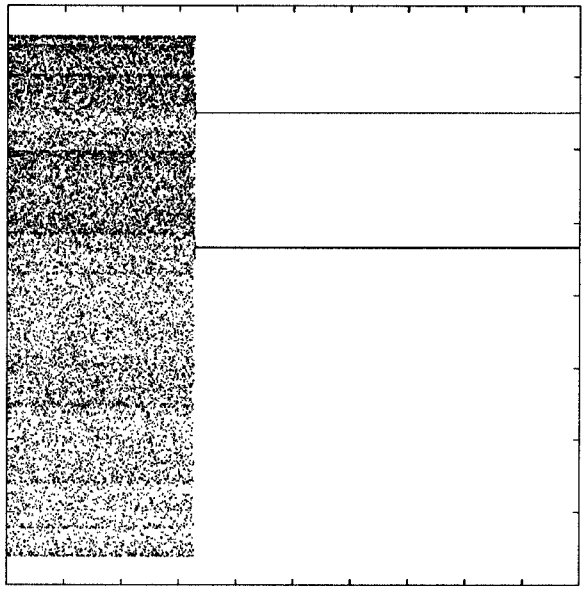

0 - n - 100000 $\quad$ -2.0 - x - 2.0

Figure 4.3: Sample time response of Hénon system with cubic control ($k_1 = 1.8$) activated after initial chaotic motion for the case $\rho = 1.4$

system is now given by Eqs. (4.27)-(4.30) along with the linear control law

$$u_n = k_2 z_n \tag{4.32}$$

With this control, the first period doubling bifurcation is postponed to greater values of ρ. The accompanying period doubling cascade and chaos are also postponed. The critical ρ_c at which the period doubling takes place after feedback is given by

$$\rho_c^* = \rho_c + \frac{2(1-p)}{2-d}k_2 + \frac{1}{(2-d)^2}k_2^2$$

Fig. 4.4 shows the effect of switching among several values of the linear feedback gain k_2 over time, for $\rho = 1.2$. Note that initially, with zero control, the system behaves chaotically. It then settles to orbits of various periods, depending on the gain k_2. The sequence of control gains used in generating Fig. 4.4 is as follows: 0, 0.165, 0.175, 0.2, 0.4, 0.7. The orbits achieved are not unstable orbits embedded in a chaotic attractor, but rather are orbits of the system for parameter values en route to chaos through the period doubling cascade. This differs from the approach of Ott, Grebogi, and Yorke [77], which entails stabilization of unstable periodic orbits embedded in a chaotic attractor.

4.6 Concluding Remarks

This chapter has investigated the design of stabilizing feedback control laws for period doubling bifurcation. The approach applies directly to nonlinear systems of any finite order, given in discrete-time form. The use of the method to remove or postpone the occurrence of a period doubling cascade to chaos was considered. Both static and dynamic feedback controllers have been studied. The dynamic feedback controllers employ washout filters and do not affect the location of

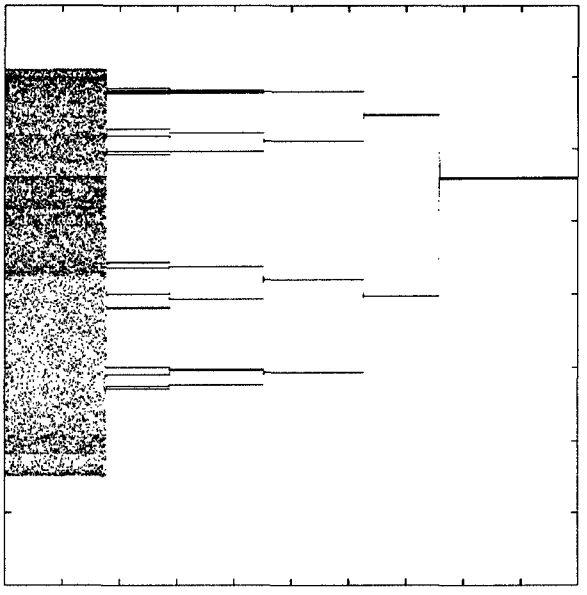

0 - n - 100000 $\quad$ -2.0 - x - 2.0

Figure 4.4: Sample time response of Hénon system under linear control with gain-switching

system fixed points. The controllers do not use measurement of the system parameter and are effective over a range of parameter values.

Chapter 5

Analysis and Control of Voltage Collapse in a Model Power System

In this chapter, the analysis and control of voltage collapse in a model electric power systems is investigated. Dynamic bifurcations, including Hopf and period-doubling bifurcations, are found to occur in a power system dynamic model recently employed in voltage collapse studies. The occurrence of dynamic bifurcations is ascertained in a region of state and parameter space linked with the onset of voltage collapse. The presence of the dynamic bifurcations, and the resulting implications for dynamic behavior, necessitate a re-examination of the role of saddle node bifurcations in the voltage collapse phenomenon. It is shown that voltage collapse can occur "prior" to the saddle node bifurcation. Moreover, a new dynamical mechanism for voltage collapse is determined: *the boundary crisis of a strange attractor* or synonymously *a chaotic blue sky bifurcation.* This mechanism results in solution trajectories containing both an oscillatory component (as predicted by recent analytical work), and a sharp, steady drop in voltage (as observed in the field). More generally, catastrophic bifurcations are identified as important mechanisms for voltage collapse.

Since nonlinear phenomena, such as bifurcations and chaos, are determined to be crucial factors in the inception of voltage collapse in power system models, in the second part of this chapter, the problem of controlling voltage collapse in the presence of these nonlinear phenomena is addressed. The bifurcation control approach is employed to modify the bifurcations and to suppress chaos. The control law is shown to result in improved performance of the system for a greater range of parameter values.

5.1 Introduction

Voltage collapse in electric power systems has recently received significant attention in the literature (see, e.g., [64] for a synopsis). This research has been motivated by increases in power demand which result in operation of electric power systems near their stability limits. A number of physical mechanisms have been identified as possibly leading to voltage collapse. From a mathematical perspective, voltage collapse has been viewed as arising from a *bifurcation* of the power system governing equations as a parameter is varied through some critical value. In a number of papers (e.g., [34], [26], [100], [57], [28]), voltage collapse is viewed as an instability which coincides with the disappearance of the steady state operating point as a system parameter, such as a reactive power demand, is quasistatically varied. In the language of bifurcation theory, these papers link voltage collapse to a *fold* or *saddle node bifurcation* of the nominal equilibrium point.

An essential distinction exists between the mathematical formulation of voltage collapse problems and transient stability problems. In studying transient

stability, one often is interested in whether or not a given power system can maintain synchronism (stability) after being subjected to a physical disturbance of moderate or large proportions. The faulted power system in such a case has been perturbed in a severe way from steady-state, and one studies the possibility of the post-fault system returning to steady-state (regaining synchronism). In the voltage collapse scenario, however, the disturbance may be viewed as a slow change in a system parameter, such as a power demand. Thus, the disturbance does not necessarily perturb the system away from steady-state. The steady-state varies continuously with the changing system parameter, until it disappears at a saddle node bifurcation point. It is because of this that saddle node bifurcation was viewed as the route to voltage collapse.

However, the presence of a saddle node bifurcation in a dynamical system does not preclude the presence of other, possibly more complex, bifurcations. In fact, the recent papers [5], [8], [27], [15] have shown that other bifurcations do occur in the example power system model studied in [34]. The bifurcations found in this model include Hopf bifurcations from the nominal equilibrium, a cyclic fold bifurcation, period doubling bifurcations, as well as a period doubling cascade leading to chaotic behavior. (See, e.g., [97] and references therein for a general discussion of these phenomena.) Other papers have also studied bifurcations in voltage dynamics in other power system models [1], [83], [98].

The fact has therefore now been established that a variety of bifurcations, static and dynamic, occur in power system models exhibiting voltage collapse. The objective of this chapter is to determine the implications of these bifurcations for the voltage collapse phenomenon and to address the issue of voltage collapse control.

5.2 Towards a Theory of Voltage Collapse

5.2.1 A Power System Model

Dobson and Chiang [34] postulated a mechanism for voltage collapse tied to the saddle node bifurcation, stressing the role of the center manifold of the system model at the bifurcation. In the same paper, they introduced a simple example power system containing a generator, an infinite bus, and a nonlinear load. The saddle node bifurcation mechanism for voltage collapse [34] was investigated for this example in subsequent papers, including [26] and [15]. On the other hand, instead of attributing voltage collapse to a single bifurcation mechanism, [98] refined the term of voltage collapse to distinguish transitions resulting from finite-sized disturbances in state space from bifurcations in parameter space. Thus in the terminology of [98], the saddle node bifurcation mechanism of voltage collapse is classified as a *parametric voltage collapse.*

In our work [8], a link was suggested between the voltage collapse phenomenon and the occurrence of dynamic bifurcations: specifically, we showed the possible role of an oscillatory transient in voltage collapse. In the proposed research, we will continue the study of dynamic bifurcations and voltage collapse, showing the possible role of catastrophic bifurcations, including crises of strange attractors [42], [43] in voltage collapse.

In this part of the research, we will focus on the model introduced by [34]. The power system is depicted in Fig. 5.1. In the study of electric power networks, one may wish to focus on a particular generating unit and nearby transmission lines and loads. Figure 5.1 is to be viewed as an equivalent circuit for a local area of interest connected to a large network. The network is modeled as an

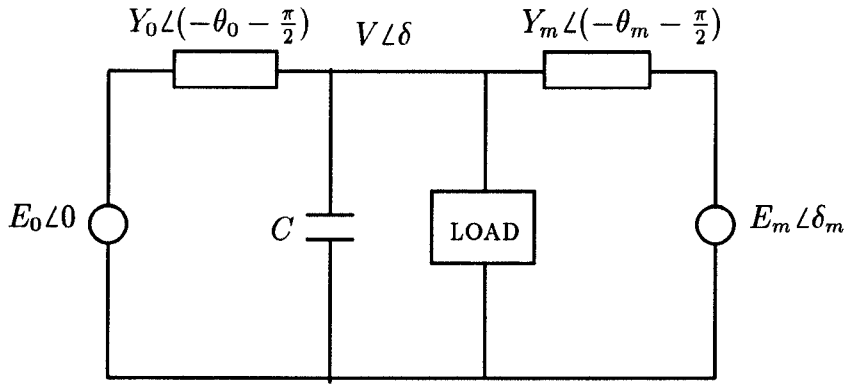

Figure 5.1: Power system model

infinite bus, i.e., a voltage source providing constant voltage magnitude and phase regardless of power flow. In Fig. 5.1, the infinite bus has terminal voltage $E_0\angle 0$ (a phasor). Here, $E_0 > 0$ is the voltage magnitude, and 0 is taken as the voltage phase angle. The generator terminal voltage is $E_m\angle\delta_m$. Figure 5.1 also shows the complex admittances of the transmission lines connected to the generator and infinite bus terminals, a load and a capacitor. Note that the load voltage is $V\angle\delta$.

The system dynamics is governed by the following four ordinary differential equations [34] ($P(\delta_m,\delta,V)$, $Q(\delta_m,\delta,V)$ are specified below):

$$\dot{\delta}_m = \omega \tag{5.1}$$

$$\begin{aligned} M\dot{\omega} &= -d_m\omega + P_m + E_m V Y_m \sin(\delta-\delta_m-\theta_m) \\ &\quad + E_m^2 Y_m \sin\theta_m \end{aligned} \tag{5.2}$$

$$K_{qw}\dot{\delta} = -K_{qv2}V^2 - K_{qv}V + Q(\delta_m,\delta,V) - Q_0 - Q_1 \tag{5.3}$$

$$\begin{aligned} TK_{qw}K_{pv}\dot{V} &= K_{pw}K_{qv2}V^2 + (K_{pw}K_{qv} - K_{qw}K_{pv})V \\ &\quad + K_{qw}(P(\delta_m,\delta,V) - P_0 - P_1) \end{aligned}$$

$$-K_{p\omega}(Q(\delta_m, \delta, V) - Q_0 - Q_1) \tag{5.4}$$

In these equations, the state variables are δ_m (the generator voltage phase angle, closely related to the mechanical angle of the generator rotor), ω (the rotor speed), δ (the load voltage phase angle) and V (the magnitude of the load voltage). A dot signifies differentiation with respect to time t. The functions $P(\delta_m, \delta, V)$, $Q(\delta_m, \delta, V)$ appearing in these equations represent, respectively, the real and reactive powers supplied to the load by the network. They are given by

$$\begin{aligned} P(\delta_m, \delta, V) &= -E_0' V Y_0' \sin(\delta + \theta_0') - E_m V Y_m \sin(\delta - \delta_m + \theta_m) \\ &\quad + (Y_0' \sin\theta_0' + Y_m \sin\theta_m) V^2 \end{aligned} \tag{5.5}$$

$$\begin{aligned} Q(\delta_m, \delta, V) &= E_0' V Y_0' \cos(\delta + \theta_0') + E_m V Y_m \cos(\delta - \delta_m + \theta_m) \\ &\quad - (Y_0' \cos\theta_0' + Y_m \cos\theta_m) V^2 \end{aligned} \tag{5.6}$$

In the above equations, instead of including the capacitor in the circuit, it is convenient to derive the Thévenin equivalent circuit with the capacitor. The adjusted values are [26]

$$\begin{aligned} E_0' &= \frac{E_0}{(1 + C^2 Y_0^{-2} - 2CY_0^{-1}\cos\theta_0)^{1/2}} \\ Y_0' &= Y_0(1 + C^2 Y_0^{-2} - 2CY_0^{-1}\cos\theta_0)^{1/2} \\ \theta_0' &= \theta_0 + \tan^{-1}\{\frac{CY_0^{-1}\sin\theta_0}{1 - CY_0^{-1}\cos\theta_0}\} \end{aligned}$$

Other quantities appearing in Eqs. (5.1)-(5.6) are constant parameters, relating to either the load or the network and generator. All of these parameters will be fixed next, except for Q_1, the reactive power demand of the load; Q_1 will be taken as the bifurcation parameter. The load parameter values are

$$K_{p\omega} = 0.4,\ K_{pv} = 0.3,\ K_{q\omega} = -0.03,\ K_{qv} = -2.8,\ K_{qv2} = 2.1,$$
$$T = 8.5,\ P_0 = 0.6,\ Q_0 = 1.3,\ P_1 = 0.0$$

The network and generator parameter values are

$$Y_0 = 20.0,\ \theta_0 = -5.0,\ E_0 = 1.0,\ C = 12.0,\ Y_0' = 8.0,\ \theta_0' = -12.0,$$

$E_0' = 2.5,$ $Y_m = 5.0,\ \theta_m = -5.0,\ E_m = 1.0,\ P_m = 1.0,\ d_m = 0.05,$

$M = 0.3.$

All angle values noted above are given in degrees.

This model has been used in [26], [34], [15] and other papers to illustrate the view that voltage collapse arises at a saddle node bifurcation. Given the highly nonlinear nature of the power system, we anticipate that a variety of nonlinear phenomena would play possible roles in voltage collapse. In the next few sections, we will use this model as well as its variations to study the dynamics associated with voltage collapse.

5.2.2 Dynamic Bifurcations and Voltage Collapse

Bifurcations

In this section, results of a detailed bifurcation study of the model (5.1)-(5.6) are presented. The continuation/bifurcation software package AUTO [35] is employed to assist this analysis. A representative bifurcation diagram for the system (5.1)-(5.6) appears in Fig. 5.2. This diagram relates the voltage magnitude V to the bifurcation parameter Q_1 (the reactive power demand). Essential features of the bifurcation diagram are summarized next.

To simplify the discussion, note first that there are six bifurcations depicted in Fig. 5.2. These are labeled HB①, CFB②, PDB③, PDB④, HB⑤ and SNB⑥. For simplicity, we may also refer to these bifurcations through their numbers ①-⑥, respectively. The acronyms indicate types of bifurcations, as follows:

- HB: Hopf bifurcation

- CFB: Cyclic fold bifurcation
- PDB: Period doubling bifurcation
- SNB: Saddle node bifurcation

For ease of reference, we denote the values of the parameter Q_1 at which the bifurcations ①-⑥ occur by $Q_1^{①}$-$Q_1^{⑥}$, respectively. In Fig. 5.2, the solid curve represents the locus of a locally asymptotically stable equilibrium point, while dashed curves correspond to unstable equilibrium points. For $Q_1 < Q_1^{①} = 10.9461\ldots$, a stable equilibrium point exists with voltage magnitude in the neighborhood of 1.2. (Upper left in Fig. 5.2.) As Q_1 is increased, an unstable ("subcritical" in the sense of increasing Q_1) Hopf bifurcation is encountered at the point labeled HB① in Fig. 5.2. As Q_1 is increased further, the stationary point regains stability at $Q_1 = Q_1^{⑤}$ through a stable ("supercritical") Hopf bifurcation. This stable equilibrium merges with another, unstable stationary branch and disappears in the saddle node bifurcation labeled SNB⑥ in Fig. 5.2. The numerical computations show that the family of periodic solutions emerging from the Hopf bifurcation at ① and the family of periodic solutions emerging from the Hopf bifurcation at⑤ are one and the same.

Besides the bifurcations of the nominal equilibrium described in the foregoing, the periodic solutions emerging from the Hopf bifurcations at ① and ⑤ themselves undergo (secondary) bifurcations. Determining the location and nature of all of the associated bifurcations is not an easy computational task, since it involves using numerical continuation to follow the bifurcated periodic solutions, as well as other solutions bifurcated from them, and so on. However, we discuss a few of these bifurcations to give an idea of the possibilities.

Since HB① is a subcritical Hopf bifurcation, it results in a family of unsta-

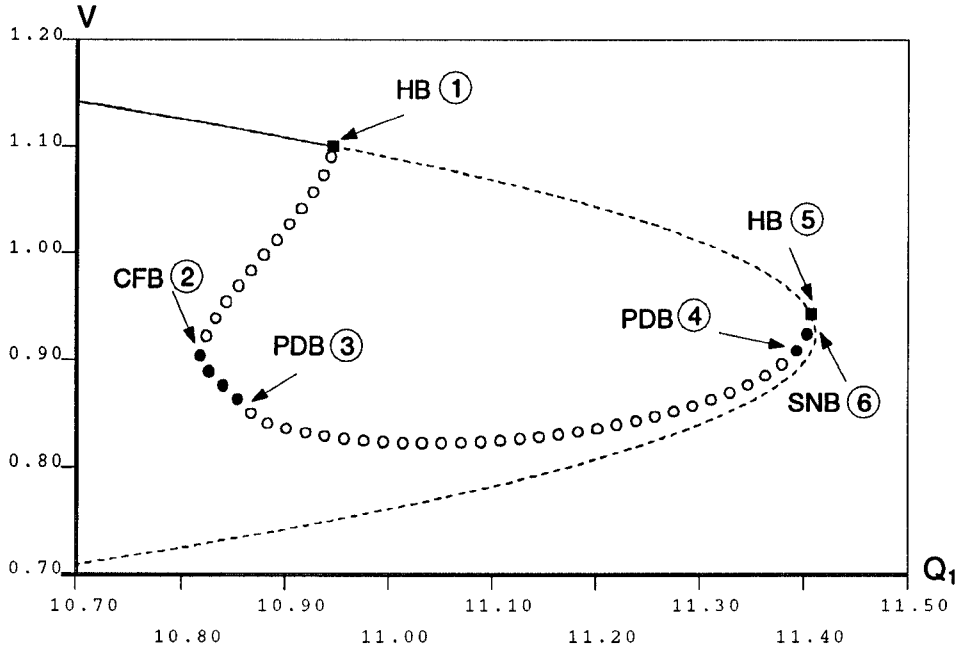

Figure 5.2: Bifurcation diagram of the model.

ble periodic solutions occurring for Q_1 slightly less than $Q_1^{①}$. In Fig. 5.2, the minimum value of this family of periodic solutions in the variable V is indicated by the circles appearing from ① and extending to the left. Open circles indicate unstable periodic solutions; filled circles denote stable orbits. At $Q_1 = Q_1^{②}$, the unstable periodic solution undergoes a *cyclic fold bifurcation.* Thus, in Fig. 5.2, the continuation of the periodic solutions for Q_1 near $Q_1^{②}$ exists for Q_1 slightly greater than $Q_1^{②}$. A cyclic fold bifurcation is simply a saddle node bifurcation of periodic solutions. Thus, the unstable periodic solution gains stability at $Q_1 = Q_1^{②}$.

The second Hopf bifurcation is supercritical. For $Q_1^{⑤} < Q_1 < Q_1^{⑥}$, i.e., just before the saddle node bifurcation SNB⑥, the equilibrium is stable. Thus, in a sufficiently small neighborhood of the parameter value $Q_1^{⑥}$, the system remains at the steady-state if its initial condition is at the nominal equilibrium. This is in

agreement with the results of [Dobson & Chiang, 1989] and [Chiang *et al.*, 1990]. Of course, it is also true that the system would in all likelihood *not* be operating at this equilibrium, due to the effects of the bifurcations discussed above.

The appearance of a window of stable large amplitude periodic orbits (see Fig. 5.2) in the parameter range $Q_1^{②} < Q_1 < Q_1^{③}$ as a result of the cyclic fold bifurcation CFB② can be verified by careful simulation. Indeed, Fig. 5.3a shows a stable periodic orbit which belongs to this family, occurring for $Q_1 = 10.8615$. The initial condition used to generate this orbit is $(\delta_m = 0.727011, \omega = 0.0345679, \delta = 0.13899, V = 0.89)$.

This large-amplitude periodic orbit loses stability at the *period doubling bifurcation* PDB③. At this bifurcation, a new periodic orbit appears which initially coincides with the original orbit, except that it is of exactly twice the period. The original orbit necessarily loses stability at such a bifurcation. The branch of period-doubled orbits is not shown in Fig. 5.2, nor any further bifurcations from that branch. However, note that another period doubling bifurcation is found to occur from the periodic orbits emanating from HB⑤; this bifurcation is labeled PDB④ in Fig. 5.2.

Simulations of the system in the parameter range corresponding to the "Hopf window" indicate the presence of further bifurcations of periodic orbits, and of aperiodic (chaotic) orbits. This is expected [33]. There are further period doublings (not shown) just beyond the period doublings PDB indicated in the figure. This indicates there is a period doubling cascade, with the resulting chaotic orbit. Indeed one surmises there are an infinite number of periodic branches, of higher and higher period, paralleling the single exhibited branch from PDB③ to PDB④. These consist almost entirely of unstable orbits. The

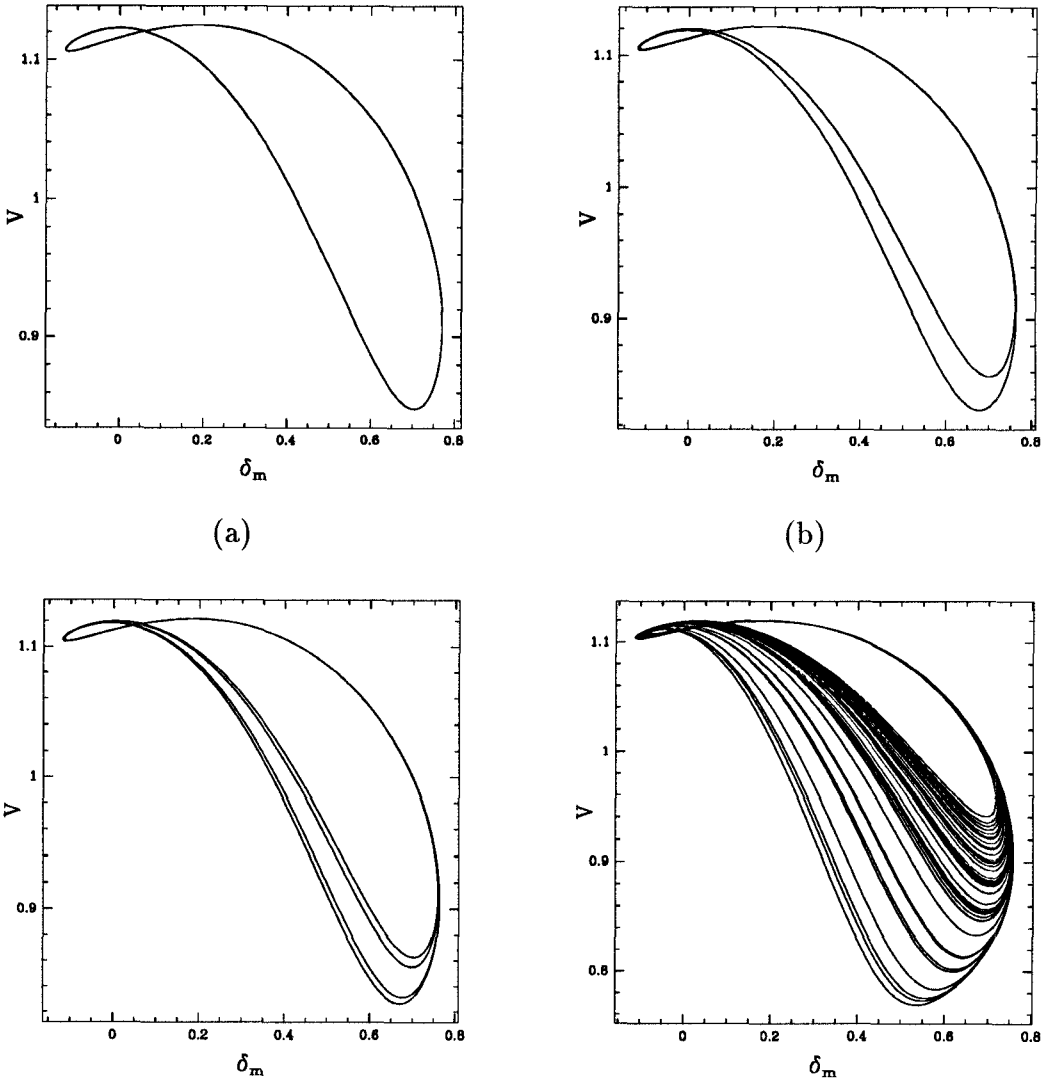

Figure 5.3: Period doubling cascade to chaos: (a) $Q_1 = 10.8615$; (b) $Q_1 = 10.8791$; (c) $Q_1 = 10.8825$; (d) $Q_1 = 10.8942$.

stable dynamical behavior is chaotic—there is some kind of strange attractor. This is what is observed. Figure 5.3(a-d) shows the period doubling cascade to chaos emerging from PDB③. (The initial condition used to generate the orbits in Fig. 5.3(b-d) agrees with that of Fig. 5.3a). Chaotic orbits resulting from this cascade occur in the approximate range $Q_1 = 10.89 - 10.8943$. There is also a period doubling cascade to chaos emerging from PDB④ (but in reverse order, w.r.t. Q_1). Figure 5.4 shows a chaotic orbit resulting from this cascade, for the parameter value $Q_1 = 11.377$. (The initial condition used to generate this orbit is $(\delta_m = 0.3503, \omega = 0.001, \delta = 0.13899, V = 0.915)$.) Fig. 5.4a represents the time simulation of V vs. time, and Fig. 5.4b gives the corresponding simulation projected in phase space onto V vs. δ_m coordinates. Chaotic orbits resulting from this cascade occur in the approximate range $Q_1 = 11.377 - 11.3825$. Note that [27] have calculated Liapunov exponents and power spectra as evidence for the presence of chaotic invariant sets. More interestingly, the strange attractor near the HB① disappears suddenly at $Q_1^* = 10.89434...$ and the strange attractor near the HB⑤ disappears at approximately $Q_1^\dagger = 11.376$. In chaos literature, the sudden death of these strange attractors is known as a *boundary crisis* [42], [43]. Here we surmise for the strange attractor nearer to HB① it is the unstable limit cycle born through the subcritical Hopf bifurcation that collides with the strange attractor. For the strange attractor near HB⑤, it is the low voltage saddle point that collides with the strange attractor.

Voltage Collapse

Analysis of the bifurcation scenario discussed in the foregoing section is important for organizing our understanding of the dynamics of voltage collapse for the

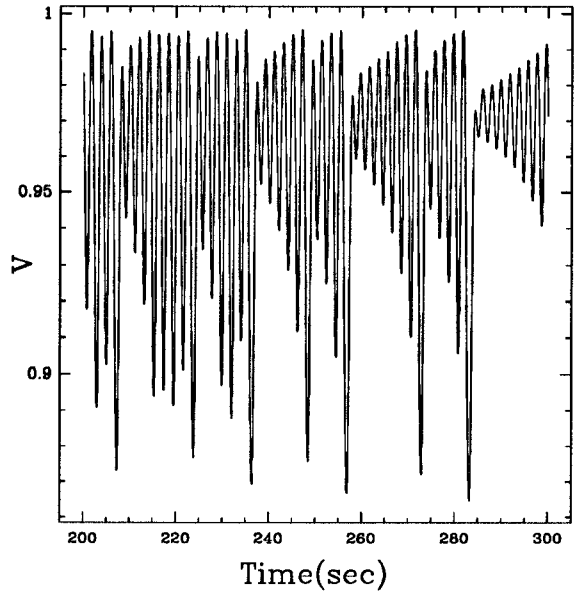

(a)

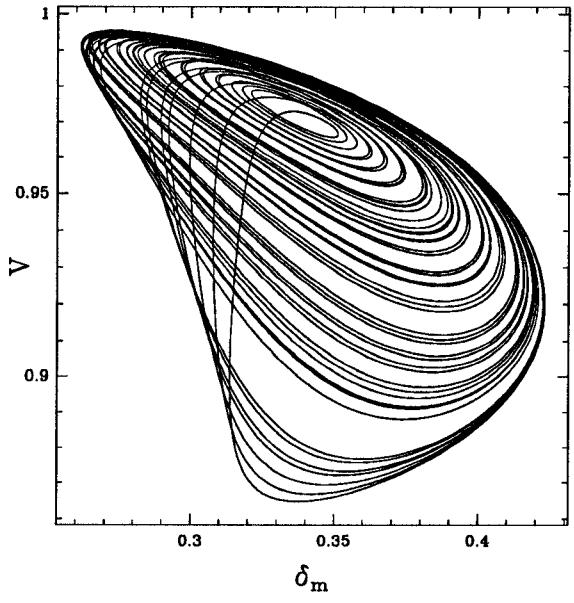

(b)

Figure 5.4: A chaotic orbit for $Q_1 = 11.377$.

model power system under consideration. To consider the implications of the bifurcations studied above in terms of the system dynamics, assume that the parameter Q_1 is quasistatically increased. For the 'usual' values of the parameter Q_1, the system operates at the stable equilibrium, At $Q_1^{②}$, we cross the cyclic fold bifurcation point. At this point, a stable/unstable limit cycle pair is born and coexists with the stable equilibrium point. The sets of initial conditions which asymptotically approach each of the two attractors is separated by the stable manifold of the saddle limit cycle born during CFB②. As Q_1 varies from $Q_1^{②}$ to $Q_1^{③}$, this periodic solution also loses stability, but in doing so gives birth to a new stable (period doubled) periodic orbit. This scenario repeats itself in a cascading fashion, each time making available a stable periodic orbit, until a strange attractor emerges. This strange attractor then disappears at Q_1^*. Notice that all these bifurcations take place prior to the HB①. Thus, in the interval of $Q_1^{②} - Q_1^*$, there exists a *partial* hysteresis loop, i.e., in addition to the stable equilibrium, there is another coexisting attractor. This means voltage collapse can occur through two different routes in this system.

In the interval of $Q_1^{②} - Q_1^*$, if the system is perturbed away from the stable equilibrium, the system may settle down to the coexisting attractor. The coexisting attractor, depending on the parameter value, is either a stable limit cycle or a strange attractor. Then as Q_1 is quasistatically increased, a boundary crisis of the strange attractor is encountered at Q_1^*, at which point voltage collapse occurs. On the other hand, even after the disappearance of the strange attractor, the nominal equilibrium of the system is still stable until the Hopf bifurcation HB①. Hence another possible mechanism of voltage collapse is linked to the subcritical Hopf bifurcation as suggested in [8]. As Q_1 passes the Hopf

bifurcation point, the excursion of voltage exhibits increasing oscillations and then a sharp decrease. Note that subcritical Hopf bifurcation is a form of catastrophic bifurcation. Hence in this example, voltage collapse is triggered either by a boundary crisis or by a catastrophic Hopf bifurcation.

We remark that for parameter values very near the saddle node bifurcation there exists a range of stable operating conditions for the system. Depending on the parameter value, this stable operating condition can be a stable equilibrium, a stable periodic orbit, or a strange attractor. However, it is also true that the system would in all likelihood not be operating at these conditions, since voltage collapse would probably have already occurred as a result of the mechanisms discussed above.

Fig. 5.5 shows an example of a typical voltage collapse within the Hopf window. The parameter value used for Fig. 5.5 is $Q_1 = 11.25$. The initial conditions used to generate the simulation of Fig. 5.5 is $(\delta_m = 0.3503, \omega = 0.001, \delta = 0.13899, V = 0.915)$. Note the oscillatory nature of the solution, and the pronounced drop in V. Fig. 5.6 shows a simulation of a "cooked" example in which collapse occurs in a nonoscillatory fashion just after the first Hopf bifurcation point (i.e., for Q_1 slightly greater than $Q_1^{\textcircled{1}}$). The parameter value used for this simulation is $Q_1 = 11.0$. What is cooked about this example is the choice of initial conditions. For the same parameter value, "most" other choices of initial conditions near the nominal stationary point give rise to oscillatory collapse, of the type illustrated in Fig. 5.5.

Fig. 5.7 shows a typical collapse simulation near to the saddle node bifurcation. This is a very sharp collapse as predicted in [34]. However, it should be noted that this behavior only occurs if the initial condition is near the nominal

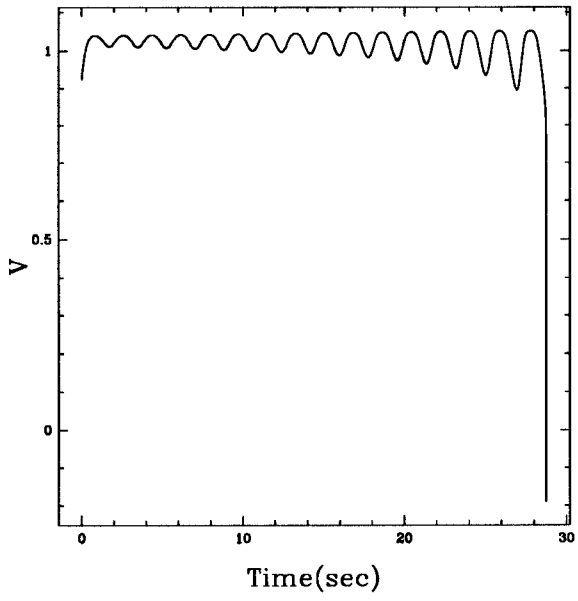

Figure 5.5: Typical voltage collapse in Hopf window.

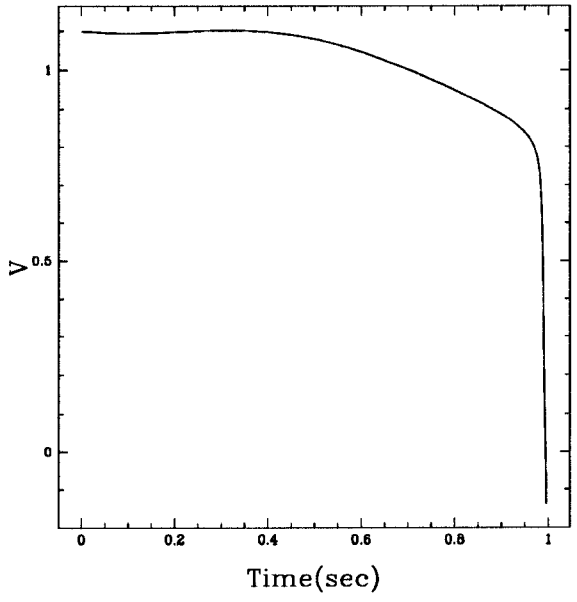

Figure 5.6: "Cooked" voltage collapse in Hopf window.

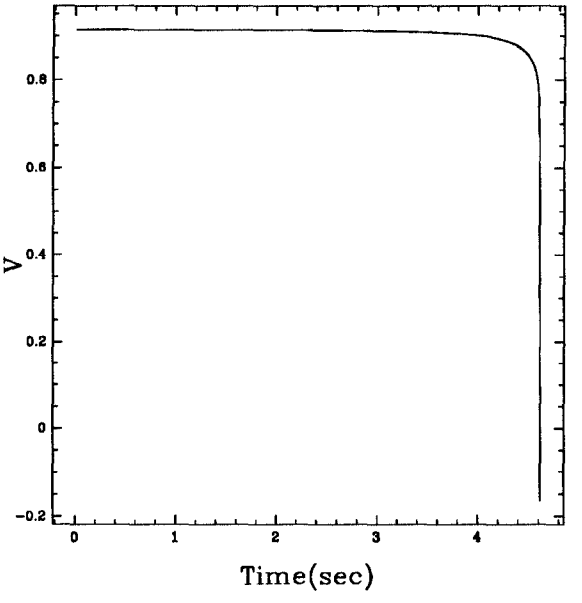

Figure 5.7: Voltage collapse near the saddle node bifurcation.

equilibrium for parameter values near $Q_1^{⑥}$. Such an initial condition is hardly likely, since the previous bifurcations discussed above will have resulted in an excursion away from the nominal equilibrium.

5.2.3 Chaotic Blue Sky Catastrophe and Voltage Collapse

Modification of the Power System Model

The power system under consideration in this section is related to one previously considered in Section 5.2.1 [34]. The example system of Section 5.2.1 includes a capacitor in parallel with a nonlinear load. The capacitor is included to raise the voltage magnitude to nearly 1 per unit. The parameter Q_1 is taken as the bifurcation parameter of the system. It is found that the value of this parameter

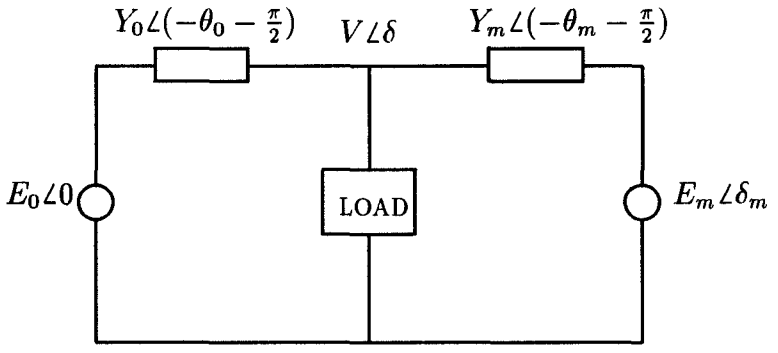

Figure 5.8: Modified power system model

at the saddle node bifurcation is approximately 11.41 per unit. This is a rather high value, and is a consequence of inclusion of the capacitor in the example system. It seems that it is rather difficult to reach this level of reactive load at normally encountered power factors.

For this reason, we modify the power system example of [34], mainly through deletion of the capacitor from the system of [34]. This reduces the reactive power load parameter prior to collapse to approximately 2.56 per unit, while reducing the voltage magnitude to approximately 0.65 per unit. The resulting power system model is depicted in Figure 5.8. Possible compromises in which a capacitor is included to raise the voltage magnitude without a large increase in load, are not given priority in this work. It follows from [34] that the system dynamics (with no capacitor) is governed by the following four differential equations ($P(\delta_m, \delta, V)$, $Q(\delta_m, \delta, V)$ are specified below):

$$\dot{\delta}_m = \omega \tag{5.7}$$

$$M\dot{\omega} = -d_m\omega + P_m - E_m V Y_m \sin(\delta_m - \delta) \tag{5.8}$$

$$K_{qw}\dot{\delta} = -K_{qv2}V^2 - K_{qv}V + Q(\delta_m, \delta, V) - Q_0 - Q_1 \tag{5.9}$$

$$
\begin{aligned}
TK_{qw}K_{pv}\dot{V} &= K_{pw}K_{qv2}V^2 + (K_{pw}K_{qv} - K_{qw}K_{pv})V \\
&\quad + K_{qw}(P(\delta_m, \delta, V) - P_0 - P_1) \\
&\quad - K_{pw}(Q(\delta_m, \delta, V) - Q_0 - Q_1) \qquad (5.10)
\end{aligned}
$$

The notation is basically identical to that of Section 5.2.1, with the caveat that there is no need for primed quantities. Primes are used to indicate Thévenin equivalent circuit values, a step which is made unnecessary since the capacitor is no longer included in the system.

The load includes a constant PQ load in parallel with an induction motor. The real and reactive powers supplied to the load by the network are

$$
\begin{aligned}
P(\delta_m, \delta, V) &= -E_0 V Y_0 \sin(\delta) + E_m V Y_m \sin(\delta_m - \delta) \qquad (5.11) \\
Q(\delta_m, \delta, V) &= E_0 V Y_0 \cos(\delta) + E_m V Y_m \cos(\delta_m - \delta) - (Y_0 + Y_m)V^2 \qquad (5.12)
\end{aligned}
$$

Most of the parameter values used in the present study agree with those of Section 5.2.1. The parameters given in Section 5.2.1 correspond to a large generator. The choice of parameter values here corresponds to a medium sized generator (500MW). Of the parameter values used here, those which differ from values given in Section 5.2.1 are as follows:

$$M = 0.01464,\ Q_0 = 0.3,\ E_m = 1.05,\ Y_0 = 3.33,\ \theta_0 = 0 \text{ and } \theta_m = 0.$$

Those which coincide with values given in Section 5.2.1 are as follows:

$$
\begin{aligned}
&K_{p\omega} = 0.4,\ K_{pv} = 0.3,\ K_{q\omega} = -0.03,\ K_{qv} = -2.8,\ K_{qv2} = 2.1, \\
&T = 8.5,\ P_0 = 0.6,\ P_1 = 0.0, \\
&E_0 = 1.0,\ Y_m = 5.0,\ P_m = 1.0,\ d_m = 0.05.
\end{aligned}
$$

All values are in per unit except for angles, which are in degrees.

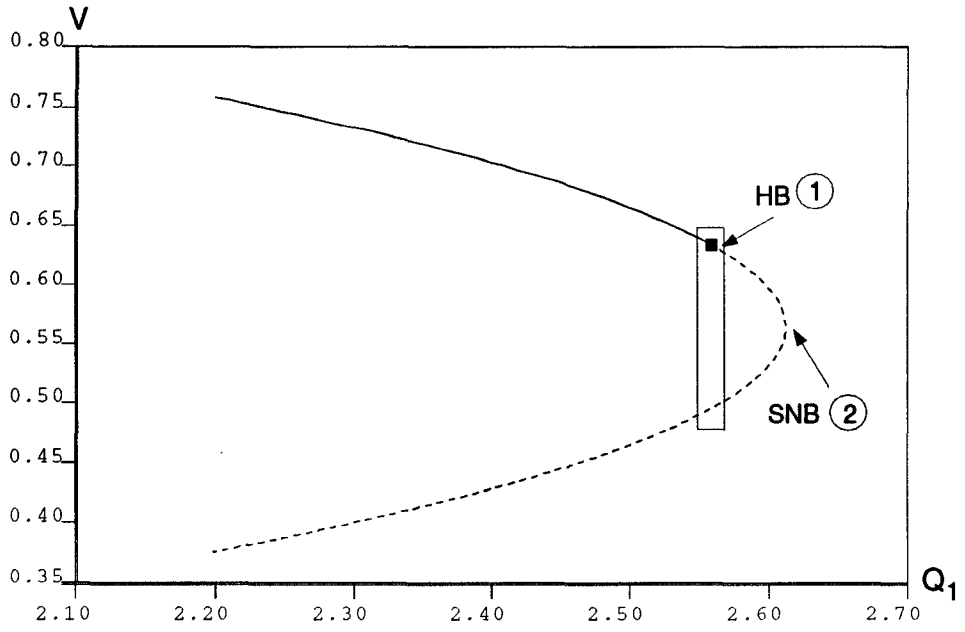

Figure 5.9: V vs. Q_1 at system equilibria

Bifurcation Analysis

In this section, the results of a bifurcation analysis of the model (5.7)-(5.12) are given. Figure 5.9 shows the dependence of the voltage magnitude V at system equilibrium points, as well as the stability of these equilibria, as a function of the bifurcation parameter Q_1. A solid line corresponds to stability of an equilibrium, while a dashed line corresponds to instability. Figure 5.10 depicts a blown-up bifurcation diagram, detailing some of the bifurcations which occur in the boxed region of Figure 5.9.

To simplify the discussion, note first that Fig. 5.9 depicts two bifurcations, and Fig. 5.10 depicts a total of five *additional* bifurcations. These seven bifurcations are labeled HB①, SNB②, CFB③, PDB④, PDB⑤, BSKY⑥ and BSKY⑦. Each of the seven bifurcations shown in Figures 5.9 and 5.10 is of one of the following types, with the corresponding acronyms:

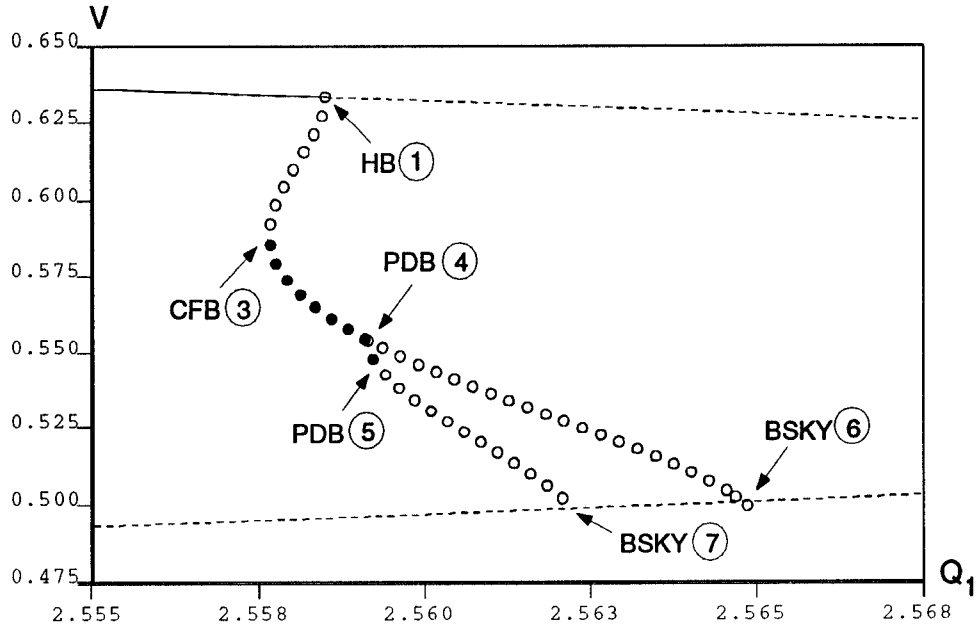

Figure 5.10: Magnified bifurcation diagram for boxed region in the previous figure

- HB: Hopf bifurcation
- SNB: Saddle node bifurcation
- CFB: Cyclic fold bifurcation
- PDB: Period doubling bifurcation
- BSKY: Blue sky bifurcation

The technical connotations of these terms will be clarified in the sequel. For ease of reference, we denote the values of the parameter Q_1 at which the bifurcations ①-⑦ occur by $Q_1^{①}$-$Q_1^{⑦}$, respectively. For $Q_1 < Q_1^{①}$, a stable equilibrium point exists with voltage magnitude in the neighborhood of 0.7. (Upper left in Fig. 5.9.) As Q_1 is increased, an unstable ("subcritical") Hopf bifurcation is encountered at the point labeled HB① in Fig. 5.9. This coincides with the point labeled HB① in Fig. 5.10. As Q_1 is increased further, the nominal stationary point

(now unstable) disappears in the saddle node bifurcation (SNB② in Fig. 5.9) at $Q_1 = Q_1^{②}$.

Besides the bifurcations of the nominal equilibrium described in the foregoing, the periodic solution emerging from the Hopf bifurcation at HB① itself undergoes bifurcations. The bifurcation HB① is a subcritical Hopf bifurcation, resulting in a family of unstable periodic solutions occurring for Q_1 slightly less than $Q_1^{①}$. In Fig. 5.10, the minimum of the variable V for members of this family of periodic solutions is indicated by the circles appearing from ① and extending to the left. Open circles indicate instability of the periodic orbits. At $Q_1 = Q_1^{③}$, the unstable periodic solution undergoes a *cyclic fold bifurcation.* Thus, in Fig. 5.10, the continuation of the sequence of circles of periodic solutions for Q_1 near $Q_1^{③}$ exists for Q_1 slightly greater than $Q_1^{③}$. A cyclic fold bifurcation is simply a saddle node bifurcation of periodic solutions. Thus, the unstable periodic solution gains stability at $Q_1 = Q_1^{③}$. The solid circles emanating from CFB③ depict the continuation of the periodic solutions; they are solid to indicate stability.

This stable periodic orbit born at CFB③ loses stability at the *period doubling bifurcation* PDB④. At this bifurcation, a new periodic orbit appears which initially coincides with the original orbit, except that it is of exactly twice the period. The original orbit necessarily loses stability at such a bifurcation. The branch of period-doubled orbits is also shown in Fig. 5.10. This branch, depicted by the solid circles emanating to the right from PDB④, undergoes a further period doubling bifurcation in short order. This occurs at PDB⑤ in Fig. 5.10. These two period doubling bifurcations are followed by a cascade of period doubling bifurcations, resulting in a strange attractor for some values of Q_1. These

further period doublings are not depicted in Fig. 5.10. However, Fig. 5.10 shows the continuation of the periodic orbits appearing at the cyclic fold bifurcation CFB③ and the period doubling bifurcation PDB④. Note that each of these periodic orbits disappears in a collision with the unstable (saddle) low voltage equilibrium point. These collisions are known by various names, including the blue sky bifurcation [97]. Thus, the disappearance of these orbits is indicated by BSKY⑥ and BSKY⑦ in Fig. 5.10. Since the system undergoes a cascade of period doubling bifurcations, one expects that each period doubled orbit undergoes such a blue sky bifurcation.

Figure 5.11 depicts several stable periodic orbits in the sequence of period doublings discussed above, along with the strange attractor resulting from the period doubling cascade.

Let us pause to consider the implications of the bifurcations studied above for the system dynamics, assuming the parameter Q_1 is quasistatically increased. For the 'usual' values of the parameter Q_1, the system operates at the stable equilibrium. As the parameter is increased, the equilibrium loses stability at the Hopf bifurcation point, giving rise to an unstable periodic orbit. Since this orbit gains stability at the cyclic fold bifurcation, a stable periodic orbit surrounds the equilibrium at and slightly beyond the Hopf bifurcation point. The system then operates at this stable periodic orbit. For greater values of the parameter Q_1, this periodic solution also loses stability, but in doing so gives birth to a new stable (period doubled) periodic orbit. This scenario repeats itself in a cascading fashion, each time making available a stable periodic orbit, until a strange attractor emerges. The system operates on the strange attractor until the strange attractor disappears ("crisis"). After this crisis, there is no stable

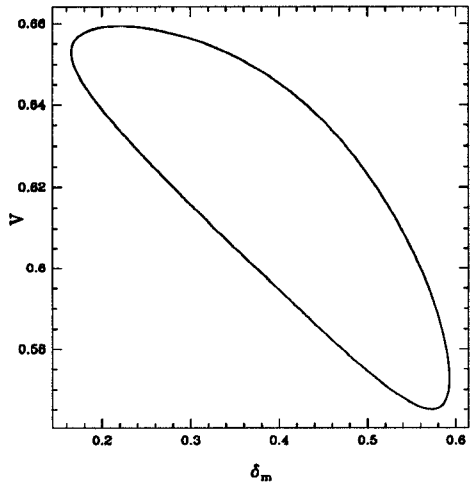

$Q_1 = 2.559$

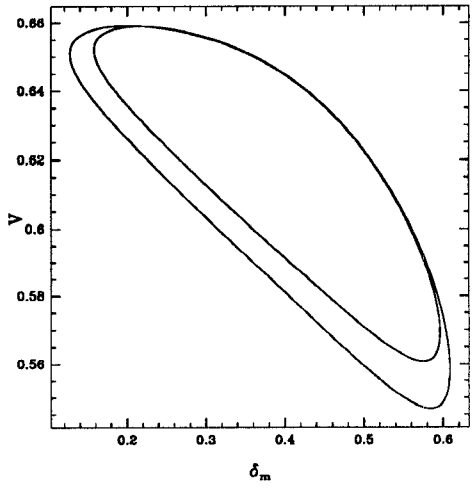

$Q_1 = 2.5601$

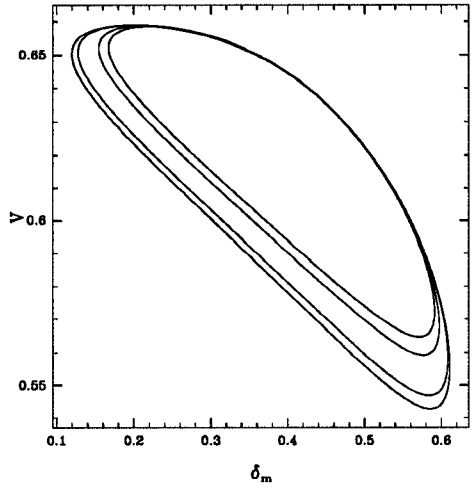

$Q_1 = 2.5602$

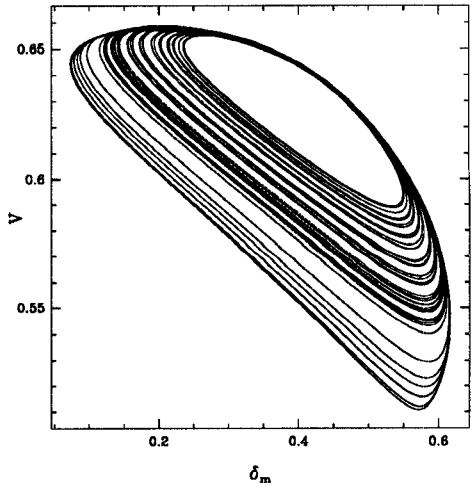

$Q_1 = 2.560378$

Figure 5.11: Period doubling cascade to chaos

invariant set in the vicinity of the nominal equilibrium at which to operate. Thus, the system must now undergo a large transient excursion. In the next section, this excursion ("voltage collapse") is tied to the disappearance of the strange attractor.

Boundary Crises, Chaotic Blue Sky Bifurcations and Voltage Collapse

The bifurcations uncovered in the foregoing analysis, and especially the sudden disappearance of the strange attractor, are crucial to the understanding of voltage collapse for the model power system under consideration. We claim that, for the model under study, voltage collapse is triggered by the *boundary crisis of the strange attractor* [42], [43] or *chaotic blue sky bifurcation* [97], i.e., its sudden destruction through collision with the low voltage saddle point.

Recall that a boundary crisis or a chaotic blue sky bifurcation involves the sudden destruction of a strange attractor through collision of the strange attractor with a saddle point, an unstable periodic orbit, or the stable manifold of such. In a boundary crisis or a chaotic blue sky bifurcation, a strange attractor exists for parameter values up to the critical value, at which the collision takes place. Subsequent to this value, the strange attractor no longer exists, but it leaves a signature, namely a transient chaotic motion. The transient chaotic motion appears chaotic for a relatively long time (depending on the initial condition), and then suddenly experiences a sharp excursion either to another, probably distant attractor, or to infinity. This excursion occurs through a tunnel in state space which necessarily follows the *unstable manifold* of the saddle point or orbit with which the collision takes place. Note the distinction with the center manifold based view adopted in [34], [15].

With this summary of boundary crises, we can return to the example at hand. An attracting invariant set exists for parameter values Q_1 up to the critical value, Q_1^*, at which the boundary crisis takes place. *Voltage collapse occurs precisely at the parameter value* $Q_1 = Q_1^*$. This gives a clear alternative to the previous view [34] that the critical value of Q_1 at which voltage collapse occurs is that associated with the saddle node bifurcation, $Q_1 = Q_1^{②}$. Note that one may view the Hopf bifurcation as an signal of impending voltage collapse, especially considering the very short interval in parameter space between the Hopf bifurcation (at $Q_1 = Q_1^{①} = 2.55919...$) and the boundary crisis of the strange attractor (at $Q_1 = Q_1^* = 2.560378...$).

Significantly, the current proposal serves to reconcile two seemingly contradictory pieces of evidence:

- First, the steady, sharp decrease in voltage observed in practice in voltage collapse; and

- Second, the presence of nonlinear phenomena such as oscillations and chaotic motion in dynamic models used in the study of voltage collapse, which is determined from analysis.

Figure 5.12 shows a projection of the dynamics onto the ω, V plane for a value of Q_1 slightly below Q_1^*. Figure 5.13 shows the same projection, for a value of Q_1 slightly greater than Q_1^*. The low voltage saddle point has one real positive eigenvalue, one real negative eigenvalue and a pair of complex conjugate eigenvalues with negative real part. Thus in both figures, the unstable manifold and only a section of the stable manifold of the low saddle point are shown. These manifolds are important to understand the underlying dynamics near crisis. At

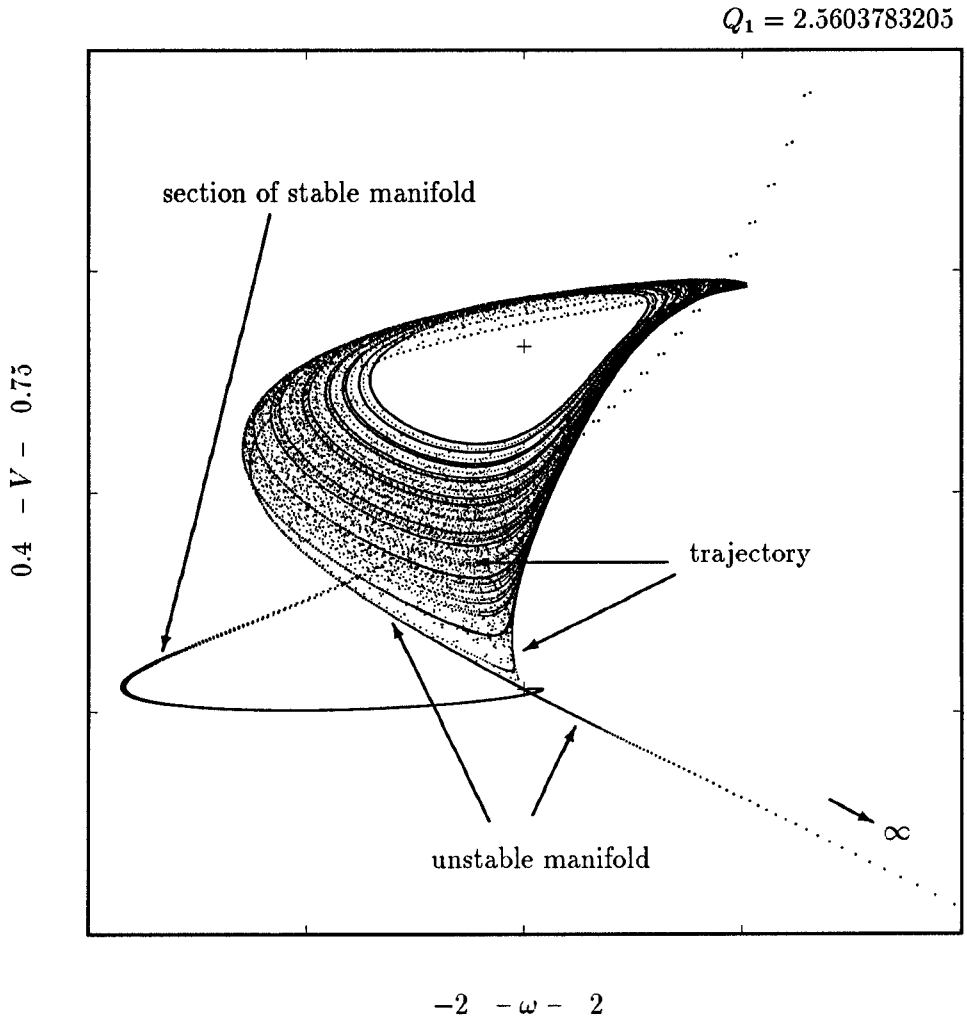

Figure 5.12: Just before boundary crisis: Strange attractor, unstable and stable manifolds of lower saddle point

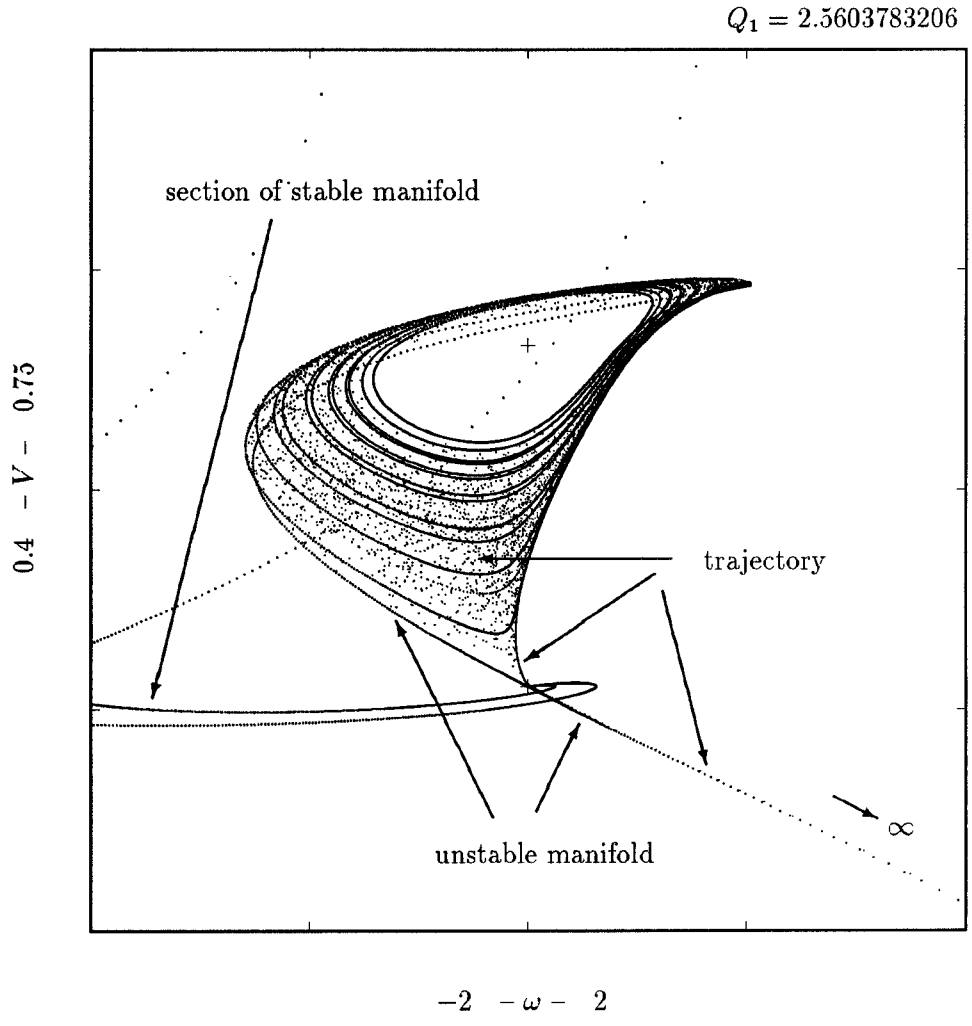

Figure 5.13: Just after boundary crisis: Transient chaos, unstable and stable manifolds of lower saddle point

$Q_1 = Q_1^*$ the closure of one of the branches of the unstable manifold of the low voltage saddle point is the strange attractor, while the stable manifold of the low voltage saddle point forms the boundary of the basin of attraction for the strange attractor for $Q_1 < Q_1^*$ [43]. In Figure 5.12, the chaotic invariant set is a strange attractor, i.e., is stable. Since the strange attractor is bounded, system trajectories are confined to a bounded subset of the state space. One of such trajectories is shown as thousands of points that flesh out the strange attractor. In Figure 5.13, the strange attractor no longer exists, and is replaced by a transient chaotic motion followed by passage of system trajectories near the low voltage saddle point, after which the trajectories follow the other branch of the unstable manifold of the saddle point. This results in a sharp decrease ("collapse") in the system voltage. Figure 5.14 represents a time simulation of V vs. time for the same value of Q_1 as that of Figure 5.13. The transient chaotic behavior and the pronounced collapse are illustrated in Figure 5.14. (Note the small magnitude of the transient oscillatory behavior.)

5.2.4 Catastrophic Bifurcations and Voltage Collapse

Related Voltage Collapse Phenomena : Differential-Algebraic Equations

The models of three preceding subsections are in the form of ordinary differential equations. This is because a dynamic load model is assumed. However, traditionally power system models are subject to algebraic constraints. More precisely, they are governed by parameter dependent differential-algebraic sys-

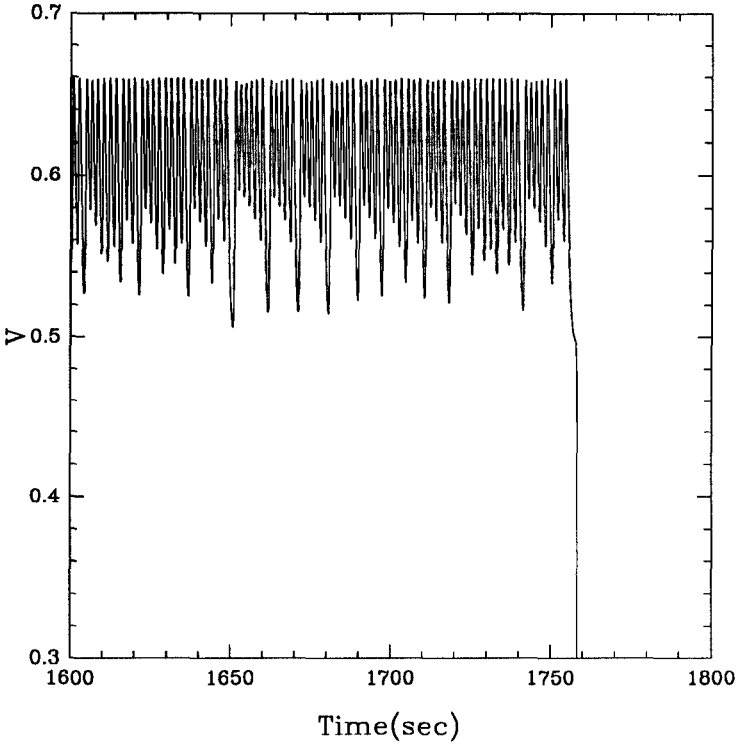

Figure 5.14: A time simulation of transient chaos and voltage collapse just after boundary crisis ($Q_1 = 2.5603783206$)

tems of the form

$$\dot{x} = f(x, y, p), \quad f : \mathbb{R}^{n+m+p} \to \mathbb{R}^n \tag{5.13}$$

$$0 = g(x, y, p), \quad g : \mathbb{R}^{n+m+p} \to \mathbb{R}^m \tag{5.14}$$

A natural question arises as to whether the voltage collapse mechanisms uncovered in the previous two subsections are applicable to the differential-algebraic system above. In [98], it was shown that in a rudimentary but representative power system model, a (parametric) voltage collapse occurs following either a subcritical Hopf bifurcation or a saddle node bifurcation as control gain and load are varied as parameters. The model is essentially two dimensional, and thus doesn't admit a strange attractor. Also the model in [98] is subject to algebraic system constraints in the form of load flow equations and thus is a differential-algebraic system. Despite the existence of singularities in the state space due to the constraints, the occurrence of the parametric voltage collapse is still triggered by catastrophic bifurcations, namely subcritical Hopf and saddle node bifurcations. In the classification of voltage collapse phenomena in [98], another type of voltage collapse is the so-called dynamic (state space) voltage collapse. Dynamic voltage collapse occurs when the post fault state lies outside the transient stability region and so the quantification of this nonlinear stability characteristic requires computing the basins of attraction of the stable equilibria. In this work, we focus on the parametric aspect of the voltage collapse phenomena. Of course, the understanding of voltage dynamics will not be complete without performing analysis in the entire state space and the entire parameter space (or a relevant region), which is beyond the scope of this study.

Voltage Collapse and Catastrophic Bifurcations

Generally speaking voltage collapse may be linked with the sudden loss of stable bounded solutions of a power system model in the vicinity of a pre-collapse operating condition. In this thesis, based on the study of our research and those of other research groups, we suggest a theory of voltage collapse in electric power systems. Our main idea is that voltage collapse is triggered by some form of catastrophic bifurcations. Two types of stability margin will be introduced: a *static stability margin* and a *dynamic stability margin.* The static stability margin is measured in parameter space from the point where the nominal equilibrium loses its stability. The dynamic stability margin is measured in parameter space from the point where voltage collapse takes place. These two stability margins are not necessarily the same.

The route to voltage collapse will differ from system to system. The responsible catastrophic bifurcation can be a catastrophic bifurcation of an equilibrium, a limit cycle, a torus or a chaotic attractor. The main ingredients of our theory are stated as follows.

From a practical point of view, the distinction between subtle and catastrophic bifurcations has very important implications. Generally we can say that a *catastrophic* bifurcation occurs at a *dangerous boundary*, while a *subtle* bifurcation occurs at a *safe boundary.* Thus a real system, such as an electric power system, evolving slowly along an equilibrium path, along a trace of limit cycles, or along a trace of strange attractors, due to the *slow* (quasistatical) variation of a parameter would experience a rapid, dynamic jump to a remote attractor at a dangerous boundary but not at a safe boundary. The type and form of the bifurcation locally tells us nothing about the new remote final state after a catastrophic jump: a saddle node bifurcation could for example trigger a jump

to a remote equilibrium, a remote limit cycle, a remote chaotic attractor, or even infinity. This is in complete contrast to the subtle bifurcation, where the type of the bifurcation tells us precisely the qualitative form of the attractor to which an evolving system would make a gradual smooth transition. There are basically three types of catastrophic bifurcations. One is the subcritical types of bifurcations. The second is the explosive birth of a different attractor. The third is the sudden death of an attractor.

In the following, we consider topological types of bifurcation that occur as a single parameter is varied, e.g.,

$$\dot{x} = f_\mu(x) \tag{5.15}$$

where μ is the distinguished bifurcation parameter. We organize the various bifurcations according to the topological dimension of the attractor on either side of the bifurcation point. Equilibrium points are zero-dimensional, limit cycles are one-dimensional, and the torus is a two-dimensional manifold. For simplicity, mappings are treated as Poincaré mappings of flows, and attractor dimension refers to the flow rather than to the mapping. Chaotic attractors are treated as three-dimensional attractors in the sense of embedding dimension, i.e., they require a phase space of at least three dimensions in order to be realized. However, it should be noted that chaotic attractors themselves are not three-dimensional manifolds, and certain rules for computing their dimension such as the Hausdorff dimension yield non-integer values greater than 2 [78].

5.3 Control of Nonlinear Phenomena at Inception of Voltage Collapse

In this section, we consider local control of voltage collapse at its inception. That is, we design controllers which can delay the occurrence of voltage collapse, as opposed to controllers for recovery from voltage collapse. The controllers we seek do not involve forced system operation in parameter ranges where voltage collapse does not occur, but are designed to work in the parameter ranges of difficulty. In order to control voltage collapse in power system models such as the one studied in the preceding section, one has to design control laws to deal with bifurcations, chaos and crises. In Chapter 3 and 4, we have seen that control laws which significantly reduce the amplitude of a bifurcated solution, or significantly enhance its stability over a nontrivial parameter range, are viable tools in the taming of chaos. Here similar techniques will be employed to control the bifurcations, chaos, and crises. In doing so we expect to increase the stability margin of the system in parameter space. In other words, voltage collapse will be 'postponed' so that stable operation of the system will be allowed beyond the point of impending collapse in the open loop system. In particular, the control laws are designed to increase two types of stability margin: a *static stability margin* and a *dynamic stability margin.* The static stability margin is measured in parameter space from the point where the nominal equilibrium loses its stability. The dynamic stability margin is measured in parameter space from the point where voltage collapse takes place. As discussed in the previous section, these two stability margins are not necessarily the same. In the system models of under study, the static stability margin is measured from the Hopf bifurcation

point $Q_1^{①}$. In the model of Section 5.2.1, dynamic stability is measured either from $Q_1^{①}$ or the crisis point Q_1^* depending on the route to collapse. In the model of Section 5.2.3, the dynamic stability is measured from the crisis point Q_1^*.

In the models under study, the stable equilibrium point loses its stability through the subcritical Hopf bifurcation HB①. The subcriticality of the Hopf bifurcation has several negative effects on the system: the system may exhibit a jump from the stable equilibrium to the coexisting attractor under perturbation, and the boundary crisis is also a direct consequence of the subcriticality of the Hopf bifurcation. Moreover, the region of attraction of the stable equilibrium is bounded by the stable manifold of the unstable limit cycle, and so this region shrinks as criticality is approached. These factors motivate the design of feedback control laws directed at the Hopf bifurcation which reduce the negative effects and increase the stability margin of the system in parameter space. As shown in [101], [9], such control action can also suppress the chaos and crises by 'squeezing' the period doubling cascades. Next we present a brief summary of the bifurcation control approach in the context of Hopf [2] and period doubling [9] bifurcation control and then proceed to use these techniques in the voltage collapse control problem.

5.3.1 Nonlinear Bifurcation Control

Consider a one-parameter family of nonlinear autonomous control systems

$$\dot{x} = f_\mu(x, u). \tag{5.16}$$

where $x \in I\!R^n$ is the state vector, $\mu \in I\!R$ is the system parameter, f_μ is a smooth map from $I\!R^n \times I\!R$ to $I\!R^n$, and u is a scalar input. Local bifurcation control deals

with the design of smooth control laws $u = u(x)$ which stabilize a bifurcation occurring in the one-parameter family of systems (5.16). These control laws exist generically, even if the critical eigenvalues of the linearized system at the equilibrium of interest are uncontrollable. The feedback control designs of [2] transform a subcritical (unstable) Hopf bifurcation to a supercritical (stable) bifurcation.

For Hopf bifurcation, the design procedure recalled in Section 3.3.2 aims to ensure the asymptotic stability of the Hopf bifurcation point as well as orbital asymptotic stability of the periodic solutions emerging from the bifurcation point for a range of parameter values. It is well known that only the quadratic and cubic terms occurring in a nonlinear system undergoing a Hopf bifurcation influence the value of β_2. Thus only the linear, quadratic, and cubic terms in an applied control u have potential for influencing β_2. If the critical mode is controllable, a linear stabilizing feedback exists. Interestingly, as discussed in Section 3.3.2, a cubic stabilizing feedback also exists in such a case. On the other hand, if the critical mode is uncontrollable, the system may still be stabilizable by a quadratic feedback control law.

Now suppose the periodic solution emerging from the Hopf bifurcation point undergoes a cascade of period doubling bifurcations to chaos. As shown in Chapter 4 and in [9], nonlinear feedback control laws can be designed which influence the degree of stability and amplitude of a given period-doubled orbit. If the amplitude of such an orbit can be constrained sufficiently, then the cascade of period doublings to chaos can be eliminated.

5.3.2 Voltage Collapse Control I

In this subsection, we carry out the design of controllers for voltage collapse in the model (5.1)-(5.4). Consider system (5.1)-(5.4) subject to a frequency-dependent control $u = u(\omega)$ by adding a control function u to the right side of Eq. (5.4) to give

$$\dot{\delta}_m = \omega \tag{5.17}$$

$$\begin{aligned} M\dot{\omega} &= -d_m\omega + P_m + E_m V Y_m \sin(\delta - \delta_m - \theta_m) \\ &\quad + E_m^2 Y_m \sin\theta_m \end{aligned} \tag{5.18}$$

$$K_{qw}\dot{\delta} = -K_{qv2}V^2 - K_{qv}V + Q(\delta_m, \delta, V) - Q_0 - Q_1 \tag{5.19}$$

$$\begin{aligned} TK_{qw}K_{pv}\dot{V} &= K_{pw}K_{qv2}V^2 + (K_{pw}K_{qv} - K_{qw}K_{pv})V \\ &\quad + K_{qw}(P(\delta_m, \delta, V) - P_0 - P_1) \\ &\quad - K_{pw}(Q(\delta_m, \delta, V) - Q_0 - Q_1) + u(\omega) \end{aligned} \tag{5.20}$$

where $P(\delta_m, \delta, V)$, $Q(\delta_m, \delta, V)$ are given by (5.5) and (5.6).

Note that the control is implemented by injecting a speed signal into the load node. The speed signal needs no washout since it does not affect the system equilibrium structure at steady state. Note also that such a controller does not affect the position of the saddle node bifurcation SNB⑥.

One control law design transforms a subcritical Hopf bifurcation into a supercritical bifurcation and ensures a sufficient degree of stability of the bifurcated periodic solutions so that chaos and crises are eliminated. This control law allows stable operation very close to the point of impending collapse (saddle node bifurcation). Because the critical mode in this case is controllable, a purely cubic control is designed to handle all these tasks. Another control design involves changing the critical parameter value at which the Hopf bifurcations occur

through a linear feedback control. Because of the special structure of the system under study, this linear feedback law eliminates the Hopf bifurcations and the resulting chaos and crises. Thus, the linearly controlled system can operate at a stable equilibrium up to the saddle node bifurcation.

Nonlinear Bifurcation Control

To render the Hopf bifurcation HB① supercritical, we employ a cubic feedback with measurement of ω. The closed loop system is Eq. (5.17)-(5.20) and u is of the form

$$u = k_n \omega^3 \tag{5.21}$$

where $k_n > 0$ is the nonlinear (cubic) feedback gain.

Values of k_n which give a supercritical HB are determined by computing the stability coefficient β_2 of the closed loop system. Since transforming HB① to a supercritical Hopf bifurcation is strictly a local result, computational analysis techniques must be used to assess the effects of the nonlinear control on the global dynamical behavior of the closed-loop system. As shown in [101], [9], larger values of the gain k_n not only enhance the stability of the bifurcation but also result in a reduced amplitude of the stable limit cycle over a range of parameter values. Recalling the discussion in Subsection 5.3.1, if the amplitude of the periodic orbit can be constrained sufficiently, then the cascade of period doublings to chaos can be eliminated. Figure 5.15 shows a bifurcation diagram for the closed loop system with control gain $k_n = 0.5$. In the closed-loop system, HB① is rendered supercritical. Moreover, the period doubling bifurcations, including the two period doubling cascades and the resulting two strange attractors and their crises are all eliminated. The benefits of changing HB① to a

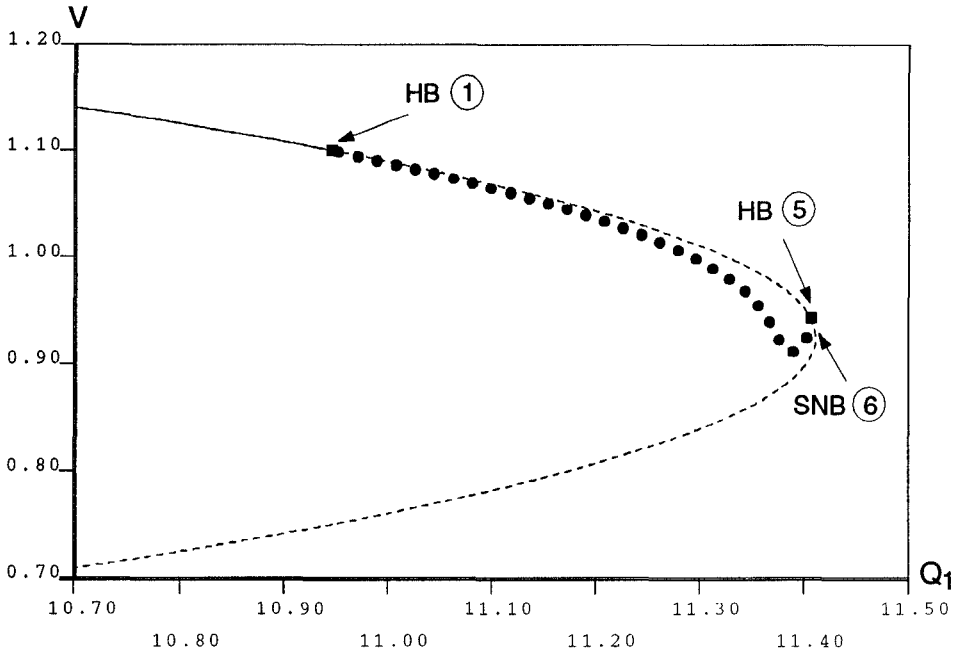

Figure 5.15: Bifurcation diagram of closed loop system with cubic control (k_n = 0.5)

supercritical bifurcation can be seen in Fig. 5.17 where the dynamic response of the system to increasing Q_1 to a value beyond HB① is shown. Transient trajectory (a) shows the increasing oscillations and ultimate voltage collapse without control. With nonlinear control and identical initial conditions, however, we see that the voltage settles to a small amplitude oscillation in trajectory (b) rather than collapsing.

Evidently such a control has a very favorable effect on the voltage collapse dynamics. By transforming the Hopf bifurcation HB① to a supercritical bifurcation, the multistability near HB① is eliminated and hence the occurrence of jump behavior of the system operating point under perturbation is prevented. More significantly, the system can operate at a small amplitude limit cycle as Q_1 crosses the previous collapse point $Q_1^{①}$ and this transition can be done in a con-

tinuous fashion. Also because of the supercriticality of the Hopf bifurcation in the closed loop system, the region of attraction of the nominal stable equilibrium is increased. As Q_1 increases further, the nominal equilibrium regains stability at $Q_1 = Q_1^{⑤}$ through the supercritical Hopf bifurcation HB⑤. The operation of the system takes yet another continuous transition from the small periodic orbit to the stable equilibrium as Q_1 crosses $Q_1^{⑤}$. The system can operate at the stable equilibrium until the saddle node bifurcation point SNB⑥ is encountered. Then a sharp drop in voltage collapse takes place.

Note that by introducing an alternative type of operating condition (a stable small amplitude limit cycle), though the static stability margin of the system remains the same as in the open loop case, the dynamic stability margin is increased up to the saddle node bifurcation point. Thus, in the closed loop system, the fatal voltage collapse then occurs at the saddle node bifurcation point (now agreeing with the scenario in [34]).

Linear Bifurcation Control

Since the critical mode is controllable, a linear stabilizing control exists for the stabilization of the Hopf bifurcation point. However, in the context of voltage collapse control, one has to consider the effect of such a control over a range of parameters. The effect may be difficult to determine since linear feedback will affect all the eigenvalues and eigenvectors. In particular, a high gain linear feedback may well destabilize modes that are open-loop stable. Also it should not be surprising that in some situations a linear feedback which locally stabilizes an equilibrium may result in globally unbounded behavior [3]. For small feedback gains, however, one can expect that the bifurcation will reappear at a different

parameter value. Fortunately, in this particular example, linear feedback with measurement of ω in the form

$$u = k_l \omega \tag{5.22}$$

can impart desirable effects on the system. In (5.22), $k_l > 0$ is the (scalar) linear feedback gain.

Since system (5.17)-(5.20) is a parametrized system, it is very difficult to study the effect of the linear control (5.22) over a range of parameter values by standard pole placement techniques directed at a particular equilibrium for a particular parameter value. However, if we consider the control gain k_l as a second parameter in the system in addition to the parameter Q_1, the effect of linear control can be tracked with two-parameter continuations of the Hopf bifurcation points (HB① and HB⑤). Recall that the control design does not affect the position of SNB⑥.

Fig. 5.16a shows a two-parameter (depending on k_l and Q_1) curve of the Hopf bifurcation points ① and ⑤. It can be seen that as k_l increases from 0, HB① and HB⑤ move closer to each other with HB① having a much faster pace. As k_l increases further, HB① merges with HB⑤ leading to their disappearance. Figs. 5.16b, 5.16c and 5.16d show that the Hopf window shrinks and ceases to exist. The benefits of eliminating the Hopf window are seen in trajectory (c) of Fig. 5.17, where increasing Q_1 to a point which is beyond the location of the original HB① results in the system settling down to the original, high voltage equilibrium branch. The initial conditions of trajectory (c) coincide with those of (a) and (b).

With linear bifurcation control (5.22), both the static and dynamic stability margins can be increased. When the Hopf bifurcations cease to exist (approxi-

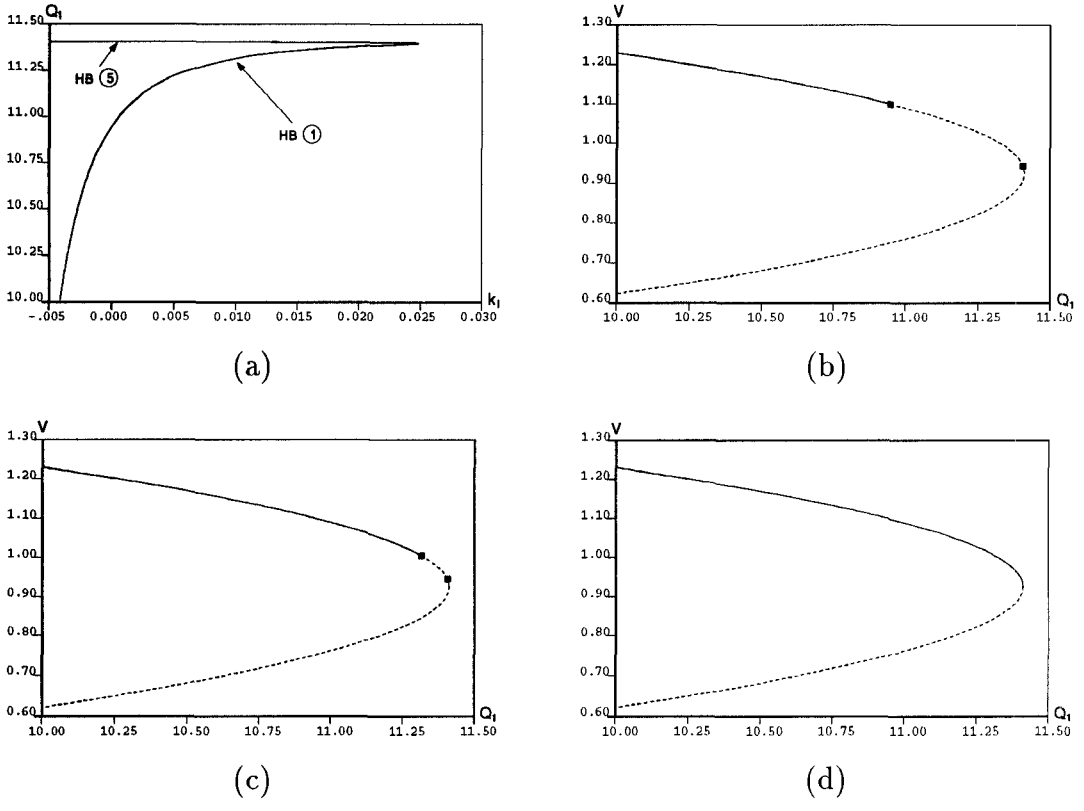

Figure 5.16: With linear bifurcation control: (a) two-parameter curves of the Hopf bifurcation points; bifurcation diagrams with (b) $k_l = 0$ (no control), (c) $k_l = 0.01$, (d) $k_l = 0.025$.

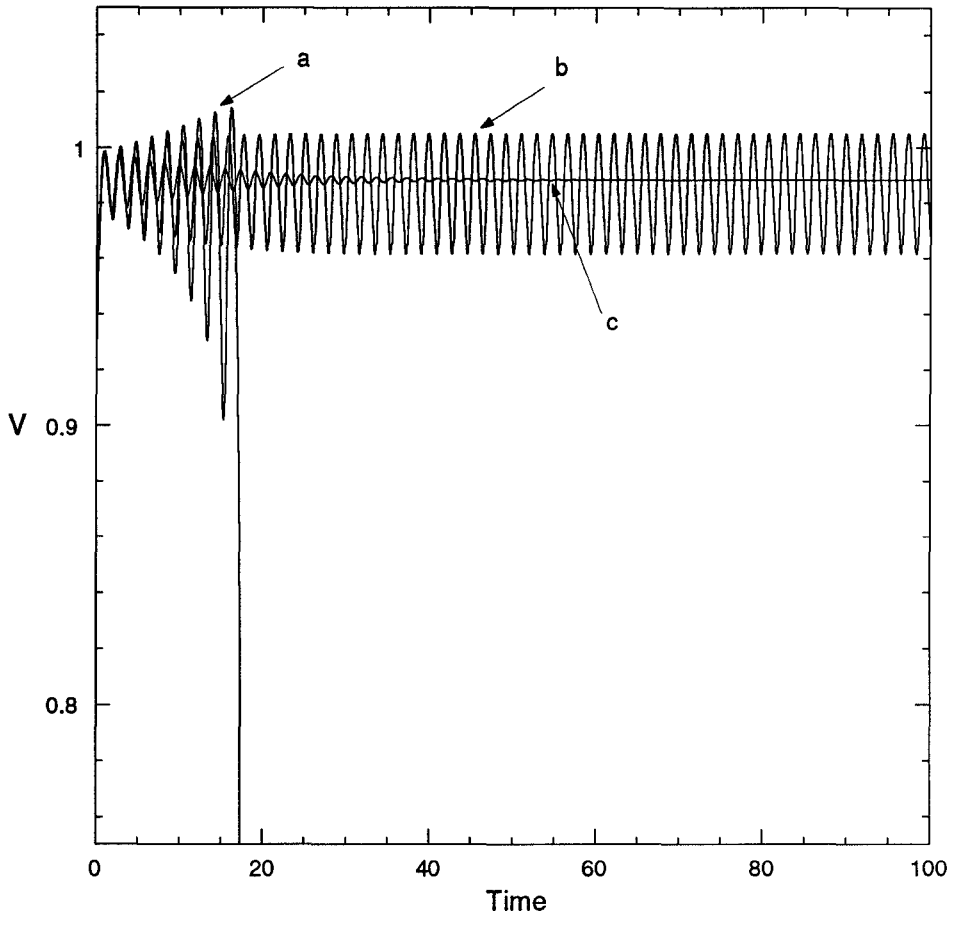

Figure 5.17: Dynamic responses of the system at $Q_1 = 11.35$: **a**. without control; **b**. with nonlinear control $k_n = 0.5$; **c**. with linear control $k_l = 0.025$.

mately for $k_l > 0.0245$), the static and dynamic stability margins are maximized in that the system can operate at a stable nominal equilibrium up to the saddle node bifurcation. Also, all the dynamic bifurcations, including Hopf bifurcations, period doubling bifurcations, period doubling cascade to chaos and crises, are extinguished.

Composite Bifurcation Control

The two types of control law given above, namely the cubic control (5.21) and the linear control (5.22), can be combined to result in a composite control law. The closed loop system is Eq. (5.17)-(5.20) with u of the form

$$u = k_l\omega + k_n\omega^3 \tag{5.23}$$

where $k_l > 0$ and $k_n > 0$ are the (scalar) linear and nonlinear feedback gains, respectively.

With this composite control, the designer has the freedom to choose proper static and dynamic stability margins. Besides the flexibility in terms of achievable behavior of the system under such control (over a range of parameter values), the nonlinear term in the control may be used to improve the transient response.

5.3.3 Voltage Collapse Control II

In this section, we consider local control of voltage collapse at its inception in the model of Section 5.2.3. The results parallel those of the subsection above, which were obtained for the model of Section 5.2.1.

In the model of Section 5.2.3, the stable equilibrium point loses its stability through the subcritical Hopf bifurcation (local), and the boundary crisis (global)

of the strange attractor triggers the voltage collapse. The subcriticality of the Hopf bifurcation has several negative effects on the system as we discussed before. The same control strategy is employed as in the previous subsection. It can be easily seen in this example that this is an approach to influence the various aspects of the global bifurcations (e.g., blue sky catastrophes) through local control.

We carry out the design of controllers for voltage collapse control for the model (5.7)-(5.10) subject to control u which is inserted additively at the right hand side of Eq. (5.10).

The objectives of control are 1) to prevent the occurrence of the jump behavior, 2) to increase the region of attraction of the stable equilibrium point, and 3) to delay the collapse (in parameter space). One control law design transforms the subcritical Hopf bifurcation into a supercritical bifurcation and ensures a sufficient degree of stability of the bifurcated periodic solutions over a range of parameter values of interest. These control laws allow stable operation close to the point of saddle node bifurcation. Another control design involves changing the critical parameter value at which the Hopf bifurcations occur through a linear feedback control. The voltage collapse can be delayed by such a linear control. Note that controllability of the critical mode facilitates the design.

Stabilizing the Hopf Bifurcation

To render the Hopf bifurcation HB① supercritical, we employ a cubic feedback with measurement of ω. The control u is of the form

$$u = -k_n \omega^3 \tag{5.24}$$

where $-k_n > 0$ is the (scalar) cubic feedback gain.

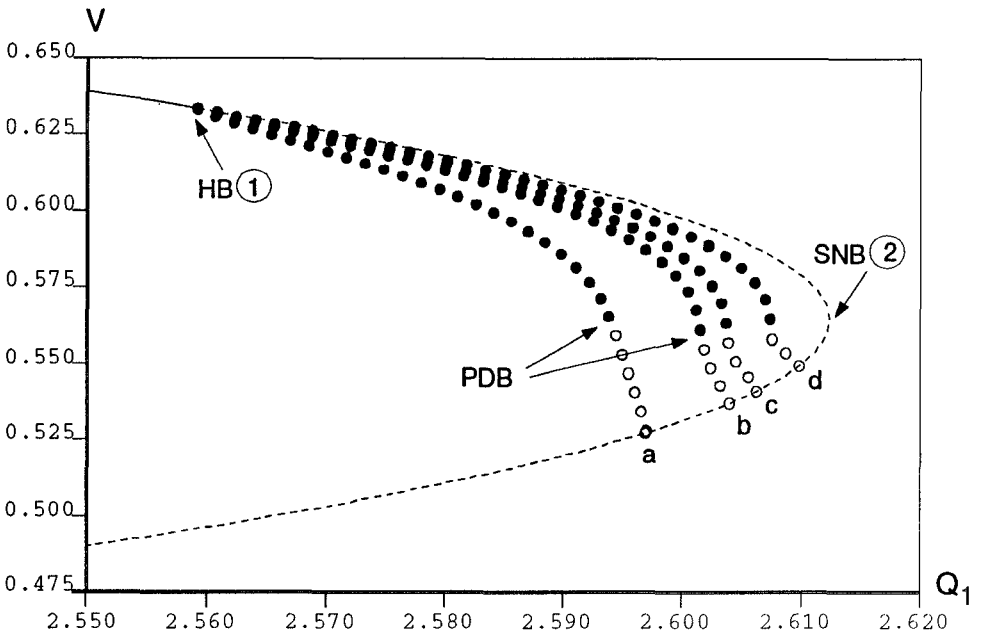

Figure 5.18: Superimposed bifurcation diagrams for cubic control with different gains: a. -0.1; b. -0.5; c. -1.0; d. -5.0

Fig. 5.18 shows superimposed bifurcation diagrams for the closed loop system with various control gains k_n. This along with simulation evidence indicates that larger values of the gain $|k_n|$ result in a reduced amplitude of the stable limit cycle. Note that the boundary crisis is delayed and the possible operating range of the system in parameter space is increased.

Delaying the Hopf Bifurcation

A linear control exists for delaying the Hopf bifurcation point:

$$u = -k_l \omega. \tag{5.25}$$

where $-k_l > 0$ is the (scalar) linear feedback gain.

Such a control is found to be able to delay the subcritical Hopf bifurcation HB① to parameter values extremely close to $Q_1^{②}$, where the saddle node bifur-

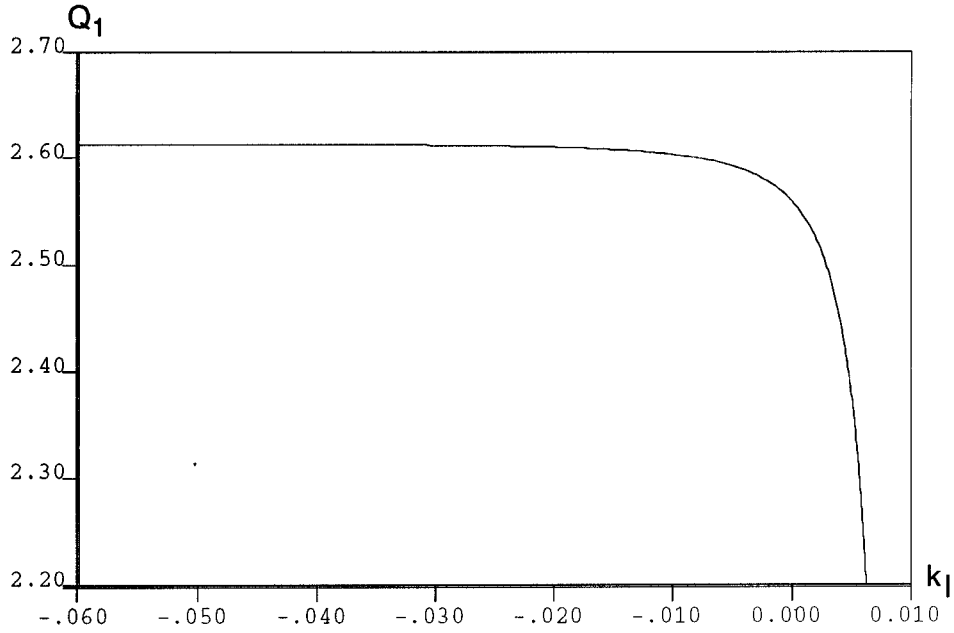

Figure 5.19: Relationship between critical Q_1 at which the Hopf bifurcation occurs and gain k_l of linear control

cation SNB② takes place. The relationship between the critical value $Q_1^{①}$ and the gain k_l in the closed loop system is found by a two-parameter (Q_1 and k_l) continuation of the Hopf bifurcation and is depicted in Fig. 5.19. Also another interesting consequence is that chaos and the boundary crisis can be eliminated by such a control.

Figure 5.20 illustrates the system responses for a value of Q_1 greater than the critical crisis value Q_1^*. Trajectory (a) is with no control, (b) is with nonlinear control (5.24), and (c) is with linear control (5.25).

The two types of control law given above, namely the cubic control (5.24) and the linear control (5.25), can be combined to result in a composite control law which both delays and stabilizes the Hopf bifurcation.

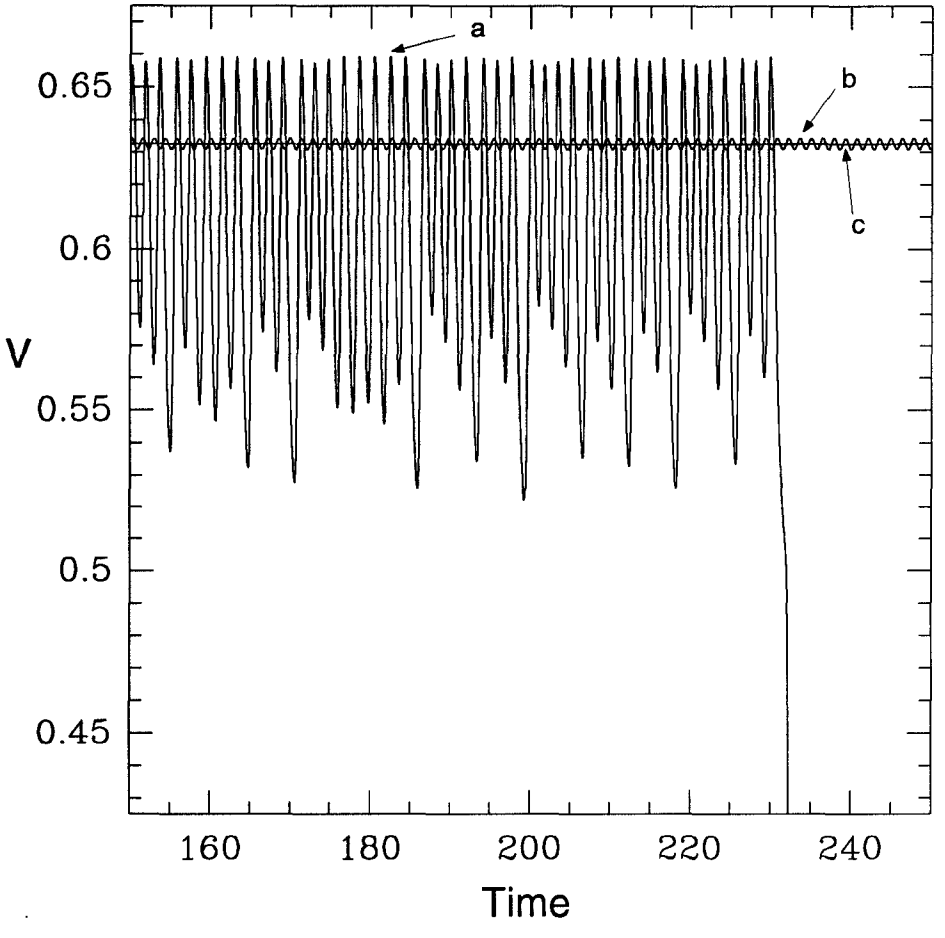

Figure 5.20: Sample trajectories of the system at $Q_1 = 2.560379$: **a.** without control; **b.** with nonlinear control $k_n = -0.1$; **c.** with linear control $k_l = -0.0618$.

5.4 Concluding Remarks

Nonlinear phenomena, including bifurcations and chaos, occurring in power system models exhibiting voltage collapse have been studied in this chapter. A new theory of voltage collapse is suggested. The theory emphasizes the role of catastrophic bifurcations in voltage collapse in electric power systems. The presence of the various nonlinear phenomena have also been determined to be crucial factors in the inception of voltage collapse in these models. Moreover, the problem of controlling voltage collapse in the presence of these nonlinear phenomena is addressed. The bifurcation control approach is employed to modify the bifurcations and to suppress chaos. The control law is shown to result in improved performance of the system for a greater range of parameter values. Although the relative importance of the effects of these nonlinear phenomena in general power systems under stressed conditions is still a topic for further research, the bifurcation control approach appears to be a viable technique for control of these systems.

Chapter 6

Active Control of Stall in Axial Flow Compressors

In this chapter, active stabilization of stall instabilities in axial flow compressors is pursued using a combination of bifurcation analysis and nonlinear control. A low-order discretization of a PDE compressor model is found to exhibit a stationary (pitchfork) bifurcation at the inception of stall. Using throttle opening as a control, analysis of the linearized system at stall shows that the critical mode (zero eigenvalue) is unaffected by linear feedback. Hence, nonlinear stabilization techniques are necessary. A nonlinear (quadratic) feedback control of the first mode amplitude is proposed based on the lower-order model and is found to eliminate or reduce the hysteresis for both the low order and high order discretizations. This improves the nonlinear stability of the compression system near the stall limit. Furthermore, the issue of designing nonsmooth feedback control laws is addressed. The merits of employing nonsmooth feedback are illustrated by bifurcation analysis of both the low order and high order discretizations. A possible mechanism for the nonsmooth feedback is suggested.

6.1 Introduction

Recent years have witnessed an increasing interest in axial flow compressor dynamics, both in terms of analysis of stall phenomena and their control [44]-[66], [50], [18]. This interest is due to the increased performance that is potentially achievable in modern gas turbine jet engines by operation near the maximum pressure rise. The increased performance comes at the price of a significantly reduced stability margin, since the steady, spatially-uniform gas flow loses stability when the system is operated near peak pressure-rise conditions. The resulting post-instability behavior leads to decreased operating performance of the compressor and to mechanical damage of the compression system.

In general there are two fundamentally different post-instability behaviors: surging flow and rotating stall [44]. Compressor *surge* occurs when the plenum gas pressure exceeds the compressor pressure rise and so low frequency (in time) oscillations of the mean gas flow rate develop. *Rotating stall* is a local aerodynamic phenomenon that occurs when the gas passing through the rotor disengages from the blade surface, reducing the local gas flow rate [31]. In this case, the bulk gas flow remains constant in time, but flow measurements taken along the circumferential coordinate (θ of Fig. 6.1) of the compressor rotor will reveal spatial variations of the local gas flow. This means the local gas velocity takes the form of a traveling wave, rotating about the compressor annulus.

Greitzer [44] developed a nondimensional fourth-order compression system model and introduced a nondimensional parameter, B, which he found to be a determinant of the nature of post-instability behavior. A global bifurcation of periodic solutions and other bifurcations were found for this model, and were used to explain the observed dependence of the dynamical behavior on the B

parameter [5], [61]. Moore and Greitzer [72] introduced a refined model to describe stall phenomena in axial flow compression systems. This model accounts for nonaxisymmetric flow patterns, whereas the model of Greitzer [44] had no means of explicitly describing spatial effects.

Our work begins with a modification [103] to the 2-dimensional partial differential equation model of Moore and Greitzer [72] to include viscous dissipative forces in the unsteady performance of a compressor blade row. The resulting compression system model, while somewhat more complicated that the original Moore-Greitzer model, is still amenable to formal local stability and bifurcation analysis. Detailed studies about the transition from steady, spatially-uniform flow to nonuniform and time-dependent gas axial velocity profiles in this modified model are presented in [13]. It is found that the first stalled-flow solution is born through a *subcritical* bifurcation, meaning the bifurcating solution is born unstable. The practical importance of the subcritical stall bifurcation, however, is that when the uniform-flow operating point is subject to perturbations, the system will jump to a large amplitude, fully developed stall cell. Subcritical bifurcations also imply hysteresis, and so returning the throttle to its original position may not bring the system out of stall.

Several techniques have been proposed for active control of stall instabilities in axial flow compressors (e.g., [79], [50], [18]). From an analytical point of view, these methods employ linear control for avoiding or delaying the occurrence of stall. Of course the physical mechanisms of a proposed control implementation differ among the proposed active control schemes. The present work and that of [62], however, begin with the recognition of the importance of local bifurcations as determinants of the nature of post-instability behavior of axial flow compres-

sion systems. In [62] a nonlinear state feedback law was proposed for the Moore and Greitzer model [72] simplified to three ordinary differential equations with a low-order Galerkin discretization. The control philosophy of this work and that of [62] is similar to that of Abed and Fu [3]. This entails determining feedback control laws which ensure the stationary bifurcation results in only stable bifurcated solutions. Thus, even though the nominal equilibrium is not stabilizable within the framework of linear theory, it may be possible to stabilize a neighborhood of the nominal solution for a range of parameter values including the stall value of the throttle opening parameter, to finite amplitude perturbations. The control law is designed analytically based on the low-order discretization and is applied to both the low-order and high-order spectral discretizations of the full system. Bifurcation analysis of a high-order discretization is used to assess the effectiveness of the controller.

In addition to the smooth feedback control design, it is found that some nonsmooth feedback controllers render surprisingly superior performance over smooth feedback designs. The merits of the nonsmooth feedback controllers are judged by bifurcation studies. Though theoretically bifurcation analysis of nonsmooth systems is still a largely open area, the results revealed in this study appear to point out a new avenue in terms of control of bifurcating systems and critical system stabilization.

The chapter proceeds as follows. In Section 6.2, modification of the Moore-Greitzer model is presented [103]. In Section 6.3, analytical computations useful in the analysis of stationary bifurcations are reviewed. These results are applied to study the stability of a low order discretization of the axial flow compression system in the vicinity of the stall point. The low order model is obtained by

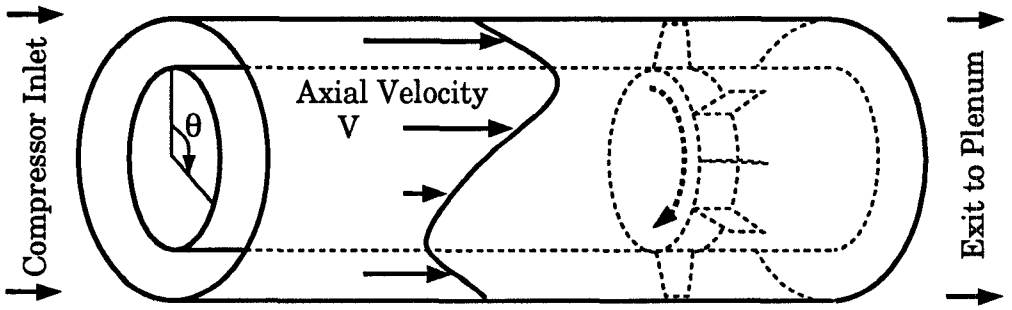

Figure 6.1: A schematic of the compressor geometry

applying Galerkin's method to the full PDE model. A pitchfork-type stationary bifurcation is observed in the model at the stall point. In Section 6.4, a throttle opening control law is given. This nonlinear control law circumvents the uncontrollability of the zero eigenvalue of the linearized model at stall. A purely quadratic state feedback using measurement of the asymmetric flow disturbance amplitude is given, and found to result in local stabilization of the bifurcation leading to stall not only in the low order model, but also in high-order discretizations of the compression system model. In Section 6.5, the use of nonsmooth feedback is discussed.

Nomenclature

a_n, b_n, A_n	mode amplitude coefficients
B	plenum/compressor volume
c	wave speed
f	axisymmetric compressor characteristic
f_0	shut-off head
F	throttle characteristic
H	pressure rise scaling factor

k	controller gain
l_c	overall compressor length
m	exit duct length factor
n	mode number
u	control input
v	axial velocity perturbation
v_0	perturbation at $\eta = 0$
V	mean axial velocity
V_{loc}	total local axial velocity
w	mean velocity scaling factor

α	internal compressor lag
γ	throttle opening
γ_0	nominal throttle opening
Δ_p	plenum-atmosphere pressure rise
η	axial coordinate
θ	circumferential coordinate
λ_n	n'th eigenvalue
μ	viscosity
τ	time

6.2 Modification of the Moore-Greitzer Model

The model is based on Moore and Greitzer's model [72], but a term which accounts for momentum transfer in the compressor section by viscous transport

is also included [103]. A local momentum balance describing the two-dimensional flow in the compressor and its associated ducting gives the partial differential equation:

$$\triangle_p = f(V + v_0) - l_C \frac{dV}{d\tau} - m\frac{\partial}{\partial\tau}\int_{-\infty}^{0} v d\eta - \frac{1}{2\alpha}\left[2\frac{\partial v_0}{\partial\tau} + \frac{\partial v_0}{\partial\theta} - \mu\frac{\partial^2 v_0}{\partial\theta^2}\right]. \quad (6.1)$$

Note that our notation differs considerably from the original notation of Moore and Greitzer [72]: V denotes the annulus-averaged (mean) gas axial velocity; v_0 is the axial velocity perturbation evaluated at $\eta = 0$ (the inlet face of the compressor); Δ_p is the plenum-to-atmosphere pressure rise; η, θ are the axial and angular coordinates, respectively; and μ is the gas viscosity.

The compressor pressure rise $f(V_{loc})$ is particular to each compressor and is obtained from experiments in the stable operating range and estimated in the nonuniform-flow range. Following Moore and Greitzer [72] we use a cubic equation in axial velocity

$$f(V_{loc}) = f_0 + H\left[1 + \frac{3}{2}\left(\frac{V_{loc}}{\omega} - 1\right) - \frac{1}{2}\left(\frac{V_{loc}}{\omega} - 1\right)^3\right] \quad (6.2)$$

where $V_{loc} = V + v_0$ (the total local axial flow) and the characteristic parameters used throughout this work are given in Table 6.1, with l_c fixed at a representative value [72, 73]. If there are no spatial variations of gas density and pressure in the plenum, an overall material balance on the gas over the plenum gives:

$$l_C \frac{d\triangle_p}{d\tau} = \frac{1}{4B^2}\left[V(\tau) - F^{-1}(\triangle_p)\right] \quad (6.3)$$

where the throttle characteristic is given by the orifice equation

$$F^{-1}(\triangle_p) = \gamma\sqrt{\triangle_p}. \quad (6.4)$$

The parameter γ is proportional to the throttle opening.

Parameter	*Value*	*Description*
α	1/3.5	internal compressor lag
l_c	8.0	overall compressor length
m	1.75	exit duct length factor
H	0.18	compressor characteristic height factor
w	0.25	compressor characteristic width factor
f_0	0.3	shut-off head
μ	0.01	fluid viscosity

Table 6.1: Values of Compressor Parameters

6.3 Stability Analysis

In this section we first recall some bifurcation-theoretic results on stability of one-parameter families of nonlinear systems. They then will be applied to study the dynamic behavior of axial flow compression systems.

6.3.1 Bifurcation Formulae

Consider a one-parameter family of nonlinear autonomous systems

$$\dot{x} = f_\mu(x), \tag{6.5}$$

with $f_\mu(x_{e,\mu}) = 0$, where $x \in \mathbb{R}^n$, μ is a real-valued parameter, f_μ is sufficiently smooth in x and μ, and $x_{e,\mu}$ is the nominal equilibrium point of the system as a function of the parameter μ. Suppose the following hypothesis holds:

(S) The Jacobian matrix of system (6.5) at the equilibrium $x_{e,\mu}$ possesses a simple eigenvalue $\lambda_1(\mu)$ with $\lambda_1(0) = 0$, $\lambda_1'(0) \neq 0$, with the remaining eigen-

values $\lambda_2(0), \cdots, \lambda_n(0)$ lie in the open left-half complex plane for μ within a neighborhood of $\mu_c = 0$.

Theorem 2.1 asserts that hypothesis (S) leads to a stationary bifurcation from $x_{e,0}$ at $\mu = 0$ for Eq. (6.5). That is, new equilibrium points bifurcate from $x_{e,0}$ at $\mu = 0$. Recall that near the point $(x_{e,0}, 0)$ of the $(n+1)$-dimensional (x, μ)-space, there exists a parameter ϵ and a locally unique curve of critical points $(x(\epsilon), \mu(\epsilon))$, distinct from $x_{e,\mu}$ and passing through $(x_{e,0}, 0)$, such that for all sufficiently small $|\epsilon|$, $x(\epsilon)$ is an equilibrium point of (6.5) when $\mu = \mu(\epsilon)$.

The parameter ϵ may be chosen so that $x(\epsilon), \mu(\epsilon)$ are smooth. The series expansion of $x(\epsilon), \mu(\epsilon)$ can be written as

$$\mu(\epsilon) = \mu_1\epsilon + \mu_2\epsilon^2 + \cdots \tag{6.6}$$

$$x(\epsilon) = x_{e,0} + x_1\epsilon + x_2\epsilon^2 + \cdots \tag{6.7}$$

If $\mu_1 \neq 0$, the system undergoes a transcritical bifurcation from $x_{e,\mu}$ at $\mu = 0$. That is, there is a second equilibrium point besides $x_{e,\mu}$ for both positive and negative values of μ with $|\mu|$ small. If $\mu_1 = 0$ and $\mu_2 \neq 0$, the system undergoes a pitchfork bifurcation for $|\mu|$ sufficiently small. That is, there are two new equilibrium points for *either* positive *or* negative values of μ with $|\mu|$ small. The new equilibrium points have an eigenvalue β which vanishes at $\mu = 0$. The series expansion of β in ϵ is given by

$$\beta(\epsilon) = \beta_1\epsilon + \beta_2\epsilon^2 + \cdots \tag{6.8}$$

with

$$\beta_1 = -\mu_1\lambda'(0), \tag{6.9}$$

and, in case $\beta_1 = 0$, β_2 is given by

$$\beta_2 = -2\mu_2\lambda'(0). \tag{6.10}$$

Thus, the system exhibits an *exchange of stabilities* at the bifurcation point $x_{e,0}$ (at $\mu = 0$).

The stability coefficients β_1 and β_2 can be determined solely by eigenvector computations and the coefficients of the series expansion of the vector field. System (6.5) can be rewritten in the series form

$$\begin{aligned}\dot{\hat{x}} &= L_\mu \hat{x} + Q_\mu(\hat{x},\hat{x}) + C_\mu(\hat{x},\hat{x},\hat{x}) + \cdots \\ &= L_0\hat{x} + \mu L_1\hat{x} + \mu^2 L_2\hat{x} + \cdots \\ &\quad + Q_0(\hat{x},\hat{x}) + \mu Q_1(\hat{x},\hat{x}) + \cdots \\ &\quad + C_0(\hat{x},\hat{x},\hat{x}) + \cdots \end{aligned} \tag{6.11}$$

Here, $\hat{x} := x - x_{e,0}$, L_μ, L_0, L_1, L_2 are $n \times n$ matrices, $Q_\mu(x,x)$, $Q_0(x,x)$, $Q_1(x,x)$ are vector-valued quadratic forms generated by symmetric bilinear forms, and $C_\mu(x,x,x), C_0(x,x,x)$ are vector-valued cubic forms generated by symmetric trilinear forms.

By assumption, the Jacobian matrix L_0 has only one simple zero eigenvalue with the remaining eigenvalues stable. Denote by l and r the left (row) and right (column) eigenvectors of the matrix L_0 corresponding to the simple zero eigenvalue, respectively, where the first component of r is set to 1 and the left eigenvector l is chosen such that $lr = 1$. It is easy to check [51, 65] that

$$\lambda'(0) = lL_1r \tag{6.12}$$

Stability criteria for system (6.11) can be summarized in the following two lemmas. For details, see [3].

Lemma 6.1 *The bifurcated solutions of (6.11) for μ near 0, which appear only for $\mu > 0$ (resp. $\mu < 0$) when $lL_1r > 0$ (resp. $lL_1r < 0$), are asymptotically*

stable if $\beta_1 = 0$ *and* $\beta_2 < 0$, *and are unstable if* $\beta_1 = 0$ *and* $\beta_2 > 0$. *Here,*

$$\beta_1 = lQ_0(r,r) \tag{6.13}$$

$$\text{and} \quad \beta_2 = 2l\{2Q_0(r,\chi_2) + C_0(r,r,r)\} \tag{6.14}$$

with χ_2 *satisfying the following equation:*

$$L_0\chi_2 = -Q_0(r,r). \tag{6.15}$$

Lemma 6.2 *Suppose the value of* β_1 *given in (6.13) above is negative. Then the bifurcated solution occurring for* $\mu > 0$ *(resp.* $\mu < 0$*) is asymptotically stable when* $lL_1r > 0$ *(resp.* $lL_1r < 0$*).*

The criterion given in Lemma 6.1 corresponds to the pitchfork (stationary) bifurcation, while the one in Lemma 6.2 is for the transcritical (stationary) bifurcation. Examples of these bifurcation diagrams can be found in many books on bifurcation theory, e.g., [53].

6.3.2 Stability Analysis of Rotating Stall

The rotating stall equilibria born at the stall bifurcation point are spatial waves of local axial velocity, rotating at a constant speed around the annulus. Rather than computing these traveling wave solutions as limit cycles in the Fourier coefficient space, a more efficient method is to introduce a rotating coordinate frame $\theta \mapsto \theta + c\tau$ so that the amplitude coefficients of the traveling waves can be found as fixed points. Making this coordinate change affects the PDE (6.1) only:

$$\begin{aligned}\Delta_p = {} & f(V + v_0) - l_C\frac{dV}{d\tau} - m\int_{-\infty}^{0}\Big[c\frac{\partial v}{\partial\theta} + \frac{\partial v}{\partial\tau}\Big]d\eta \\ & -\frac{1}{2\alpha}\Big[2c\frac{\partial v_0}{\partial\theta} + 2\frac{\partial v_0}{\partial\tau} + \frac{\partial v_0}{\partial\theta} - \mu\frac{\partial^2 v_0}{\partial\theta^2}\Big].\end{aligned} \tag{6.16}$$

Near the bifurcation point, the amplitude of the bifurcating mode will dominate the shape of the stall cell. Thus, in the neighborhood of the bifurcation point we can approximate v by the eigenfunction associated with the critical eigenvalue λ_n

$$v = \exp(n\eta)\left[a_n \cos(n\theta) + b_n \sin(n\theta)\right] \tag{6.17}$$

(and so $v_0 = a_n \cos(n\theta) + a_n \sin(n\theta)$), substitute (6.17) into (6.16) to form the residual, use Galerkin's method to determine the amplitude coefficients, and constrain the Fourier coefficients by the relationship

$$A_n^2 = a_n^2 + b_n^2, \tag{6.18}$$

we obtain the greatly simplified, third-order set of ODEs (c.f. eqns (58-61) of Moore and Greitzer (1986) [72]):

$$\frac{m\alpha + n}{n\alpha}\frac{dA_n}{d\tau} = \left[\frac{3HV}{2\omega^3}(2\omega - V) - \frac{\mu n^2}{2\alpha}\right] A_n - \frac{3H}{8\omega^3}A_n^3, \tag{6.19}$$

$$l_C \frac{dV}{d\tau} = -\triangle_p + f_0 + \frac{HV^2}{2\omega^3}(3\omega - V) + \frac{3H}{4\omega^3}(\omega - V)A_n^2, \tag{6.20}$$

$$l_C \frac{d\triangle_p}{d\tau} = \frac{1}{4B^2}\left[V - \gamma\sqrt{\triangle_p}\right]. \tag{6.21}$$

Our control design will be carried out based on the stability analysis of system (6.19)-(6.21) for the case $n = 1$ (the first harmonic of the flow disturbance). The controller, however, will be applied to a high-order discretization in the ensuing numerical analysis. To solve for an equilibrium point of (6.19)-(6.21), it is easy to see that $A_1 = 0$ is always a solution of $dA_1/d\tau = 0$ for the right hand side of Eq. (6.19). However, $A_1 = 0$ may not be the necessary condition for the existence of equilibrium point for (6.19)-(6.21). Denote $\hat{x} = (0, \hat{V}, \hat{\triangle}_p)^T$ as an equilibrium point for (6.19)-(6.21) at $\gamma = \gamma^0$. $\hat{V}$ and $\hat{\triangle}_p$ should then satisfy the relationships $\hat{V} = \gamma\sqrt{\hat{\triangle}_p}$ and $\hat{\triangle}_p = f(\hat{V})$. Under the assumption $A_1 = 0$, $\hat{x}$ denotes a *uniform*

flow equilibrium point for the axial flow compression model (6.19)-(6.21), which depends on the throttle control parameter γ^0. In the following, we consider the stability conditions for the uniform flow equilibrium $\hat{x}$ and treat γ as a bifurcation parameter to seek possible bifurcating stalled-flow solutions emanating from $\hat{x}$ such that $A_1 \neq 0$.

Let $X = (x_1, x_2, x_3)^T$ denote the state variation of the third order model above near the uniform flow equilibrium point $\hat{x}$, where $x_1 = A_1, x_2 = V - \hat{V}$ and $x_3 = \triangle_p - \hat{\triangle}_p$. The linearization of (6.19)-(6.21) at $\hat{x}$ for $\gamma = \gamma^0$ is

$$\frac{dX}{dt} = L_0 X, \tag{6.22}$$

where

$$L_0 = \begin{pmatrix} \left[\frac{3H\hat{V}}{2\omega^3}(2\omega - \hat{V}) - \frac{\mu}{2\alpha}\right]\frac{\alpha}{m\alpha+1} & 0 & 0 \\ 0 & \frac{3H\hat{V}}{2\omega^3}(2\omega - \hat{V})\frac{1}{l_C} & -\frac{1}{l_C} \\ 0 & \frac{1}{4B^2 l_C} & -\frac{\gamma^0}{8B^2\sqrt{\hat{\triangle}_p} l_C} \end{pmatrix}. \tag{6.23}$$

From (6.23), the linearization of (6.19)-(6.21) has one zero eigenvalue when $\frac{3H\hat{V}}{2\omega^3}(2\omega - \hat{V}) = \frac{\mu}{2\alpha}$. This implies a stationary bifurcation may occur from the equilibrium point $\hat{x}$ for some value of γ_0. The bifurcation calculations of the preceding subsection will now be applied to derive the conditions for existence and stability of such a bifurcation.

Let $\hat{x}$ be the equilibrium point at which $\frac{3H\hat{V}}{2\omega^3}(2\omega - \hat{V}) = \frac{\mu}{2\alpha}$ for $\gamma = \gamma^0$. Taking the Taylor series expansion of (6.19)-(6.21) at the point $(\hat{x}, \gamma^0)$, we have

$$\frac{dX}{dt} = L_0 X + Q_0(X, X) + C_0(X, X, X) + (\gamma - \gamma^0) L_1 X + \cdots \tag{6.24}$$

where L_0 is as in (6.23) and

$$Q_0(X,X) = \begin{pmatrix} \frac{\alpha}{m\alpha+1}\frac{3H}{\omega^3}(\omega-\hat{V})x_1x_2 \\ \frac{3H}{4\omega^3}(\omega-\hat{V})(x_1^2+2x_2^2)\frac{1}{l_C} \\ \frac{\gamma^0}{32B^2l_C\hat{\Delta}_p\sqrt{\hat{\Delta}_p}}x_3^2 \end{pmatrix}, \tag{6.25}$$

$$C_0(X,X,X) = \begin{pmatrix} -\frac{\alpha}{m\alpha+1}\frac{3H}{8\omega^3}(x_1^3+4x_1x_2^2) \\ -\frac{3H}{\omega^3}(\frac{1}{4}x_1^2x_2+\frac{1}{6}x_2^3)\frac{1}{l_C} \\ -\frac{\gamma^0}{64B^2l_C\hat{\Delta}_p^2\sqrt{\hat{\Delta}_p}}x_3^3 \end{pmatrix}, \tag{6.26}$$

$$L_1 = \begin{pmatrix} \frac{\alpha}{m\alpha+1}\frac{3H}{\omega^3}(\omega-\hat{V})\frac{\partial\hat{V}}{\partial\gamma} & 0 & 0 \\ 0 & \frac{1}{l_C}\frac{3H}{\omega^3}(\omega-\hat{V})\frac{\partial\hat{V}}{\partial\gamma} & 0 \\ 0 & 0 & -\frac{1}{8B^2\sqrt{\hat{\Delta}_p}l_C}\left[1-\frac{\gamma^0}{2\hat{\Delta}_p}\frac{\partial\hat{\Delta}_p}{\partial\gamma}\right] \end{pmatrix}. \tag{6.27}$$

Choose $l=(1,0,0)$ and $r=l^T$ as the left and right eigenvectors corresponding to the zero eigenvalue of L_0. The dynamical behavior of (6.19)-(6.21) with respect to variation of γ near the unstalled point $\hat{x}$ is obtained as follows.

The transversality condition $lL_1r \neq 0$ is obtained as

$$lL_1r = \frac{\alpha}{m\alpha+1}\frac{3H}{\omega^3}(\omega-\hat{V})\frac{\partial\hat{V}}{\partial\gamma} \neq 0, \tag{6.28}$$

and the bifurcation stability coefficients are calculated, using Eqs. (6.13) and (6.14), as

$$\beta_1 = lQ_0(r,r) = 0 \tag{6.29}$$

$$\begin{aligned} \beta_2 &= 2l\{2Q_0(r,\chi_2)+C_0(r,r,r)\} \\ &= \frac{\alpha}{m\alpha+1}\frac{3H}{4\omega^3}(8(\omega-\hat{V})\zeta-1) \end{aligned} \tag{6.30}$$

where

$$\zeta = \frac{-\frac{3H}{4\omega^2}+\frac{3H\hat{V}}{4\omega^3}}{\frac{\mu}{2\alpha}-\frac{2\sqrt{\hat{\Delta}_p}}{\gamma^0}} \tag{6.31}$$

$$= \frac{3H(\hat{V}-\omega)\gamma^0}{6H\hat{V}(2\omega-\hat{V})\gamma^0 - 8\omega^3\sqrt{\hat{\Delta}_p}}. \tag{6.32}$$

Note that at $\gamma = \gamma^0$

$$\frac{3H\hat{V}}{2\omega^3}(2\omega-\hat{V}) = \frac{\mu}{2\alpha} \tag{6.33}$$

The next result follows readily from Lemma 6.1 and the discussions above.

Theorem 6.3 (Stability) *Suppose the quantity lL_1r given in (6.28) is nonzero as is the stability coefficient β_2 given in (6.30). Then system (6.19)-(6.21) exhibits a pitchfork-type stationary bifurcation with respect to the small variation of γ at the point $(\hat{x}, \gamma^0)$, where Eq. (6.33) holds. Moreover, if $\beta_2 < 0$ (resp. $\beta_2 > 0$) the local bifurcated solutions near $\hat{x}$ will be asymptotically stable (resp. unstable).*

The uniform-flow equilibrium point becomes unstable after the parameter γ crosses the critical value γ^0, the *stall bifurcation point.* Moreover, according to Theorem 6.3 the local bifurcated solutions, near the stall point, may not be stable. If such a condition occurs, the compression system will exhibit a jump from the stable nominal equilibrium when the parameter γ crosses the critical value γ^0. Also the subcritical nature of the stall bifurcations along with secondary limit-point bifurcations leads to operating conditions featuring multistability: conditions where the locally stable uniform flow solution coexists with a locally stable fully developed stall cell. This results in a *hysteresis loop* of the stable equilibria with respect to the parameter γ near the stall point. Practically this means that the system will jump from the uniform-flow operating point to a fully developed stall cell under perturbations in the range of multistability.

Numerical bifurcation analysis was carried out to verify the predicted compression system behavior and to study the bifurcation behavior of the stalled-flow

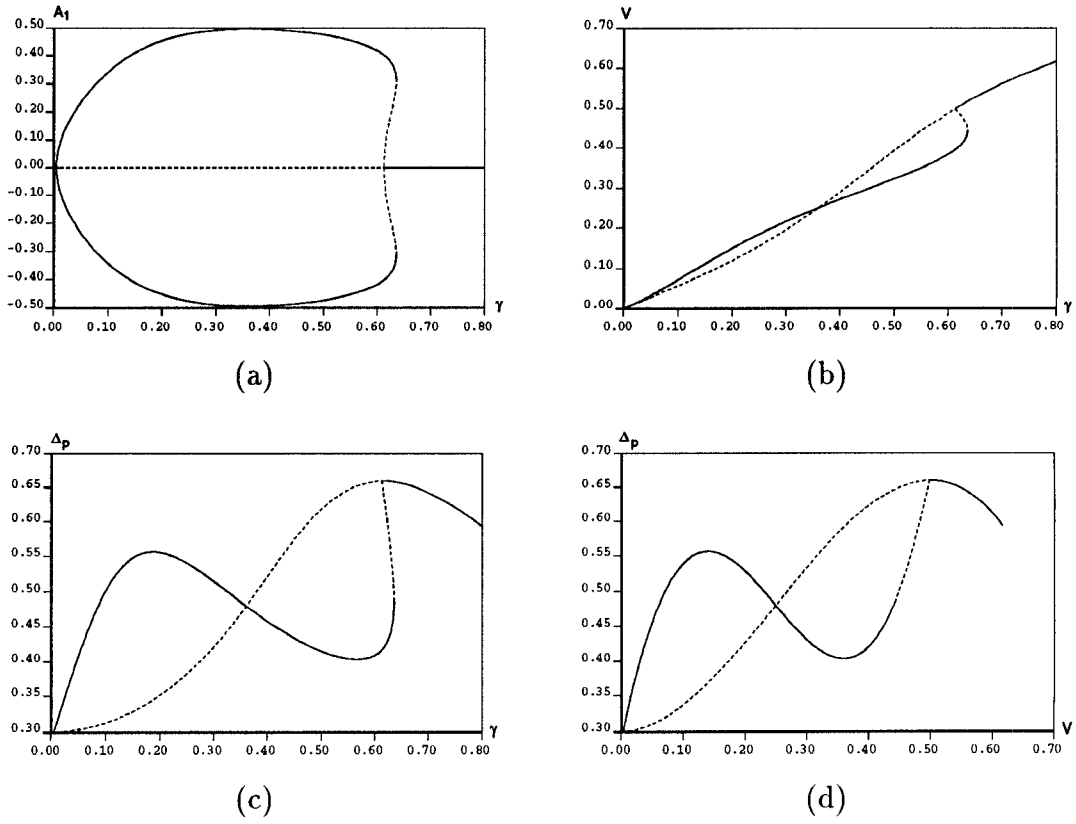

Figure 6.2: Subcritical pitchfork stationary bifurcations in the open loop axial flow compression system

solutions outside the range of validity of the local analysis. The results are shown in Fig. 6.2. In Fig. 6.2, a solid curve represents a locus of locally asymptotically stable equilibrium points, while dashed curves correspond to unstable branches. There are two pitchfork stationary bifurcations, one stable and the other unstable. The numerical analysis vividly demonstrates the large magnitude of the jump resulting from the hysteresis loop associated with the unstable bifurcation point. It is not possible to observe the pitchfork bifurcation phenomena in Figs. 6.2(b), 6.2(c), and 6.2(d) since the stalled-flow solutions $(A_1, \hat{V}, \hat{\triangle}_p)$ possess the symmetry $\hat{V}(A_1) = \hat{V}(-A_1)$ and $\hat{\triangle}_p(A_1) = \hat{\triangle}_p(-A_1)$.

6.4 Stabilization of Rotating Stall Using Smooth Feedback

In this section, we seek possible feedback control laws based on regulating the throttle setting which improve the operability near the stall point by eliminating the hysteresis loop and preventing the jump behavior associated with the unstable stall bifurcation. So $\gamma = \gamma^0 + u$ is substituted into the plenum mass balance (6.3). This type of control appears to be simpler to implement than those techniques depending on directly affecting the flow field in the compress inlet duct [79], [32]. Moreover, successful experimental results have been reported [36].

6.4.1 Low-Order Model

Denote $(\hat{x}, \gamma^0)$ as the stall point and let $\gamma := \gamma^0 + u$, where u is the control input. We then can rewrite system (6.19)-(6.21) as a throttle control system given by

$$\frac{m\alpha + n}{n\alpha}\frac{dA_n}{d\tau} = \left[\frac{3HV}{2\omega^3}(2\omega - V) - \frac{\mu n^2}{2\alpha}\right]A_n - \frac{3H}{8\omega^3}A_n^3, \tag{6.34}$$

$$l_C\frac{dV}{d\tau} = -\triangle_p + f_0 + \frac{HV^2}{2\omega^3}(3\omega - V) + \frac{3H}{4\omega^3}(\omega - V)A_n^2, \tag{6.35}$$

$$l_C\frac{d\triangle_p}{d\tau} = \frac{1}{4B^2}\left[V - (\gamma^0 + u)\sqrt{\triangle_p}\right]. \tag{6.36}$$

We observed from (6.34) that $A_1 = 0$ is an invariant submanifold of (6.34)-(6.36) unaffected by the value of control input u, which implies that (6.34)-(6.36) is uncontrollable. Moreover, it is not difficult to check that system (6.34)-(6.36) possesses an uncontrollable zero eigenvalue at the stall point. This means that we can not extend the range γ where the uniform-flow solution is locally asymptotically stable with any type of state feedback in (6.34)-(6.36).

Next, we consider the design of a control law which guarantees stability of the local bifurcated solutions near the stall point. From the property of the exchange of stability, the system will not jump from the stable uniform-flow equilibrium near the stall point if the local bifurcated solutions are stable. In the following, for simplicity, we consider the control input u to be a *purely nonlinear* feedback of the state variations as given by

$$u = k_1 x_1^2 + k_2 x_1 x_2 + k_3 x_1 x_3 + k_4 x_2^2 + k_5 x_2 x_3 + k_6 x_3^2 + U(x_1, x_2, x_3) \qquad (6.37)$$

where U is a high order function. Using formulae (6.13) and (6.14) to calculate the stability coefficients β_1^* and β_2^* for the controlled model (6.34)-(6.36) at $\hat{x}$, we obtain

$$\begin{aligned} \beta_1^* &= \beta_1 = 0 \qquad (6.38) \\ \beta_2^* &= \beta_2 + 4\frac{\alpha}{m\alpha+1}\frac{3H}{\omega^3}(\omega - \hat{V})\frac{k_1}{2}\frac{2\hat{\Delta}_p}{\frac{\mu\gamma^0}{2\alpha} - 2\sqrt{\hat{\Delta}_p}} \\ &= \beta_2 + Ck_1 \qquad (6.39) \end{aligned}$$

where β_1 and β_2 are the stability coefficients of the uncontrolled version of (6.34)-(6.36). It is observed from the expression of β_2^* that only the quadratic feedback $k_1 A_1^2$ contributes to the determination of system stability. We have the following result

Theorem 6.4 (Stabilization) *The stationary bifurcation of (6.34)-(6.36) at the point $(\hat{x}, \gamma^0)$ can be guaranteed to be a supercritical pitchfork bifurcation by a purely quadratic feedback control if $C \neq 0$. The feedback control is of the form $u = k_1 A_1^2$.*

The numerical results for the controlled case are given in Fig. 6.3. By Theorem 6.4, we find that purely quadratic feedback control laws will stabilize bifur-

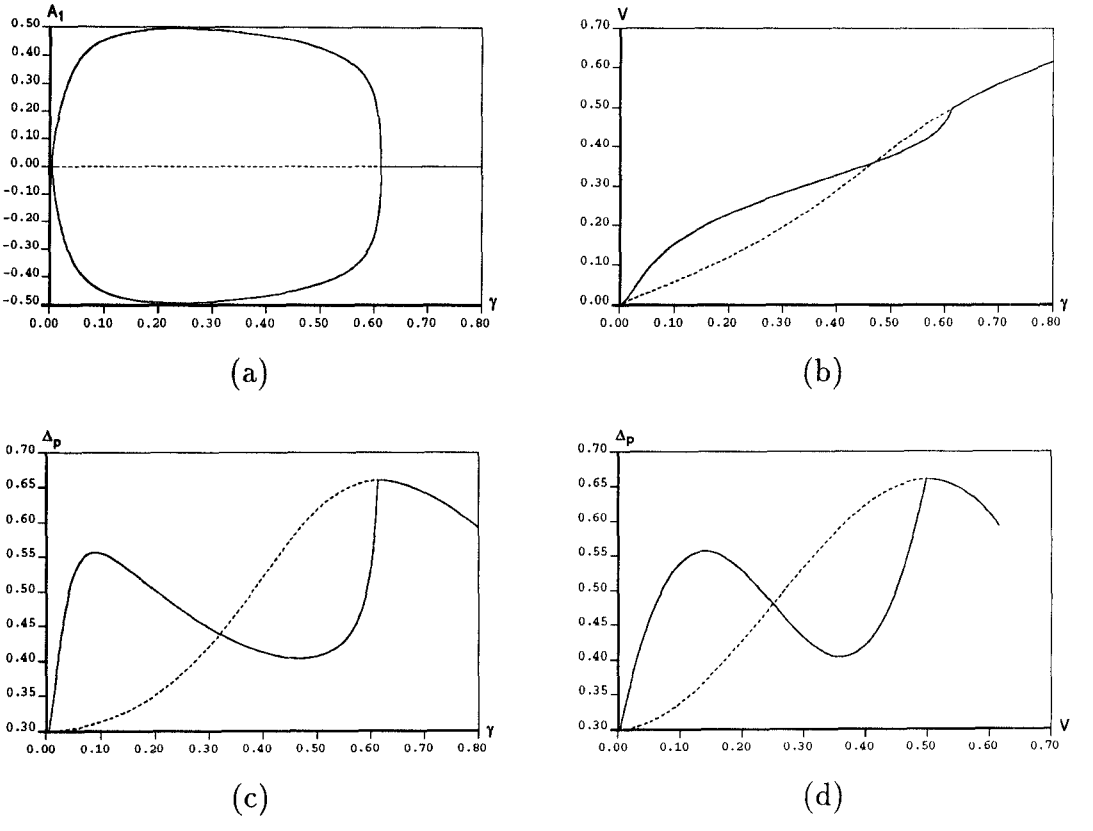

Figure 6.3: Supercritical pitchfork bifurcations in the closed-loop axial flow compression system

cated equilibrium solutions. The control input is given by

$$u = k_1 A_1^2 \tag{6.40}$$

with $k_1 = 0.5$. It is not difficult to see that the hysteresis loops of the stable system equilibria shown in Fig. 6.2 no longer exist in Fig. 6.3.

6.4.2 High-Order Models

We have designed the control law based on a highly truncated discretization of the flow field perturbation. To test the controller in a more realistic manner, the

gas axial velocity perturbation v is approximated by

$$v = \sum_{n=1}^{N} \exp(n\eta) \left[a_n \cos(n\theta) + b_n \sin(n\theta) \right] \tag{6.41}$$

and, as before, the axial velocity profile at the inlet guide vanes is denoted v_0 (at $\eta = 0$). Substituting the Fourier expansion into the local momentum balance PDE and using Galerkin's method to determine the amplitude coefficients, we obtain

$$\left\{ \frac{m}{n} + \frac{1}{\alpha} \right\} \dot{a}_n = \frac{1}{\pi} \int_0^{2\pi} f \cos(n\theta) d\theta - \frac{\mu n^2}{2\alpha} a_n - \frac{n}{2\alpha} b_n \tag{6.42}$$

$$\left\{ \frac{m}{n} + \frac{1}{\alpha} \right\} \dot{b}_n = \frac{1}{\pi} \int_0^{2\pi} f \sin(n\theta) d\theta - \frac{\mu n^2}{2\alpha} b_n + \frac{n}{2\alpha} a_n \tag{6.43}$$

along with the ODEs

$$l_C \frac{dV}{d\tau} = -\Delta_p + \frac{1}{2\pi} \int_0^{2\pi} f d\theta \tag{6.44}$$

$$l_C \frac{d\Delta_p}{d\tau} = \frac{1}{4B^2} \left[V(\tau) - F^{-1}(\Delta_p) \right]. \tag{6.45}$$

The only nonlinearities in the ODEs above are the throttle and compressor performance characteristics. One of the advantages of using the cubic compressor characteristic is that the integrals can be evaluated explicitly. These results are discussed in detail by Adomaitis [13] and are given in Appendix 6.A. Thus, we obtain a large set of ordinary differential equations in time describing the dynamics of the Fourier mode amplitude coefficients.

Denoting γ^0 as the nominal stall point of the throttle opening parameter and letting $\gamma := \gamma^0 + u$, where u is the control input, we consider feedback of *only* the amplitude of the first Fourier mode of the flow disturbance in the controller:

$$u = k(a_1^2 + b_1^2). \tag{6.46}$$

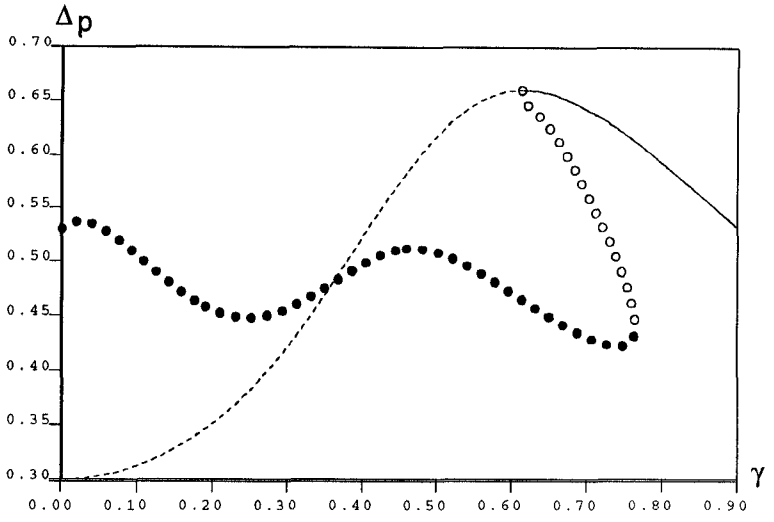

Figure 6.4: Bifurcation diagram of open loop high-order system

Using the same numerical bifurcation analysis techniques discussed in the previous section and extensive simulation studies, we find controller (6.46) is effective in eliminating the hysteresis loop in the vicinity of stall point for high-order discretizations (large N in (6.41)). Thus the occurrences of jump behavior of the stable system equilibria are prevented.

For the results reported in this work, we take $N = 2$. See [14] for representative results on $N = 6$. Figure 6.4 is a bifurcation diagram of the open-loop system. Note that the stall bifurcation is a subcritical Hopf bifurcation. The bifurcated solution becomes stable through a cyclic fold bifurcation, resulting a hysteresis loop near the stall point. Since the Hopf bifurcation is linearly uncontrollable, results from Section 3.3.2, especially Theorem 3.2 show that only quadratic terms in the feedback control can influence the value of stability coefficient β_2. Thus control function (6.46) is a logical choice.

To see the effect of the nonlinear controller (6.46), bifurcation analysis of the high-order discretization under control is carried out. In Fig. 6.5 a bifurcation

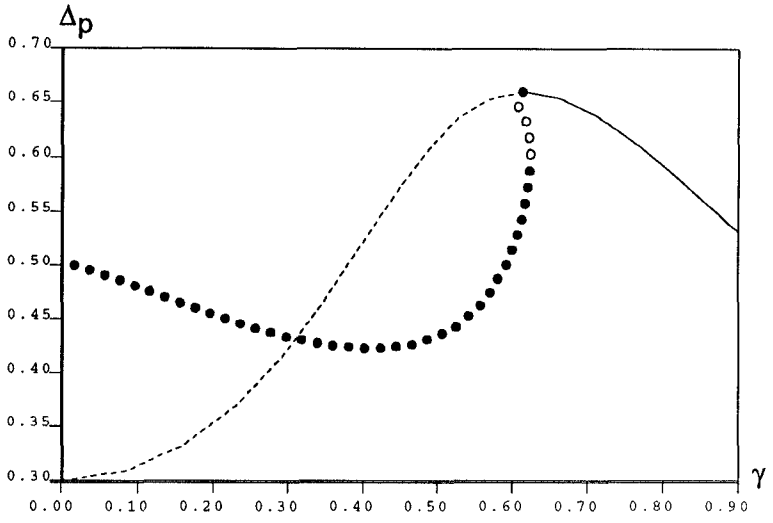

Figure 6.5: Bifurcation diagram of closed-loop high-order system ($k = 2.5$)

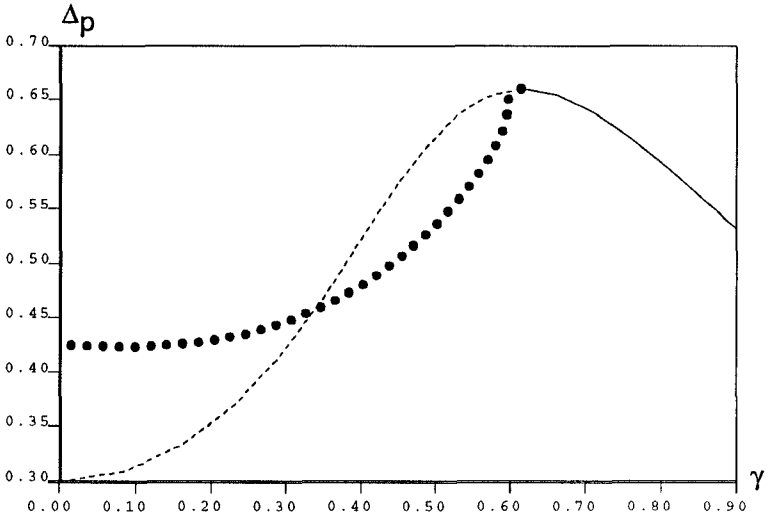

Figure 6.6: Bifurcation diagram of closed-loop high-order system ($k = 5.0$)

diagram of the closed-loop system with $k = 2.5$ is shown. Locally the stall bifurcation is now a supercritical Hopf bifurcation. However, the bifurcating stalled flow solution becomes unstable giving rise to a hysteresis loop. Even with increased controller gain (Fig. 6.6 $k = 5$), the hysteresis loop still persists (not discernible from Fig. 6.6, but can be seen if the region near the stall point is magnified) but with a reduced range in parameter space. While hysteresis is not completely eliminated in this case, the stability of the system to finite sized perturbation in the axial velocity profile is still improved and the range of the hysteresis is also reduced under this control.

6.5 Stabilization of Rotating Stall Using Non-smooth Feedback

As shown in the last section, the hysteresis can not be completely eliminated by the controller (6.46) with even a rather large gain. So far in this dissertation, we have only considered smooth feedback. Our theory results in a quadratic controller. The topological characteristic of the controller of the form $u = kx^2$ is (See Fig. 6.7)

- symmetric in x
- monotone in $|x|$.

Based on this observation, we conjecture that any controller having these two properties at least locally around $x = 0$ would locally stabilize the stall bifurcation.

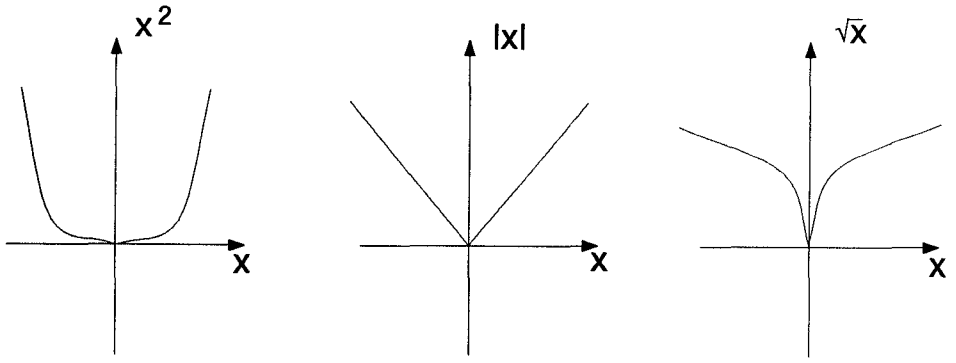

Figure 6.7: Qualitative characteristic of control functions

6.5.1 Low-Order Model

The conjecture above is supported by the bifurcation analysis of the low-order system under the following nonsmooth feedback control:

$$u = k|A_1| \tag{6.47}$$

and

$$u = k\sqrt{|A_1|} \tag{6.48}$$

Figure 6.8 illustrates the effect of such nonsmooth controllers. It can be clearly seen that the use of such nonsmooth controllers has significant advantages. With less control energy, the nonsmooth controllers effectively eliminate the hysteresis loop. More significantly, the pressure rise can be kept at a high level beyond the stall point.

We remark that the two controllers above are just a subset of a family of controllers that will show such advantages over the smooth feedback design. For example any controller of the form

$$u = k|A_1|^{\beta_n/\beta_d} \qquad \beta_n \leq \beta_d \tag{6.49}$$

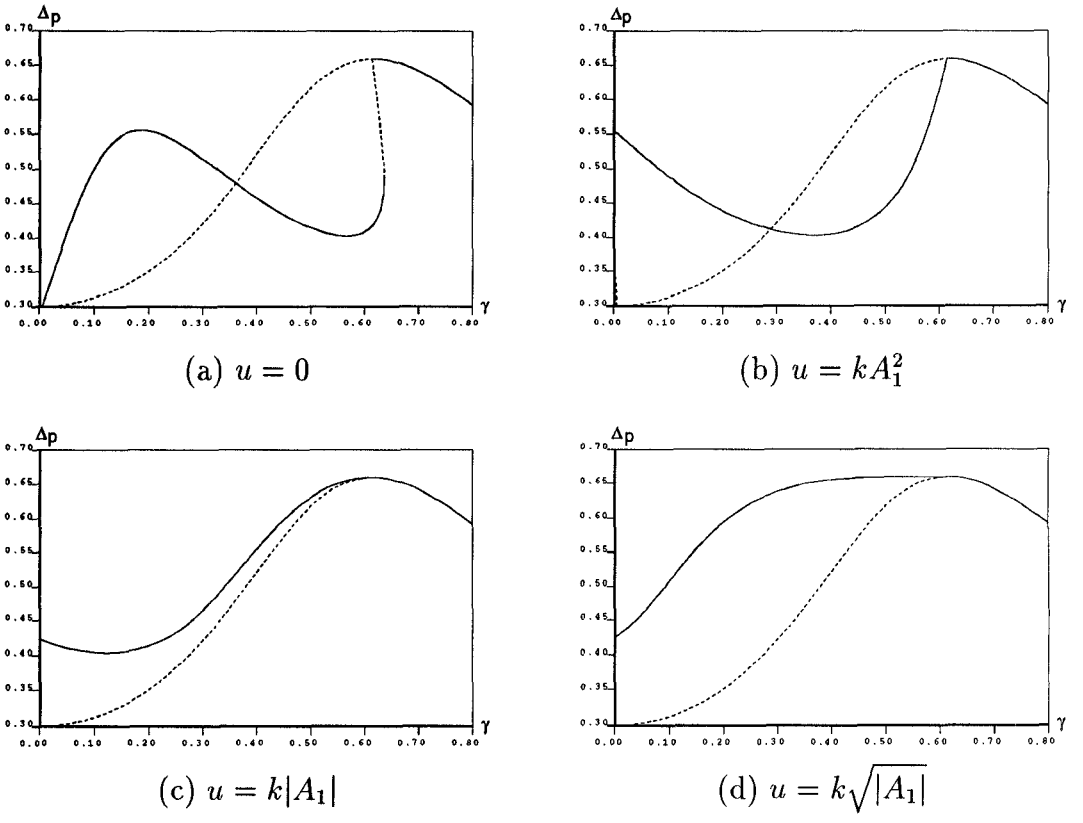

(a) $u = 0$ (b) $u = kA_1^2$

(c) $u = k|A_1|$ (d) $u = k\sqrt{|A_1|}$

Figure 6.8: Bifurcation diagrams in low-order model: smooth vs. nonsmooth feedback ($k = 1.0$)

belongs to such a family. Next we consider the use of nonsmooth feedback in the high-order discretization models.

6.5.2 High-Order Models

Two representative controllers are applied to the high-order model:

$$u = k\sqrt{a_1^2 + b_1^2} \tag{6.50}$$

and

$$u = k(a_1^2 + b_1^2)^{\frac{1}{4}}. \tag{6.51}$$

Figure 6.9 the illustrates the effect of the two controllers above vs. the open-loop case and that of smooth feedback. The nonsmooth controllers can completely eliminate the hysteresis loop with less control energy than smooth feedback. Also the pressure rise is kept at a high level beyond the stall point.

This brings up the natural question, presently under investigation, of the bifurcation mechanisms associated with nonsmooth systems. General theory on bifurcation of nonsmooth systems is in general an open area. Some case studies [76] exist in the literature. In terms of controllers (6.48) and (6.51) etc., the common feature is that the derivatives of the control function at the origin are infinity (see Fig. 6.7 and 6.10). This indicates "infinite local stabilizing power." In this regard, there is a strong resemblance to the terminal attractor theory of [106]. In the case of controllers (6.47) and (6.50), though the local stabilizing power is not infinite, it is still larger than those of controllers (6.40) and (6.46). The use of nonsmooth feedback in bifurcation control theory or even the general control theory is a worthy new avenue.

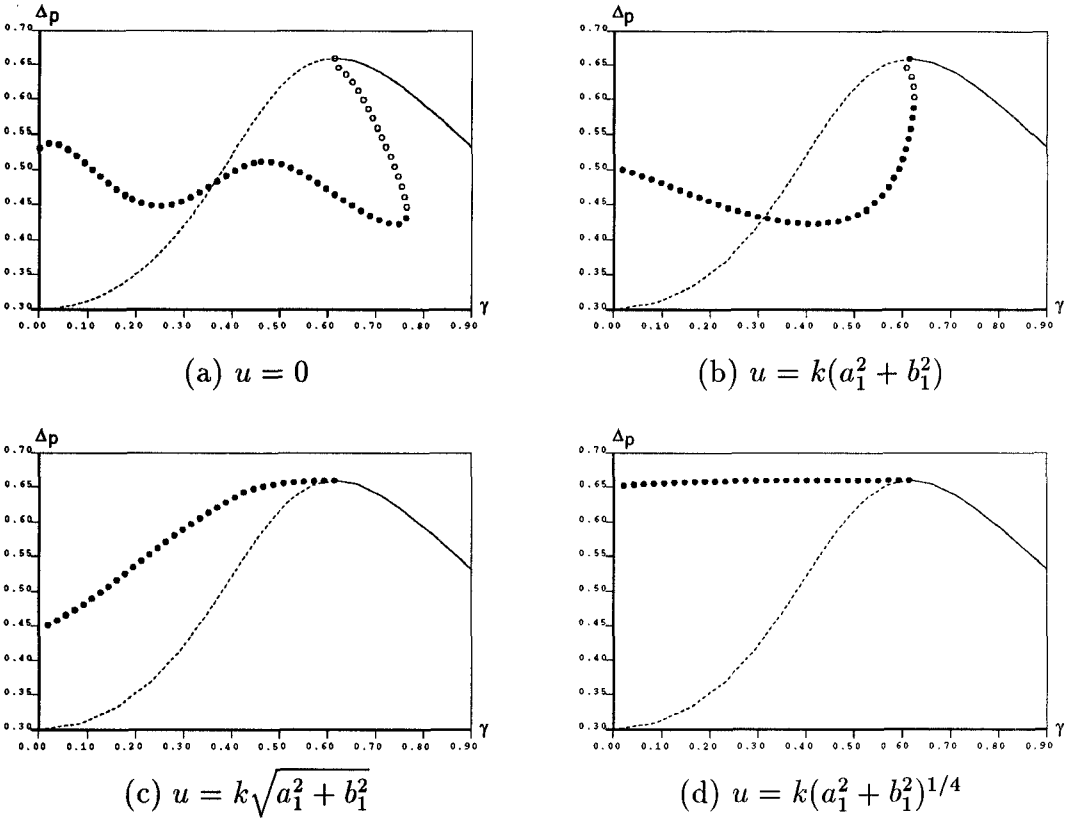

(a) $u = 0$ (b) $u = k(a_1^2 + b_1^2)$

(c) $u = k\sqrt{a_1^2 + b_1^2}$ (d) $u = k(a_1^2 + b_1^2)^{1/4}$

Figure 6.9: Bifurcation diagrams in high-order model ($N = 2$): smooth vs. nonsmooth feedback ($k = 2.5$)

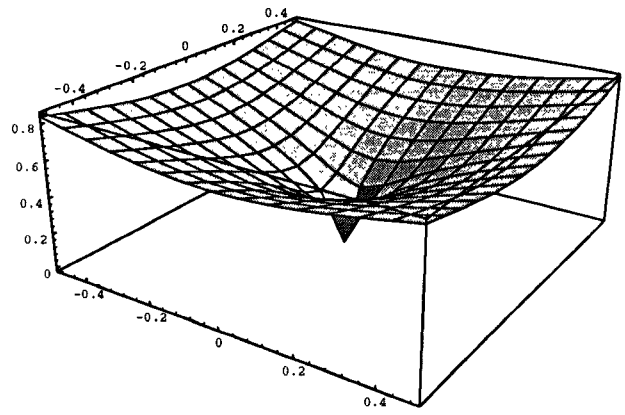

Figure 6.10: Plot of $f(x,y) = (x^2 + y^2)^{1/4}$

Controllers such as (6.46), (6.47), (6.50) have been successfully implemented in experiments [36].

6.6 Concluding Remarks

This chapter has investigated the design of stabilizing feedback control laws for rotating stall in axial flow gas compressors. The proposed approach begins with recognizing the importance of local bifurcations in determining the nature of post-instability behavior of axial flow compression systems. The controllers are (analytically) designed based on a highly-truncated discretization of a compressor model, and then are applied to both the low-order model and high-order discretizations. Although the results are obtained using a particular dynamical model, the bifurcation based control approach appears to be a viable technique for control of these systems.

Appendix 6.A

The integral found in the average momentum balance ODE is [13]:

$$\frac{1}{2\pi}\int_0^{2\pi} f\,d\theta = P_{co} + \frac{HV^2(3w-V)}{2w^3} + \frac{3H(w-V)}{4w^3}\sum_{i=1}^{N}\left(a_i^2+b_i^2\right)$$

$$-\frac{H}{8w^3}\sum_{i,j=1}^{N}\left[a_ia_j(2a_{i-j}+a_{i+j})+3a_ib_j(b_{j-i}-b_{i-j}+b_{i+j})\right]$$

for arbitrary truncation number N. Evaluation of the $\cos(n\theta)$ moment gives

$$\frac{1}{\pi}\int_0^{2\pi} f\cos(n\theta)d\theta = \frac{3HV(2w-V)}{2w^3}a_n + \frac{3H(w-V)}{4w^3}\sum_{i=1}^{N}\left[a_i(a_{i-n}+a_{i+n}+a_{n-i})\right.$$

$$\left.+b_i(b_{i-n}+b_{i+n}-b_{n-i})\right]-\frac{H}{8w^3}\sum_{i,j=1}^{N}\left[a_ia_j(2a_{i-j-n}+2a_{i-j+n}+a_{i+j-n}+a_{i+j+n}+a_{n-i-j})\right.$$

$$\left.+\,3a_ib_j(b_{j-i-n}+b_{j-i+n}+b_{i+j-n}+b_{i+j+n}-b_{i-j-n}-b_{i-j+n}-b_{n-i-j})\right]$$

and the $\sin(n\theta)$ moment gives

$$\frac{1}{\pi}\int_0^{2\pi} f\sin(n\theta)d\theta = \frac{3HV(2w-V)}{2w^3}b_n + \frac{3H(w-V)}{2w^3}\sum_{i=1}^{N}\left[a_i(b_{i+n}-b_{i-n}+b_{n-i})\right]$$

$$-\frac{H}{8w^3}\sum_{i,j=1}^{N}\left[3a_ia_j(2b_{i-j+n}-2b_{i-j-n}+b_{i+j+n}+b_{n-i-j}-b_{i+j-n})\right.$$

$$\left.+\,b_ib_j(2b_{i-j+n}-2b_{i-j-n}+b_{i+j-n}-b_{i+j+n}-b_{n-i-j})\right].$$

Chapter 7

Conclusions and Suggestions for Further Research

We have focused on the the control of nonlinear instabilities in high performance engineering systems. These belong to the class of problems that cannot be adequately addressed without recourse to results from nonlinear dynamics. As system parameters vary to satisfy the high performance requirement, nonlinear phenomena grow and dominate the control problems. In such cases one needs to study control of nonlinear phenomena such as bifurcations and chaos.

A new approach to the control of chaotic dynamical systems has been presented, namely the bifurcation control approach. The idea has been illustrated in the context of a thermal convection loop model. A washout filter-aided feedback control stabilizes a primary bifurcation in a sequence of bifurcations leading to chaos. It has been shown that feedback controls achieving a sufficient degree of stability for the primary bifurcation also extinguishes transient chaos and chaos. The technique results in equilibrium preservation even in the face of model uncertainty.

To further complement the work on bifurcation control of routes to chaos,

the stabilization of period doubling bifurcations for discrete-time nonlinear systems has been investigated. Both static and dynamic feedback controllers have been studied. It has been shown that generically such bifurcations can be stabilized using smooth feedback, even if the linearized system is uncontrollable at criticality. In the course of the analysis, expressions have been derived for bifurcation stability coefficients of general n-dimensional systems undergoing period doubling bifurcation. A connection has been determined between control of the amplitude of a period doubled orbit and the elimination of a period doubling cascade to chaos. For illustration, the results have been applied to the Hénon system.

Most of the major electric power system breakdowns in recent years have been caused by the dynamic response of the system to disturbances. Moreover, in response to today's ever-increasing demands for increased performance, there is considerable interest in operating a power system ever close to the edge of the stability boundary. Thus dynamic security assessment of power systems is becoming increasingly important. One type of system instability which occurs for a heavily loaded electric power system is voltage collapse. In this dissertation, the analysis and control of voltage collapse in electric power systems have been considered. We have challenged the existing theory of linking voltage collapse exclusively to a saddle node bifurcation by showing a variety of nonlinear phenomena existing in power system models exhibiting voltage collapse. A new mechanism of voltage collapse has been suggested based on the framework of catastrophic bifurcations. More significantly, active control of voltage collapse has been addressed. Bifurcation control laws have been designed to control the nonlinear phenomena at the inception of voltage collapse. The control laws have

been shown to result in improved performance of the system for a greater range of parameter values.

Another very important example of engineering systems near the limits of their operating envelope is the stall phenomena in modern axial gas flow compressors. The operation of compression systems is prone to the dynamic instabilities of surge and rotating stall, either of which can lead to catastrophic failure of the compression system. In this dissertation, we have used a combination of bifurcation analysis and nonlinear control to study the dynamics and active control of rotating stall in an axial flow compressor model. It has been found that the stalled flow solutions are born in subcritical bifurcations and the effect of secondary bifurcations leads to hysteresis. Practically this means that the system will jump from the uniform-flow operating point to a fully developed stall cell under perturbations. Moreover, because of hysteresis the system cannot recover from stall by returning the throttle to its original position. Using throttle opening as a control, it was also found that the stall bifurcations are not linearly stabilizable. Hence nonlinear stabilizing control laws have been designed. A nonlinear (quadratic) feedback control of the first mode amplitude has been proposed based on the lower-order model and has been found to eliminate or reduce the hysteresis for both the low order and high order discretizations. This control design has improved the nonlinear stability of the compression system near the stall margin. Furthermore, the issue of designing nonsmooth feedback control laws has been addressed. The merits of employing nonsmooth feedback have been illustrated by bifurcation analysis of both the low order and high order discretizations. A possible mechanism for nonsmooth feedback was suggested. Successful experimental results have been reported regarding both the smooth

and nonsmooth feedback controllers designed in this work.

To further extend the research covered in this dissertation, several possible directions are noted as follows. Some of these problems are currently under investigation.

1. Most of the existing results on controlling chaos are directed towards low-dimensional systems. By contrast, our methodology is applicable to systems with arbitrary (finite) dimensions. Some intriguing applications are "controlling weather" and "controlling turbulence." These cases usually deal with systems with very high dimensionality. A good starting point is the two-layer quasi-model introduced by Lorenz [63], but with modifications to include the beta effect and bottom topography [56], [24]. It is our hope that our research on controlling chaos can serve as a humble step towards the seemingly impossible task of controlling weather and turbulence.

2. The stabilization of period doubling bifurcations is achieved in the setting of discrete time systems. However, to apply the results to continuous-time nonlinear systems, one has to first construct a Poincaré map. The procedure for constructing the Poincaré map is usually very unsystematic and in most cases it is impossible to get an analytical form for this map. Thus it is highly desirable to extend the results to continuous-time nonlinear systems. One possible approach to this problem is to use the exchange of stability property which is well known in bifurcation theory. Combining this property with the describing function method, it can be determined whether the bifurcated period-doubled orbits occur supercritically or subcritically.

This determines their stability, and further calculations determine the degree of stability.

3. To extend the results on voltage collapse in electric power systems, one can add an excitation system to the models considered in this dissertation. Similar techniques can be used then to study the relationship between voltage collapse and excitation control.

4. Another problem currently under investigation is the control of nonlinear systems near fold bifurcations. The idea is to extend the operating range of a system by introducing secondary attractors beyond the fold bifurcation point.

5. We have demonstrated that nonsmooth feedback can deliver surprisingly superior performance in the active control stall in axial flow compressors. The impact is two-fold: i) The theory on bifurcation analysis of nonsmooth systems is still a largely open problem; ii) The bifurcation control, critical system stabilization or even the general nonlinear control theory will be reshaped by developments in nonsmooth feedback design.

Bibliography

[1] E.H. Abed and P.P. Varaiya, "Nonlinear oscillations in power systems," *Int. J. Elec. Power and Energy Syst.*, Vol. 6, 1984, pp. 37-43.

[2] E.H. Abed and J.-H. Fu, "Local feedback stabilization and bifurcation control, I. Hopf bifurcation," *Systems and Control Letters*, Vol. 7, 1986, pp. 11-17.

[3] E.H. Abed and J.-H. Fu, "Local feedback stabilization and bifurcation control, II. Stationary bifurcation," *Systems and Control Letters*, Vol. 8, 1987, pp. 467-473.

[4] E.H. Abed, P.K. Houpt and W.M. Hosny, "Bifurcation analysis of surge and rotating stall in axial flow compressors," *Proc. 1990 American Control Conference*, San Diego, 1990, pp. 2239-2246. Also *ASME J. Turbomachinery*, Vol. 115, 1993, pp. 817-824.

[5] E.H. Abed, A.M.A. Hamdan, H.-C. Lee and A.G. Parlos, "On bifurcations in power system models and voltage collapse," *Proceedings of the 29th IEEE Conference on Decision and Control*, Honolulu, 1990, pp. 3014-3015.

[6] E.H. Abed and H.-C. Lee, "Nonlinear stabilization of high angle of attack flight dynamics using bifurcation control," *Proc. 1990 American Control Conf.*, May 1990, pp. 2235-2238.

[7] E.H. Abed, *Notes for ENEE769D: Bifurcation and Chaos in Feedback Systems*, Dept. of Electrical Engineering, Univ. of Maryland, College Park, Fall 1991.

[8] E.H. Abed, J.C. Alexander, H. Wang, A.M.A. Hamdan and H.-C. Lee, "Dynamic bifurcations in a power system model exhibiting voltage collapse," *Proceedings of the 1992 IEEE Int. Symp. on Circuits and Systems*, San Diego, May 1992.

[9] E.H. Abed, H.O. Wang and R.C. Chen, "Stabilization of period doubling bifurcations and implications for control of chaos," *Proceedings of the 31th IEEE Conference on Decision and Control*, Tucson, Arizona, December 1992, pp. 2119-2124.

[10] E.H. Abed and H.O. Wang, "Feedback control of bifurcation and chaos in dynamical systems," *Recent Developments in Stochastic and Nonlinear Dynamics: Applications to Mechanical Sysstems*, a volume commemorating the 60th birthday of Professor S.T. Ariaratnam, CRC Press, 1993, N. Sri Namachchivaya and W. Kliemann, Editors.

[11] R. H. Abraham, "Chaostrophes, intermittency, and noise," *Chaos, Fractals, and Dynamics*, P. Fischer and W.R. Smith (eds), Dekker, New York, 1985.

[12] R. H. Abraham and J. Robbin, *Transversal Mappings and Flows*, New York: W.A. Benjamin, Inc., 1967.

[13] R.A. Adomaitis and E. H. Abed, "Bifurcation analysis of nonuniform flow patterns in axial-flow gas compressors," *Proc. 1992 World Cong. Nonlinear Analysts*, Tampa, FL, 1992.

[14] R.A. Adomaitis and E.H. Abed, "Local nonlinear control of stall inception in axial flow compressors," *Proc. 29th Joint Propulsion Conference and Exhibit*, Monterey, CA, June 1993; in press.

[15] V. Ajjarapu and B. Lee, "Bifurcation theory and its application to nonlinear dynamical phenomena in an electrical power system," *IEEE Trans. on Power Systems*, Vol. 7, 1992, pp. 424-431.

[16] P.M. Anderson and A.A. Fouad, *Power System Control and Stability,* Iowa State Univ. Press, Ames, IA, 1977.

[17] V.I. Arnold, *Geometrical Methods in the Theory of Ordinary Differential Equations*, Springer Verlag, New York, 1983.

[18] O.O. Badmus, C.N. Nett and F. J. Schork, "An integrated, full-range surge control/rotating stall avoidance compressor control system," *Proc. 1991 Amer. Contr. Conf.*, Boston, 1991, pp. 3173-3179.

[19] J. Baillieul, R.W. Brockett and R.B. Washburn, "Chaotic motion in nonlinear feedback systems," *IEEE Trans. Circuits and Systems*, Vol. CAS-27, 1980, pp. 990-997.

[20] R.L. Bishop and S.I. Goldberg, *Tensor Analysis on Manifols*, Dover Publications, New York, 1980.

[21] A.M. Bloch and J.E. Marsden, "Controlling homoclinic orbits," *Theoret. Comput. Fluid Dynamics*, Vol. 1, 1989, pp. 179-190.

[22] J. Casti, *Connectivity, Complexity, and Catastrophe in Large-Scale Systems*, Wiley-Interscience, Chichester, 1979.

[23] H.-C. Chang and L.-H. Chen, "Bifurcation characteristics of nonlinear systems under conventional PID control," *Chemical Engineering Science*, Vol. 39, 1984, pp. 1127-1142.

[24] J.G. Charney and D.M. Straus, "Form-drag instability, multiple equilibria and propagating planetary waves in baroclinic, orographically forced, planetary wave systems," *J. Atmos. Sci.*, Vol. 37, 1980, pp. 1157-1176.

[25] L.-H. Chen and H.-C. Chang, "Global effects of controller saturation on closed-loop dynamics," *Chemical Engineering Science*, Vol. 40, 1984, pp. 2191-2205.

[26] H.-D. Chiang, I. Dobson, R.J. Thomas, J.S. Thorp and L. Fekih-Ahmed, "On voltage collapse in electric power systems," *IEEE Trans. on Power Systems*, Vol. 5, 1990, pp. 601-611.

[27] H.-D. Chiang, C.-W. Liu, P.P. Varaiya, F.F. Wu and M.G. Lauby, "Chaos in a simple power system," Paper No. 92 WM 151-1 PWRS, *IEEE Winter Power Meeting*, 1992.

[28] J.C. Chow, R. Fischl and H. Yan, "On the evaluation of voltage collapse criteria," *IEEE Trans. on Power Systems*, Vol. 5, 1990, pp. 612-620.

[29] M. Cibrario and J. Lévine, "Saddle-node bifurcation control with application to thermal runaway of continuous stirred tank reactors," *Proc. 1991 IEEE Conference on Decision and Control*, Brighton, England, December 1991, pp. 1551-1552.

[30] M.W. Davis, Jr. and W.F. O'Brien, "A stage-by-stage post-stall compression system modeling technique," *AIAA, SAE, ASME, and ASEE, Joint Conference, 23rd,* San Diego, CA, June 29-July 2, 1987, AIAA Paper 87-2088.

[31] I.J. Day, "Stall inception in axial flow compressors," *Proc. 1991 ASME Gas Turbine Conf.*, Orlando.

[32] I.J. Day," Active suppression of rotating stall and surge in axial compressors," *ASME J. Turbomachinery*, Vol. 115, 1993, pp. 40-47.

[33] R.L. Devaney, *An Introduction to Chaotic Dynamical Systems*, Second Edition, Redwood City, CA: Addison-Wesley, 1989.

[34] I. Dobson and H.-D. Chiang, "Towards a theory of voltage collapse in electric power systems," *Systems and Control Letters*, Vol. 13, 1989, pp. 253-262.

[35] E.J. Doedel, "AUTO: A program for the automatic bifurcation analysis of autonomous systems," *Cong. Num.*, Vol. 30, 1981, pp. 265-284.

[36] K.M. Eveker and C.N. Nett, "Control of compression system surge and rotating stall: a laboratory-based 'hands-on' introduction," reprint, 1993.

[37] T.B. Fowler, "Application of stochastic control techniques to chaotic nonlinear systems," *IEEE Trans. Automatic Control*, Vol. AC-34, 1989, pp. 201-205.

[38] G.F. Franklin, J.D. Powell and A. Emami-Naeini, *Feedback Control of Dynamic Systems*, Addison Wesley, Reading, MA, 1986.

[39] J.-H. Fu and E.H. Abed, " Families of Liapunov functions for nonlinear systems in critical cases," *IEEE Trans. Automatic Control*, Jan. 1993.

[40] A. Fukuma, M. Matsubara, N. Watanabe and K. Onogi, "Bifurcations in the frequency response of nonlinear feedback control systems," *IEEE Trans. Automatic Control*, Vol. AC-29, 1984, pp. 450-452.

[41] R. Genesio and A. Tesi, "Harmonic balance methods for the analysis of chaotic dynamics in nonlinear systems," *Automatica*, Vol. 28, 1992, pp. 531-548.

[42] C. Grebogi, E. Ott and J.A. Yorke, "Chaotic attractors in crisis," *Physical Review Letters*, Vol. 48, No. 22, May 1982, pp. 1507-1510.

[43] C. Grebogi, E. Ott and J.A. Yorke, "Crises, sudden changes in chaotic attractors, and transient chaos," *Physica*, Vol. 7D, 1983, pp. 181-200.

[44] E.M. Greitzer, "Surge and rotating stall in axial flow compressor, Part I: Theoretical compression system model," *ASME J. Engineering for Power*, 1976, pp. 190-198.

[45] J. Guckenheimer and P. Holmes, *Nonlinear Oscillations, Dynamical Systems, and Bifurcations of Vector Fields*, Springer-Verlag, New York, 1986.

[46] Hao Bai-Lin, Ed., *Chaos II*, World Scientific, Singapore, 1990.

[47] B.D. Hassard, N.D. Kazarinoff and Y.-H. Wan, *Theory and Applications of Hopf Bifurcation*, Cambridge, U.K.: Cambridge University Press, 1981.

[48] K. Hopffman and R. Kunze, *Linear Algebra*, Second Edition, Prentice-Hall, Englewood, Cliffs, N.J., 1971.

[49] P. Holmes, "Dynamics of a nonlinear oscillator with feedback control I: local analysis," *Journal of Dynamic Systems, Measurement, and Control*, Vol. 107, 1985, pp. 159-165.

[50] W.M. Hosny, L. Leventhal and W.G. Steenken, "Active stabilization of multi-stage axial-compressor aerodynamic system instabilities," *Proc. 1991 ASME Gas Turbine Conference*, Orlando, FL, June 1991.

[51] L.N. Howard, "Nonlinear oscillations," in *Nonlinear Oscillations in Biology*, F.C. Hoppensteadt, ed. Amer. Math. Soc., Providence, R.I., 1979, pp. 1-68.

[52] A. Hübler, "Adaptive control of chaotic systems, " *Helvetica Physica Acta*, Vol. 62, 1989, pp. 343-346.

[53] G. Iooss and D.D. Joseph, *Elementary Stability and Bifurcation Theory*, Second Edition, Springer-Verlag, New York, 1990.

[54] E.A. Jackson, *Perspectives of Nonlinear Dynamics II*, Cambridge University Press, Cambridge, 1990.

[55] T. Kailath, *Linear Systems*, Prentice-Hall, Englewood Cliffs, NJ, 1980.

[56] V. Krishnamurthy, "A predictability study of Lorenz's 28-variable model: Application of dynamical systems theory," preprint, 1992.

[57] H.G. Kwatny, A.K. Pasrija and L.Y. Bahar, "Static bifurcation in electric power networks: Loss of steady-state stability and voltage collapse," *IEEE Trans. Circuits Syst.*, Vol. CAS-33, 1986, pp. 981-991.

[58] H.-C. Lee and E.H. Abed, "Washout filters in the bifurcation control of high alpha flight dynamics," *Proc. 1991 American Control Conference*, Boston, pp. 206-211.

[59] H.C. Lee, "Robust Control of Bifurcating Nonlinear Systems with Applications," University of Maryland, College Park, Ph.D. Dissertation, 1991.

[60] D.-C. Liaw and E.H. Abed, "Stabilization of tethered satellites during station keeping," *IEEE Trans. Automatic Control*, Vol. AC-35, No. 11, 1990, pp. 1186-1196.

[61] D.-C. Liaw, R.A. Adomaitis, and E.H. Abed, "Two-parameter bifurcation analysis of axial flow compressor dynamics," *Proc. 1991 IEEE American Control Conference*, Boston, MA, June 26-28, 1991, pp. 2955-2960.

[62] D.-C. Liaw and E.H. Abed, "Analysis and control of rotating stall," *Proceedings of NOLCOS'92: Nonlinear Control System Design Symposium*, (M. Fliess, Ed.), June 24-26, 1992, Bordeaux, France, pp. 88-93; Published by the International Federation of Automatic Control.

[63] E.N. Lorenz, "A study of the predictability of a 28-variable atmospheric model," *Tellus*, Vol. 17, 1965, pp. 321-333.

[64] Y. Mansour, Ed., *Voltage Stability of Power Systems: Concepts, Analytical Tools, and Industry Experience*, New York: IEEE Press, (Publ. 90TH0358-2-PWR), 1990.

[65] J.E. Marsden and M. McCracken, *The Hopf Bifurcation and Its Applications*, New York: Springer-Verlag, 1976.

[66] F.E. McCaughan, "Application of bifurcation theory to axial flow compressor instability," *ASME J. Turbomachinery*, Vol. 111, 1989, pp. 426-433.

[67] P.E. McDermott and H.-C. Chang, "On the global dynamics of an autothermal reactor stabilized by linear feedback control," *Chemical Engineering Science*, Vol. 39, 1984, pp. 1347-1356.

[68] D. McRuer, I. Ashkenas and D. Graham, *Aircraft Dynamics and Automatic Control,* Princeton University Press, Princeton, N.J., 1973.

[69] A.I. Mees, *Dynamics of Feedback Systems*, Wiley, New York, 1981.

[70] P.K. Mehra, "Catastrophe theory, nonlinear system identification and bifurcation control," *Proc. of the Joint Automatic Control Conference*, 1977, pp. 823-831.

[71] R.K. Mehra, W.C. Kessel, and J.V. Carroll, "Global stability and control analysis of aircraft at high angles-of-attack," ONRCR-215-248-1, U.S. Office of Naval Research, Arlington, VA, June 1977.

[72] F.K. Moore and E.M. Greitzer, "A theory of post-stall transients in axial compression systems: Part I–Development of equations," *ASME J. Engineering for Gas Turbines and Power*, Vol. 108, 1986, pp. 68-76.

[73] F.K. Moore and E. M. Greitzer, "A theory of post-stall transients in axial compression systems: Part II—Application," *ASME J. of Engineering for Gas Turbines and Power*, Vol. 108, 1986, pp. 231-239.

[74] M.A. Nayfeh, A.M.A. Hamdan and A.H. Nayfeh, "Chaos and instability in a power system: Primary resonant case," *Nonlinear Dynamics*, Vol. 1, 1990, pp. 313-339.

[75] H.E. Nusse and J.A. Yorke, *Numerical Investigations of Chaotic Systems: A Handbook for JAY's Dynamics*, Draft, Institute for Physical Science and Technology, University of Maryland, College Park, MD, 1992.

[76] H.E. Nusse, and J.A. Yorke, "Border-collision bifurcations including 'period two to period three' for piecewise smooth systems," *Physica D*, Vol. 57, 1992, pp. 39-57.

[77] E. Ott, C. Grebogi and J.A. Yorke, "Controlling chaos," *Physical Review Letters*, Vol. 64, 1990, pp. 1196-1199.

[78] E. Ott, *Chaos in Dynamical Systems*, Cambridge University, Cambridge, 1993.

[79] J. Paduano, A. H. Epstein, L. Valavani, J. P. Longley, E. M. Greitzer, and G. R. Guenette, "Active control of rotating stall in a low-speed axial compressor, " *ASME J. Turbomachinery*, Vol. 115, 1993, pp. 48-56.

[80] B.B. Peckham and I.G. Kevrekidis, "Period doubling with higher order degeneracies," *SIAM J. Math. Anal.*, Vol. 22, 1991, pp. 1552-1574.

[81] H. Poincaré, *Les méthodes nouvelles de la mécanique celeste*, Vols. 1-3, Gauthier-Villars, Paris.

[82] Qin Hua-Shu, "On the regulation of a system losing stability of branching type," *Recent Developments in Control Theory and its Applications*, Proc. of the Bilateral Meeting on Control Systems, Science Press, Beijing, China, 1982, pp. 499-509.

[83] C. Rajagopalan, P.W. Sauer and M.A. Pai, "Analysis of voltage control systems exhibiting Hopf bifurcation," *Proc. 28th IEEE Conf. Dec. Contr.*, Tampa, 1989, pp. 332-335.

[84] B.B. Reinhold and R.T. Pierrehumbert, "Dynamics of weather regimes: Quasi-stationary waves and blocking," *Mon. Wea. Rev.*, Vol. 110, 1982, pp. 1105-1145.

[85] F.J. Romeiras, E. Ott, C. Grebogi and W.P. Dayawansa, "Controlling chaotic dynamical systems," *Proc. 1991 American Control Conference*, Boston, 1991, pp. 1113-1119.

[86] D.L Russell, "Optimal orbital regulation in dynamical systems subject to Hopf bifurcation," J. Differential Equations, Vol. 44, 1982, pp. 188-223.

[87] F.M.A. Salam, J.E. Marsden and P.P. Varaiya, "Arnold diffusion in the swing equations of a power system," *IEEE Trans. Circuits and Systems*, Vol. CAS-31, 1984, pp. 673-688.

[88] T. Shinbrot, C. Grebogi, E. Ott, J.A. Yorke, "Using small perturbations to control chaos," *Nature*, Vol. 363, 1993, pp. 411-417.

[89] A.N. Shoshitaishvili, "Singularities for projections of integral manifolds with applications to control and observation problems," *Advances in Soviet Mathematics*, Vol. 1, 1990, pp. 295-333.

[90] A.N. Shoshitaishvili, "Structural control of nonlinear systems," Translated from *Avtomatika i Telemekhanika*, No. 8, 1991, pp. 71-79.

[91] A.N. Shoshitaishvili, "On control branching in systems with degenerate linearization," *Proc. of the Second NOLCOS (Nonlinear Control System Design) Conference*, June 24-26, 1992, Bordeaux, France, pp. 495-500.

[92] L.P. Sil'nikov, "A case of the existence of a denumerable set of periodic motions," *Soviet Math. Dokl.*, Vol. 6, 1965, pp. 163-166.

[93] J. Singer, Y.Z. Wang and H.H. Bau, " Controlling a chaotic system," sl Physical Review Letters, Vol. 66, No. 9, 1991, pp. 1123-1125.

[94] J. Singer and H.H. Bau, "Active control of convection," *Phys. Fluids A* 3 (1991), pp. 2859-2865.

[95] C. Sparrow, *The Lorenz Equations: Bifurcations, Chaos, and Strange Attractors*, Springer-Verlag, New York, 1982.

[96] I. Stakgold, *Green's Functions and Boundary Value Problems*, Wiley-Interscience, New York, 1976.

[97] J.M.T. Thompson and H.B. Stewart, *Nonlinear Dynamics and Chaos*, Wiley, Chichester, 1986.

[98] V. Venkatasubramanian, H. Schättler and J. Zaborszky, "Voltage dynamics: Study of a generator with voltage control, transmission and matched MW load," *IEEE Trans. Automatic Control*, Vol. 37, 1992, pp. 1717-1733.

[99] T.L. Vincent and J. Yu, "Control of a chaotic system," *Dynamics and Control*, Vol. 1, pp. 35-52, 1991.

[100] K.T. Vu and C.C. Liu, "Dynamic mechanisms of voltage collapse," *Systems and Control Letters*, Vol. 15, 1990, pp. 329-338.

[101] H. Wang and E.H. Abed, "Bifurcation control of chaotic dynamical systems," *Proc. of the Second NOLCOS (Nonlinear Control System Design) Conference*, June 24-26, 1992, Bordeaux, France.

[102] H. Wang, E.H. Abed and A.M.A. Hamdan, "Is voltage collapse triggered by the boundary crisis of a strange attractor?," *Proceedings of the 1992 American Control Conference*, Chicago, June 1992, pp. 2084-2088.

[103] H.O. Wang, R.A. Adomaitis and E.H. Abed, "Active Stabilization of Rotating Stall in Axial-Flow Compressors," *Proc. 1st IEEE Regional Conf. on Aerospace Control Systems*, Thousand Oaks, CA, May 1993; in press.

[104] H.O. Wang and E.H. Abed, "Control of nonlinear phenomena at the inception of voltage collapse," *Proc. 1993 American Control Conference*, San Francisco, CA, June 1993, pp. 2071-2075.

[105] Y. Wang, J. Singer and H.H. Bau, "Controlling chaos in a thermal convection loop," *J. Fluid Mechanics*, 237 (1992), pp. 479-498.

[106] M. Zak, "Terminal attractors for addressable memory in neural networks," *Physics Letters A*, Vol. 133, 1988, pp. 218-222.